



The Large Hadron Collider

Philippe Lebrun
CERN, Geneva, Switzerland

African School of Physics 2010
Stellenbosch, South Africa, 1-21 August 2010



Contents

- The LHC in a nutshell
- Performance
 - Energy
 - Luminosity
 - Collective effects
 - Dynamic aperture
- Technology
 - Superconducting magnets
 - Powering and protection
 - Cryogenics
 - Vacuum

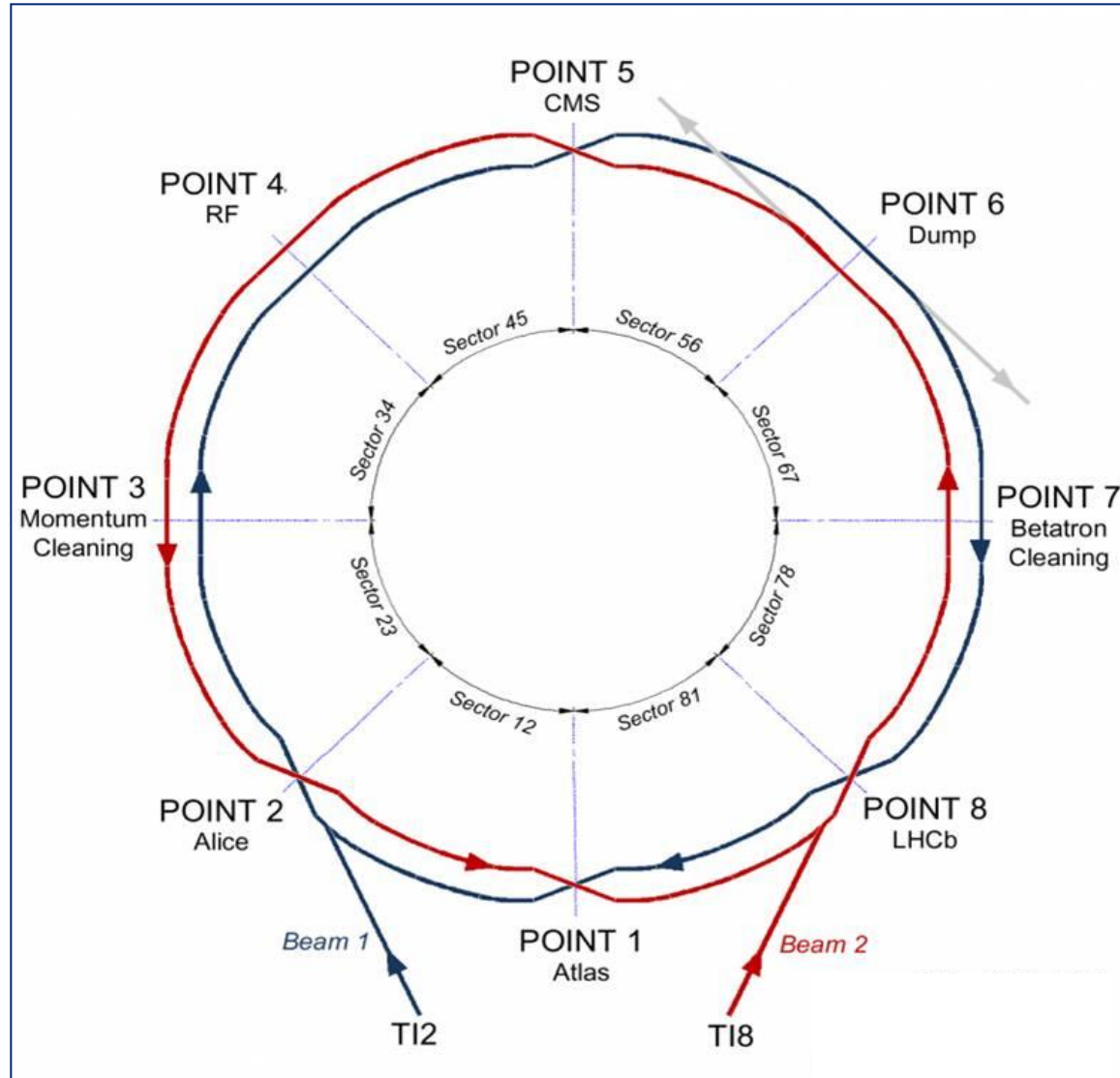


The largest scientific instrument in the world



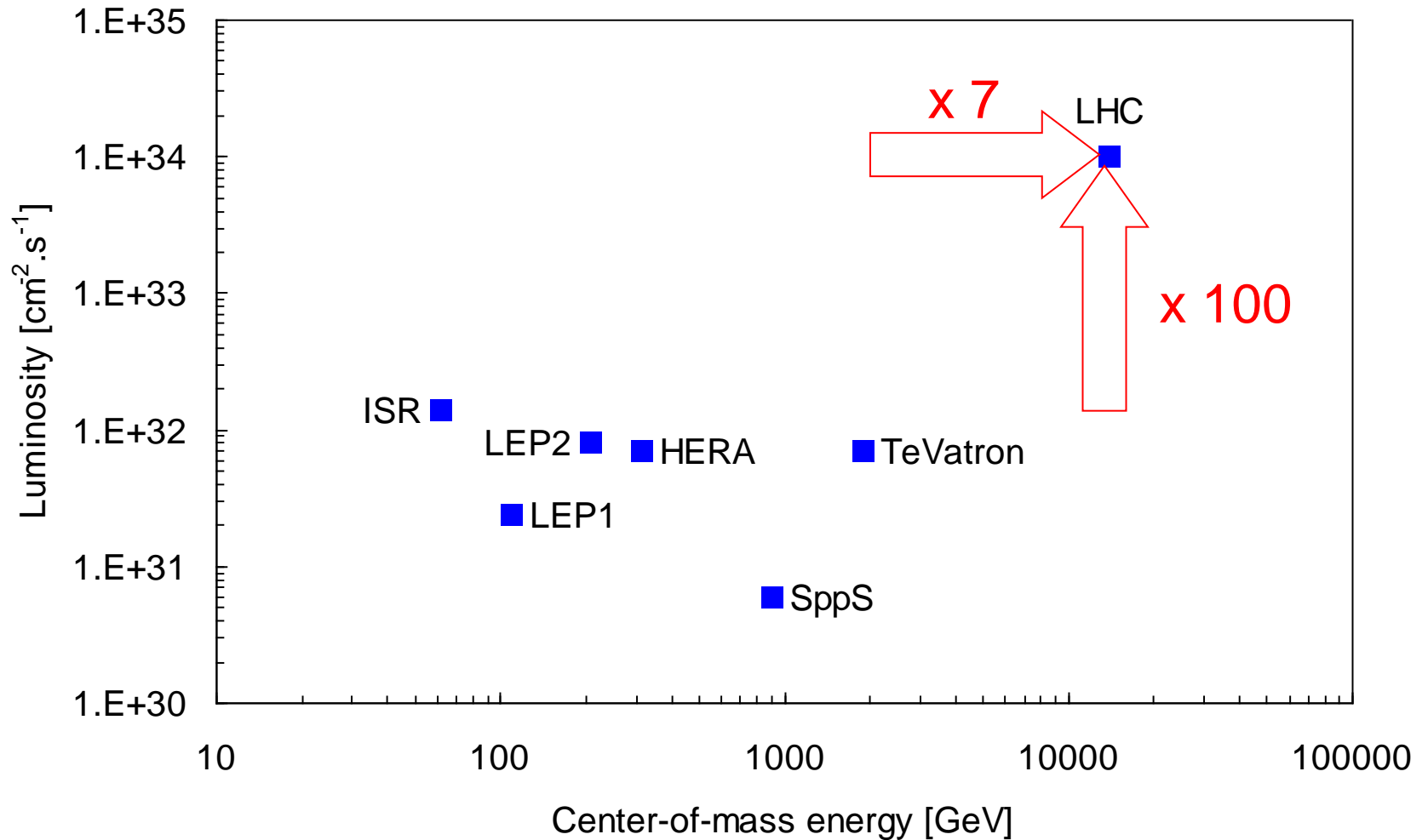


Colliding counter-rotating beams of hadrons at the center of four large particle detectors





A new territory in energy and luminosity





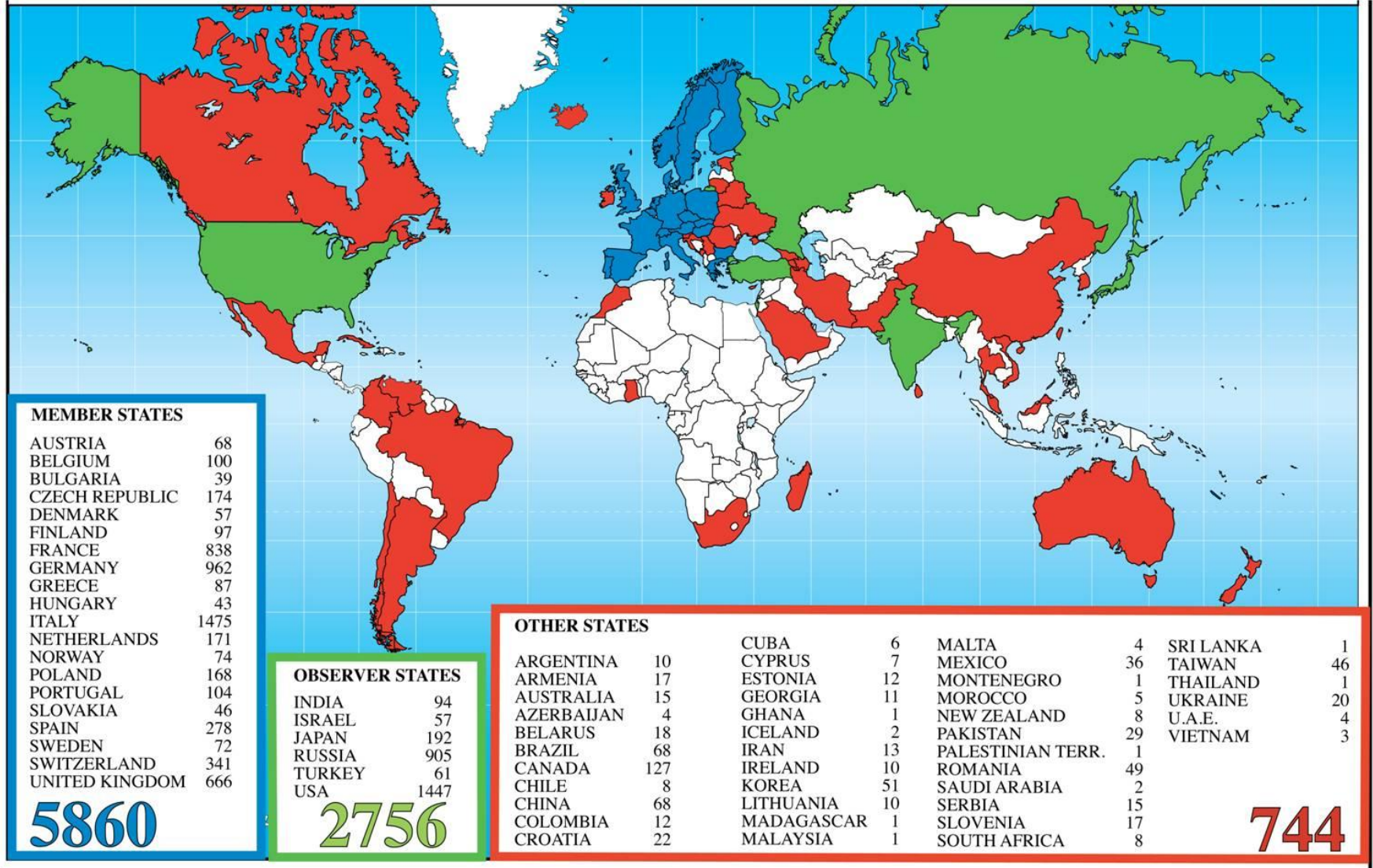
Advanced technology at work

23 km of superconducting magnets
cooled in superfluid helium at 1.9 K



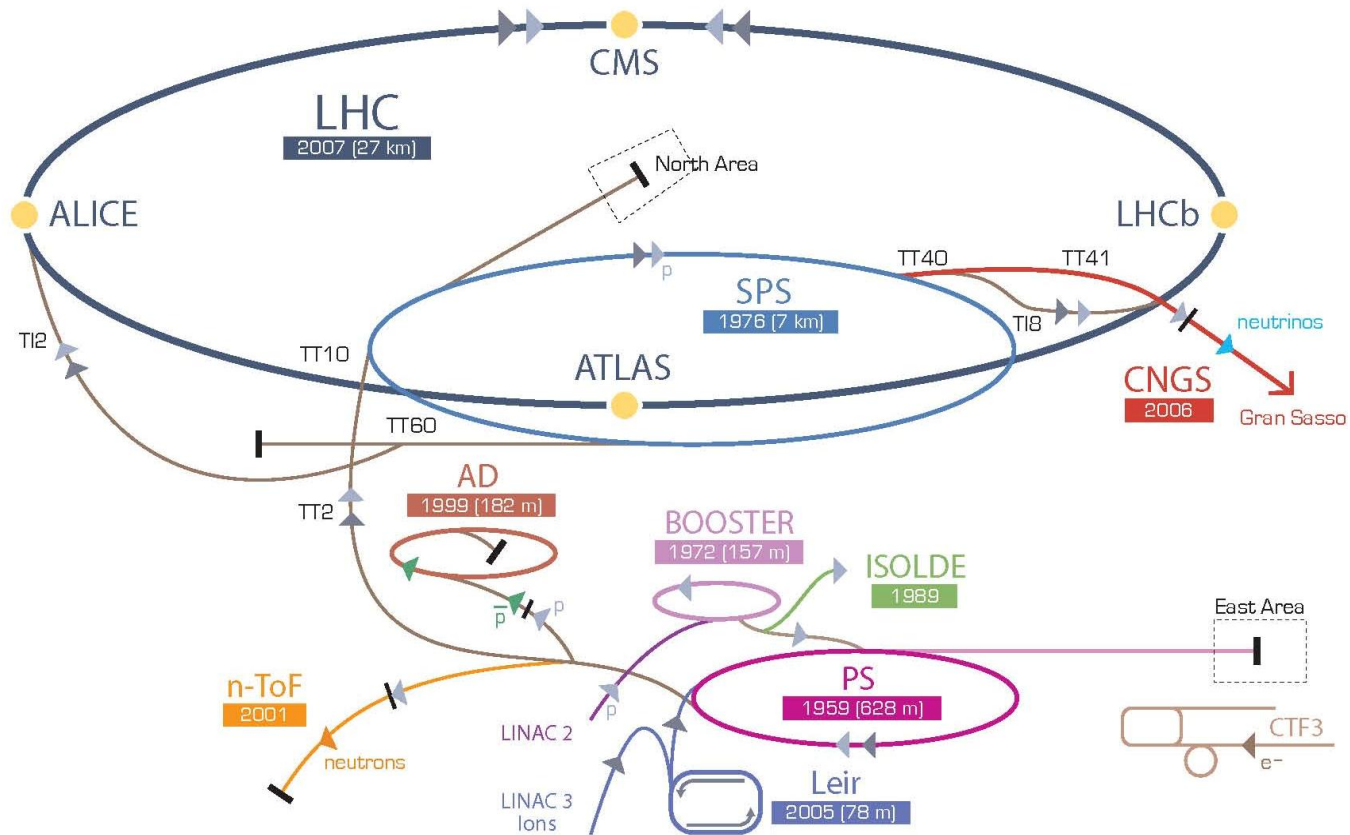


A global project serving the world community of particle physicists





Making best use of CERN's infrastructure



▶ p (proton) ▶ ion ▶ neutrons ▶ \bar{p} (antiproton) ↔ proton/antiproton conversion ▶ neutrinos ▶ electron

LHC Large Hadron Collider SPS Super Proton Synchrotron PS Proton Synchrotron

AD Antiproton Decelerator CTF3 Clic Test Facility CNGS Cern Neutrinos to Gran Sasso ISOLDE Isotope Separator OnLine DEvice

LEIR Low Energy Ion Ring LINAC LINear ACcelerator n-ToF Neutrons Time Of Flight



Main parameters of LHC (p-p)

• Circumference	26.7	km
• Beam energy at collision	7	TeV
• Beam energy at injection	0.45	TeV
• Dipole field at 7 TeV	8.33	T
• Luminosity	10^{34}	$\text{cm}^{-2}.\text{s}^{-1}$
• Beam current	0.58	A
• Protons per bunch	1.15×10^{11}	
• Number of bunches	2808	
• Nominal bunch spacing	24.95	ns
• Normalized emittance	3.75	$\mu\text{m}.\text{rad}$
• Total crossing angle	285	μrad
• Energy loss per turn	6.7	keV
• Critical synchrotron energy	44.1	eV
• Radiated power per beam	3.6	kW
• Stored energy per beam	362	MJ
• Stored energy in magnets	11	GJ
• Operating temperature	1.9	K



Contents

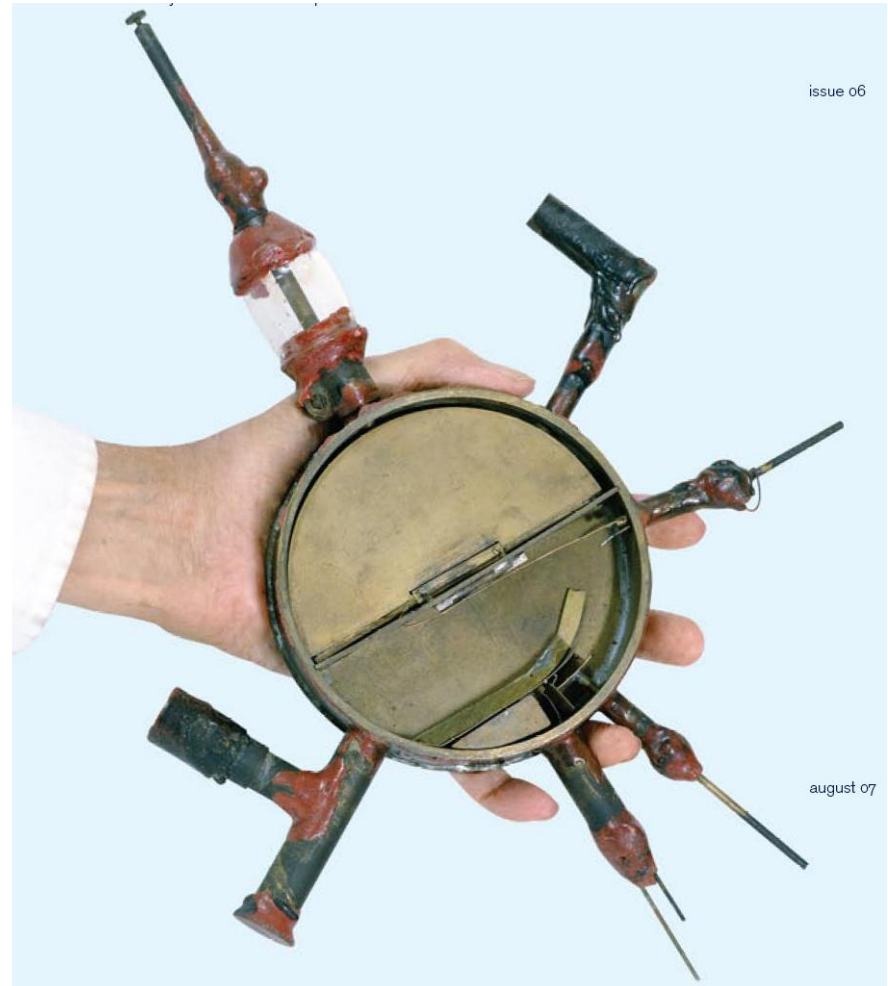
- The LHC in a nutshell
- **Performance**
 - Energy
 - Luminosity
 - Collective effects
 - Dynamic aperture
- Technology
 - Superconducting magnets
 - Powering and protection
 - Cryogenics
 - Vacuum

The first circular accelerator

Lawrence and Livingston's 80 keV cyclotron (1930)



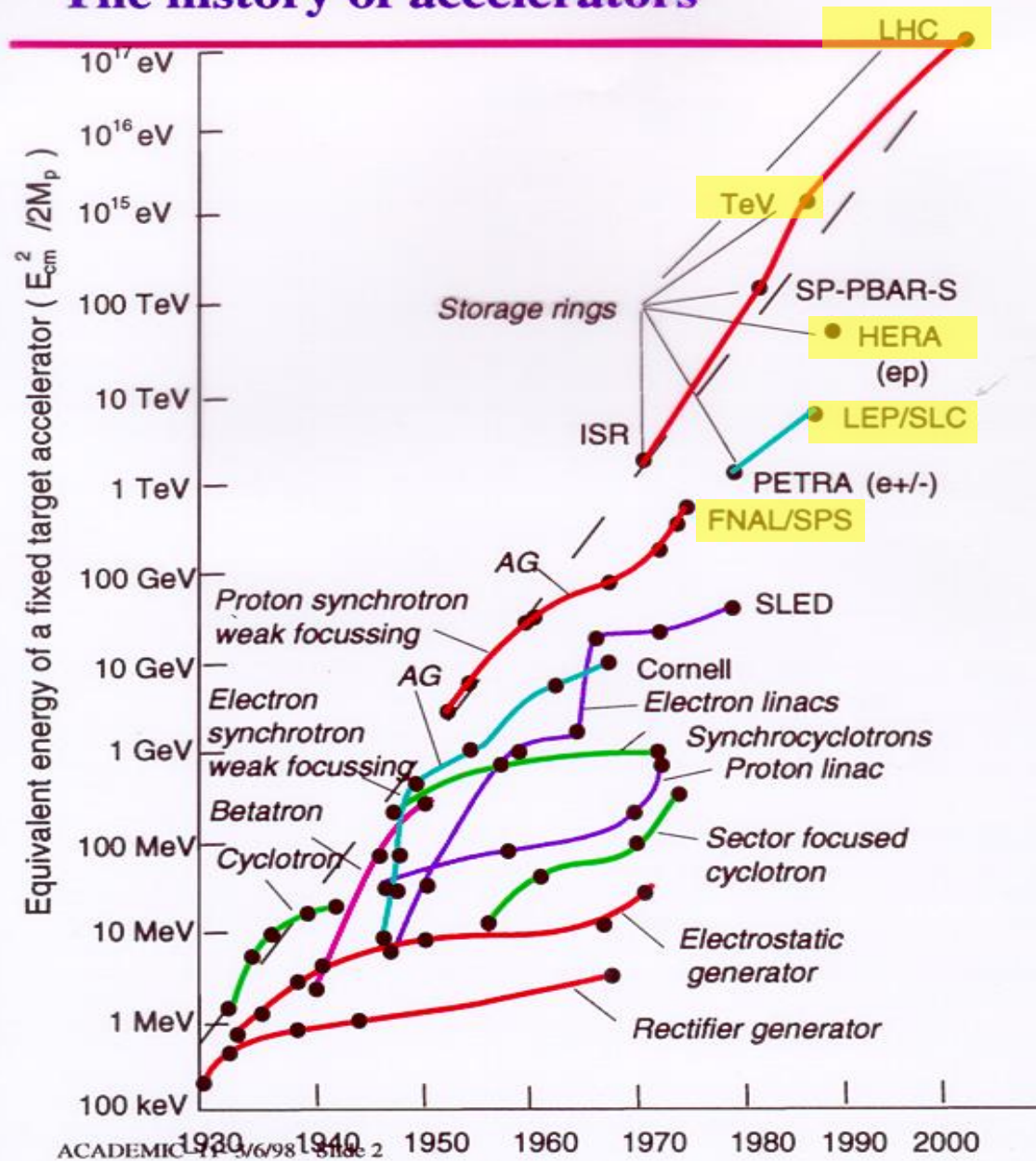
Ernest O. Lawrence





The history of accelerators

- sustained exponential development for more than 70 years
- progress achieved through repeated jumps from saturating to emerging technologies
- **superconductivity**, key technology of high-energy machines since the 1980s





Beam energy and bending field

Lorentz force on charged particle

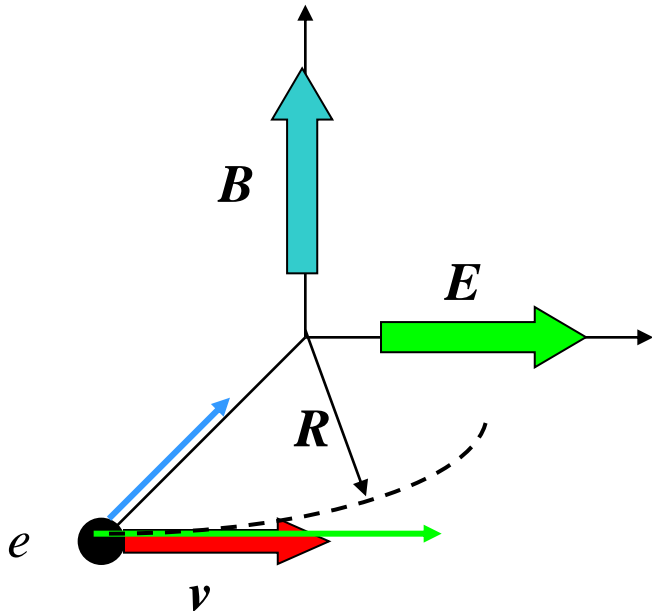
$$\vec{F} = e \vec{E} + \vec{v} \wedge \vec{B}$$

Charge

Electric field

Velocity

Magnetic field

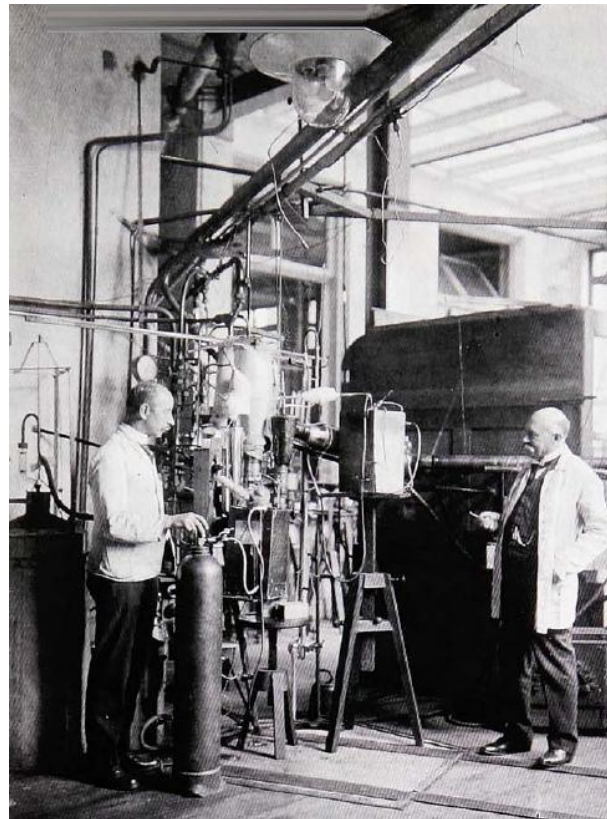


In a circular accelerator

Particle momentum \longrightarrow $p = e B R$ \longleftarrow Radius of curvature

$$p \text{ [GeV / c]} \approx 0.3 B \text{ [T]} R \text{ [m]}$$

The LHC needs a field of 8.33 T to bend 7 TeV beams along the curvature of the tunnel, with a radius of 2804 m

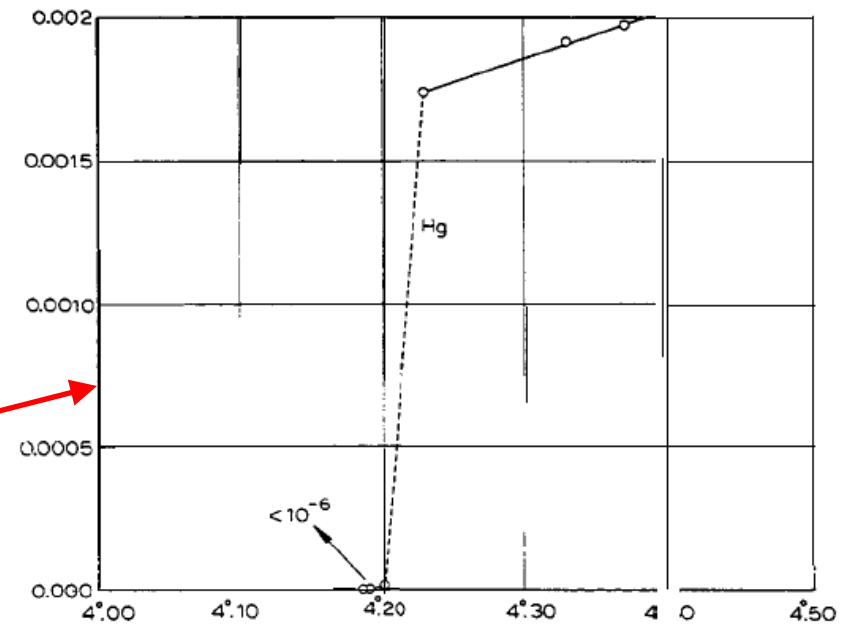
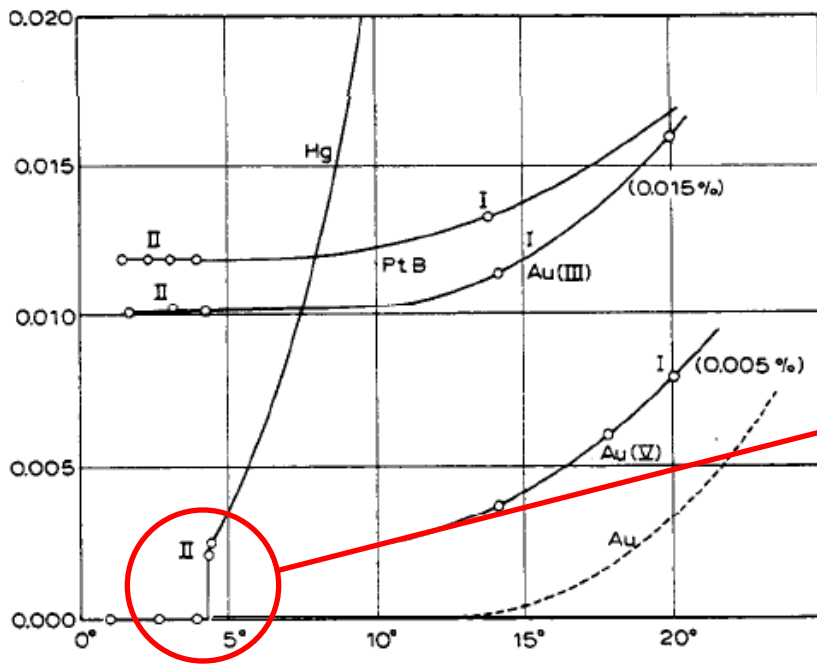


HEIKE KAMERLINGH ONNES

Investigations into the properties of substances at low temperatures, which have led, amongst other things, to the preparation of liquid helium

Nobel Lecture, December 11, 1913

Discovery of superconductivity (1911)



Thus the mercury at 4.2°K has entered a new state, which, owing to its particular electrical properties, can be called the state of superconductivity.



First idea of superconducting magnets (H. K. Onnes 1913)

dendum 2.) There is also the question as to whether the absence of Joule heat makes feasible the production of strong magnetic fields using coils without iron,* for a current of very great density can be sent through very fine, closely wound wire spirals. Thus we were successful in sending a current of 0.8 amperes, i.e. of 56 amperes per square millimetre, through a coil, which contained 1,000 turns of a diameter of $1/70$ square mm per square centimetre at right angles to the turns.

critical field of superconductors!

after this lecture was given and produced surprising results. In fields below a threshold value (for lead at the boiling point of helium 600 Gauss), which was not reached during the experiment with the small coil mentioned in the text, there is no magnetic resistance at all. In fields above this threshold value a relatively large resistance arises at once, and grows considerably with the field. Thus in an unexpected way a difficulty in the production of intensive magnetic fields with coils without iron faced us. The discovery of the

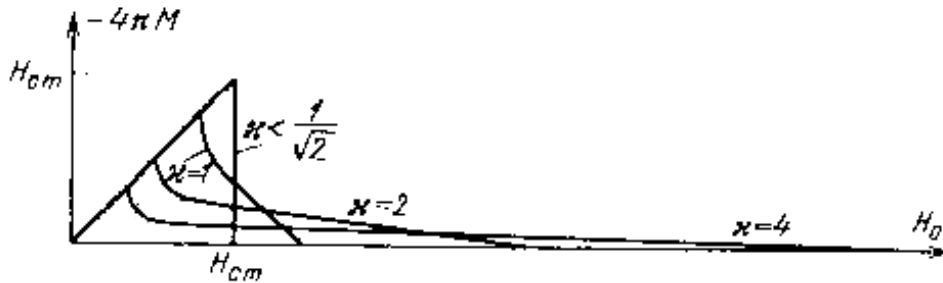
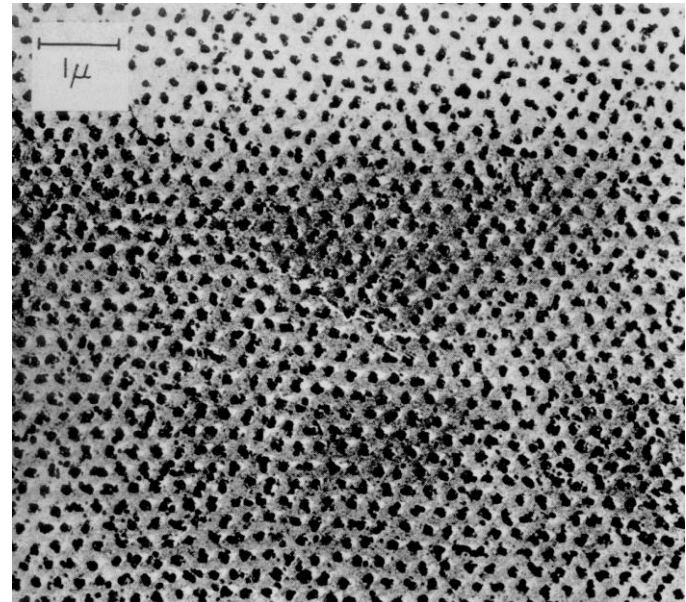
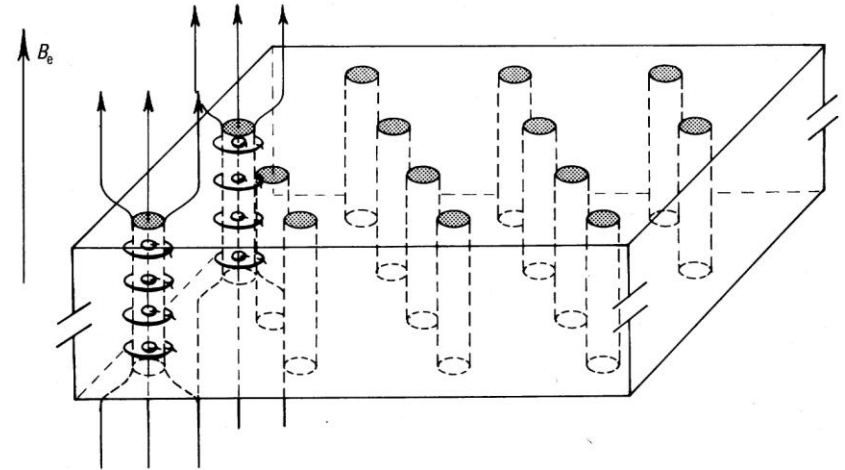


Vortex lattice of type-II superconductors (1954)

Field penetrates locally without destroying superconductivity in bulk

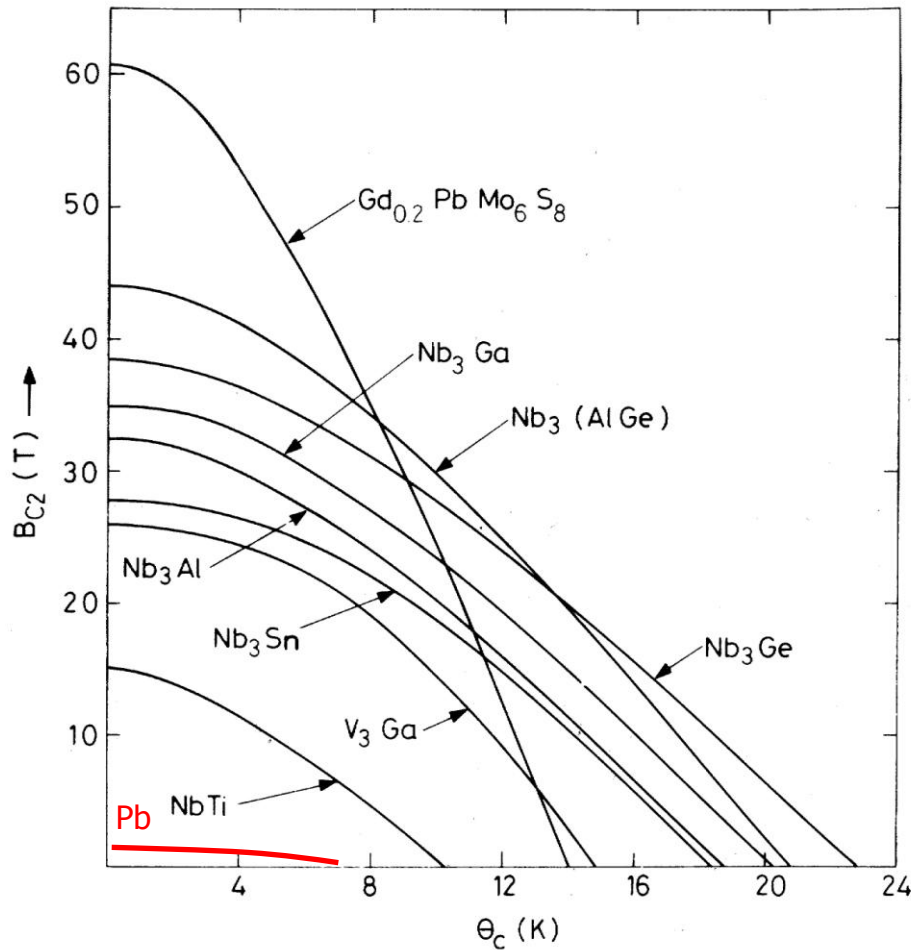


Alexei Abrikosov





Upper critical field of type II superconductors is compatible with magnet applications





First « high-field » superconducting magnet (1960)

April 14, 1964

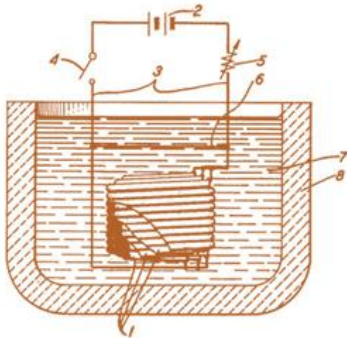
J. E. KUNZLER

3,129,359

SUPERCONDUCTING MAGNET CONFIGURATION

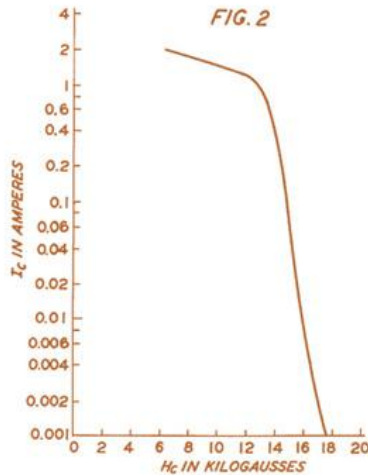
Filed Sept. 19, 1960

FIG. 1



Patent filed in 1960 by J. Kunzler, of Bell Laboratories (registered in 1964)

1.5 T reached with magnet wound from molybdenum-rhenium alloy wire



INVENTOR
J. E. KUNZLER
BY
George S. Brady
ATTORNEY



Discovery of Nb-Ti alloys (1961)

Superconducting Solid Solution Alloys of the Transition Elements

J. K. HULM AND R. D. BLAUGHER

Westinghouse Research Laboratories, Pittsburgh, Pennsylvania

(Received April 19, 1961)

The solid solution alloys formed by the incomplete *d*-shell metals in groups 4, 5, 6, and 7 have been tested for superconductivity down to 1°K. For alloys formed between neighboring elements in a given row of the periodic table, two transition temperatures are observed, one of which is approximately equal to 4.7 and 6.4, respectively, for the two elements. The upper maximum is absent. Similar maximums are observed for alloys formed between neighboring elements in adjacent rows of the periodic table, thus confirming the normal density-of-states function, $N(0)$, for these peaks lying at about the same composition. The relationship of T_c to $N(0)$ is also presented for alloys composed of elements in adjacent rows. In this case, the form of the relationship is

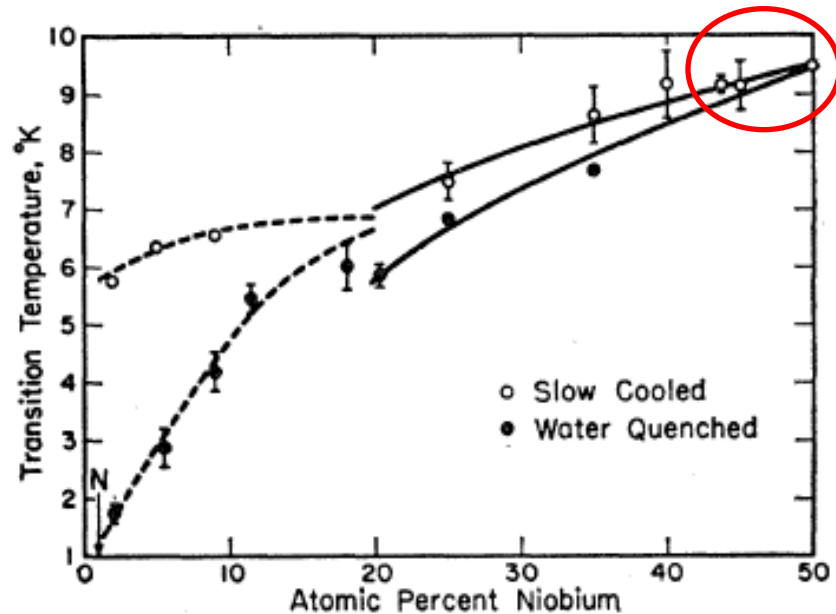


FIG. 6. Transition temperature versus composition for titanium-niobium alloys prepared by different types of heat treatment.



High-energy circular accelerators using superconducting magnets

HERA proton ring at DESY, Germany (1992)



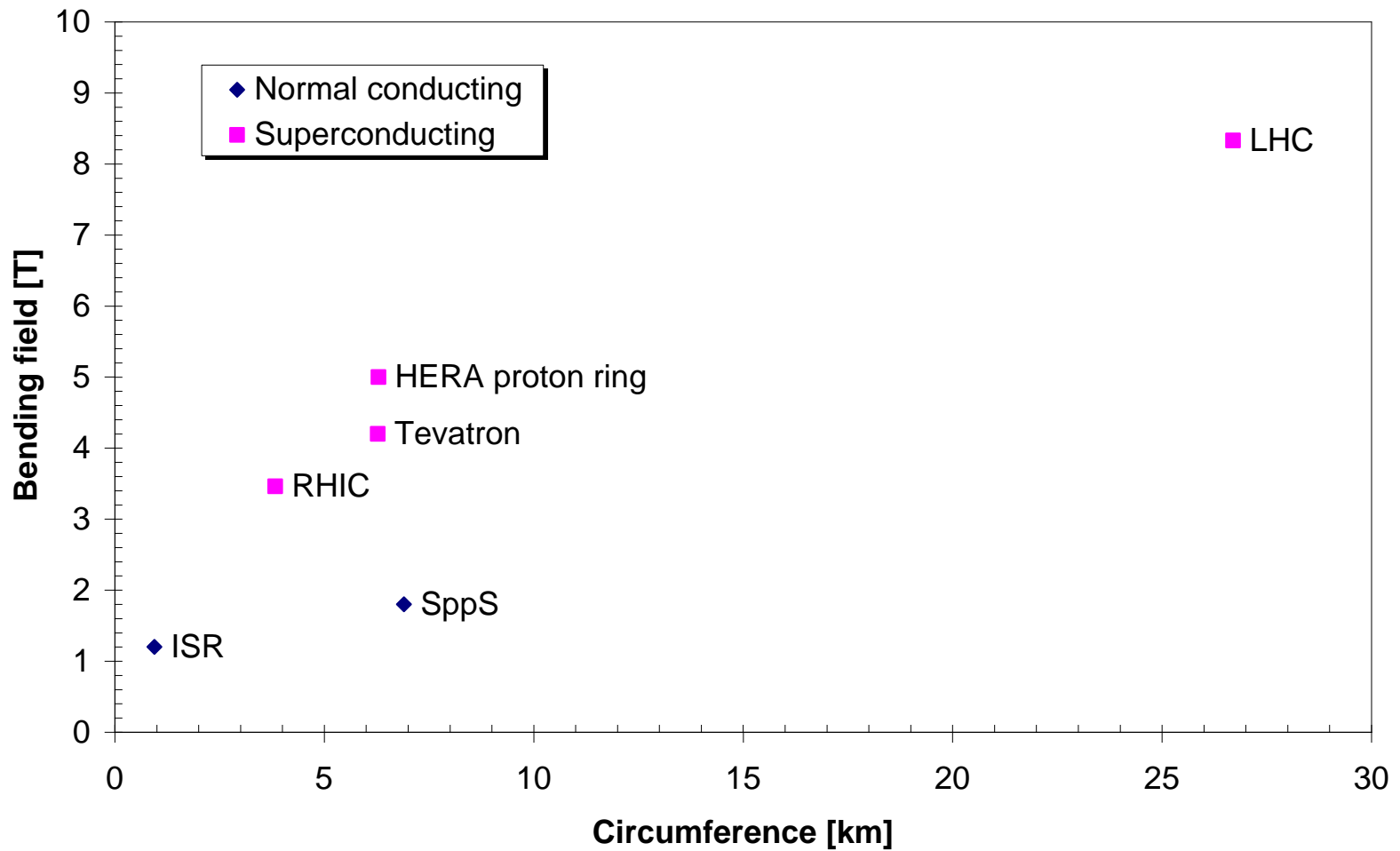
The Tevatron at Fermilab, USA (1983)



RHIC at Brookhaven National Lab, USA (2000)

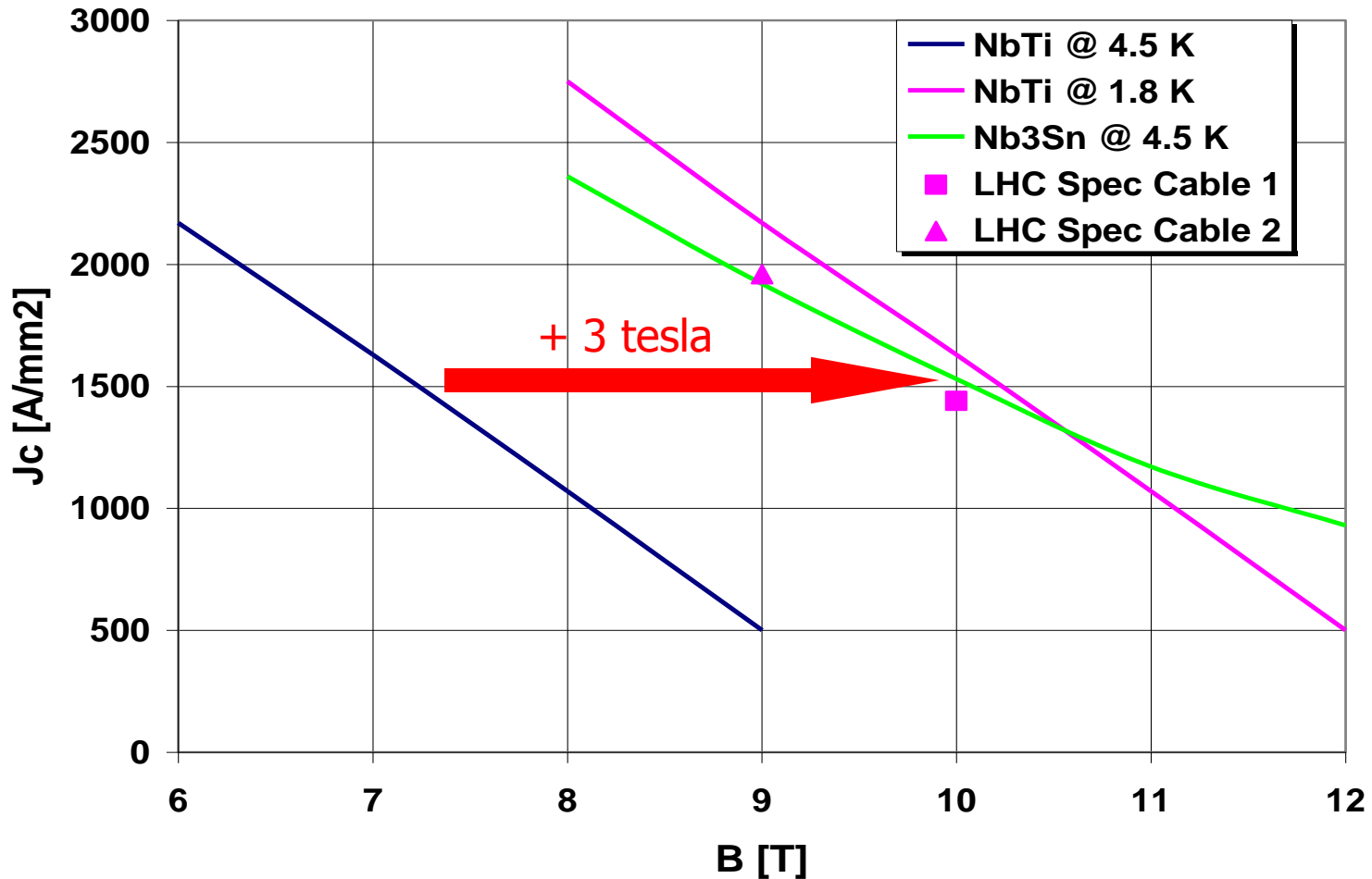


Circumference & bending field of hadron colliders





Rationale for LHC basic technical design





Contents

- The LHC in a nutshell
- **Performance**
 - Energy
 - **Luminosity**
 - Collective effects
 - Dynamic aperture
- Technology
 - Superconducting magnets
 - Powering and protection
 - Cryogenics
 - Vacuum



Event rate and luminosity

$$R = L \sigma$$

Event rate

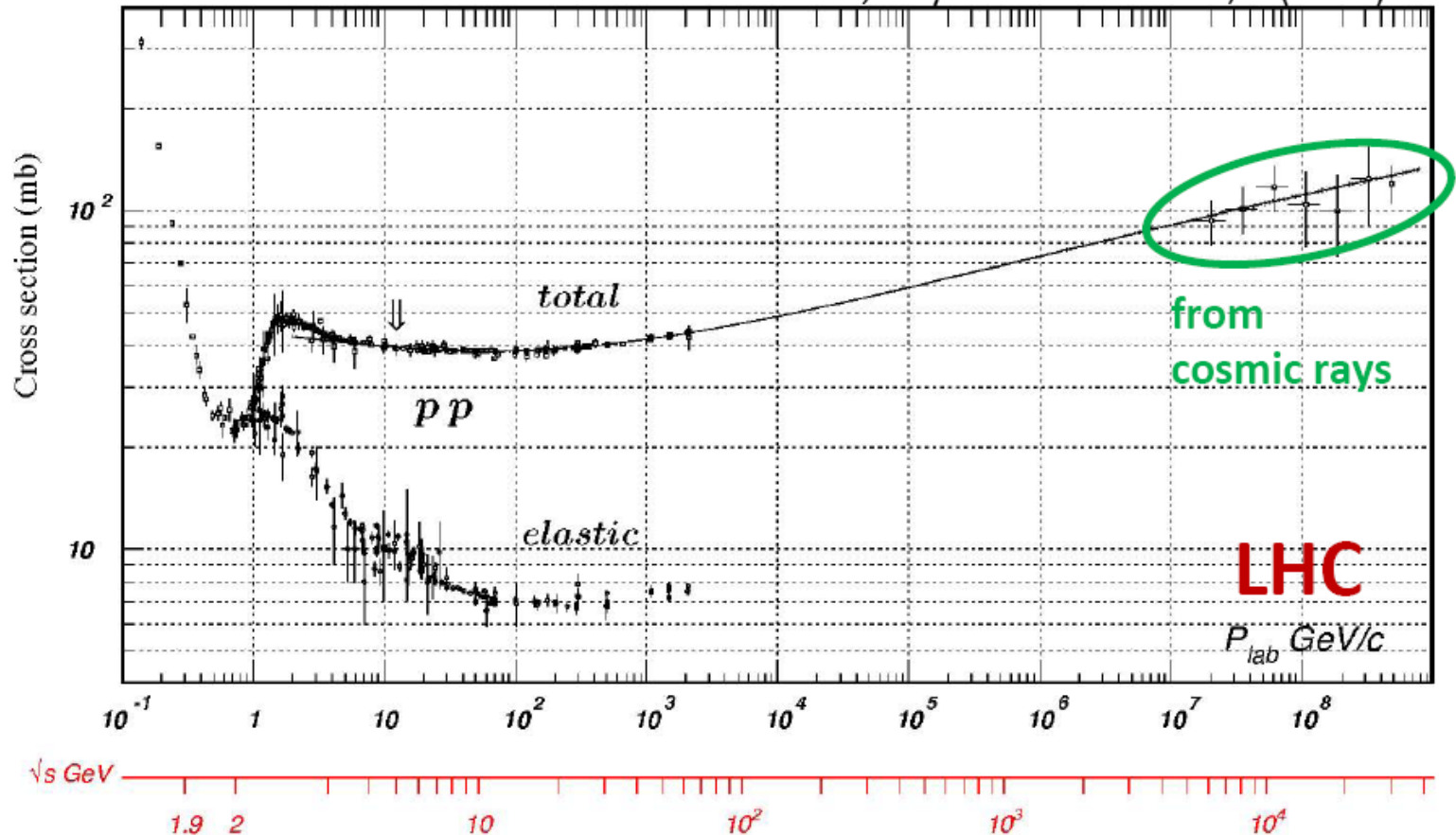
Luminosity

Cross-section

$$\sigma_{\text{TOT}} \sim 100 \text{ mbarn} = 10^{-25} \text{ cm}^2$$

$$\sigma_{\text{inelastic}} \sim 60 \text{ mbarn} = 6 \cdot 10^{-26} \text{ cm}^2$$

C. Amsler *et al.*, Physics Letters **B667**, 1 (2008)





Luminosity with colliding beams

$$L = \frac{N_b^2 n_b f_{rev} \gamma}{4 \pi \varepsilon_n \beta^*} F$$

Number of bunches

Number of particles per bunch

Revolution frequency

Relativistic factor

Geometric factor linked to crossing angle

Normalized emittance

Beta function at collision point

- To maximize luminosity
 - increase bunch number, bunch population
 - reduce emittance, beta function at collision point
 - cross at small angle

} *limits?*



Beam stored energy

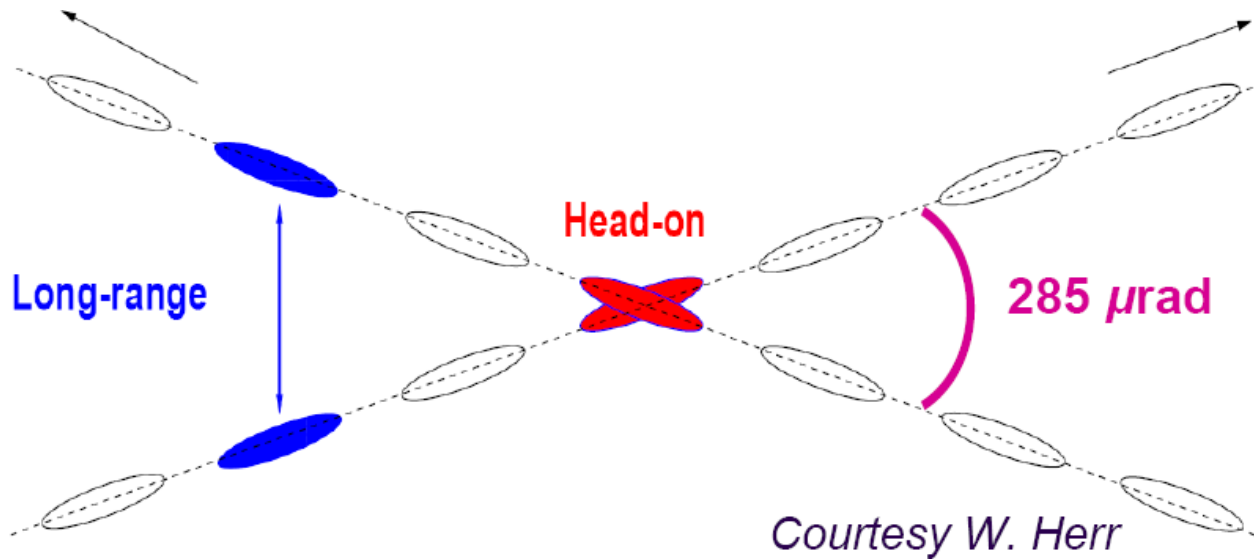
- Energy stored in circulating beam

$$E_{beam} = m_0 c^2 \gamma N_b n_b$$

With 2808 bunches of $1.1 \cdot 10^{11}$ protons at 7 TeV, $E_{beam} = 362$ MJ,
equivalent to 80 kg TNT!

$$L = \frac{N_b f_{rev}}{4 \pi m_0 c^2 \epsilon_n \beta^*} F E_{beam} = \frac{1}{4 \pi m_0 c^2} \underbrace{f_{rev}}_{\text{Set by machine circumference}} \underbrace{\frac{N_b}{\epsilon_n}}_{\text{Set by injector chain}} \underbrace{\frac{F}{\beta^*}}_{\text{Set by collision optics}} E_{beam}$$

Beam-beam effects



- Particle trajectories in one beam perturbed by e-m field of the other
 - Head-on crossing
 - Excites betatron resonances
 - Generates tune spread
 - Long-range
 - Additional non-linear tune spread
 - Minimum crossing angle $>$ beam divergence at collision point
- tune footprint must not cross low-order resonances*



Head-on beam-beam tune shift

Number of collision points

$$\xi_{total} = \frac{k N_b r_p}{4 \pi \epsilon_n} F < \xi_{max}$$

~ 0.01 (pointing to ξ_{total})

Should not exceed 0.015 (empirical limit) (pointing to ξ_{max})

- Strategy to maximize luminosity
 - Operate at beam-beam limit
 - Maximize number of bunches, bunch population
 - Decrease beta at collision point

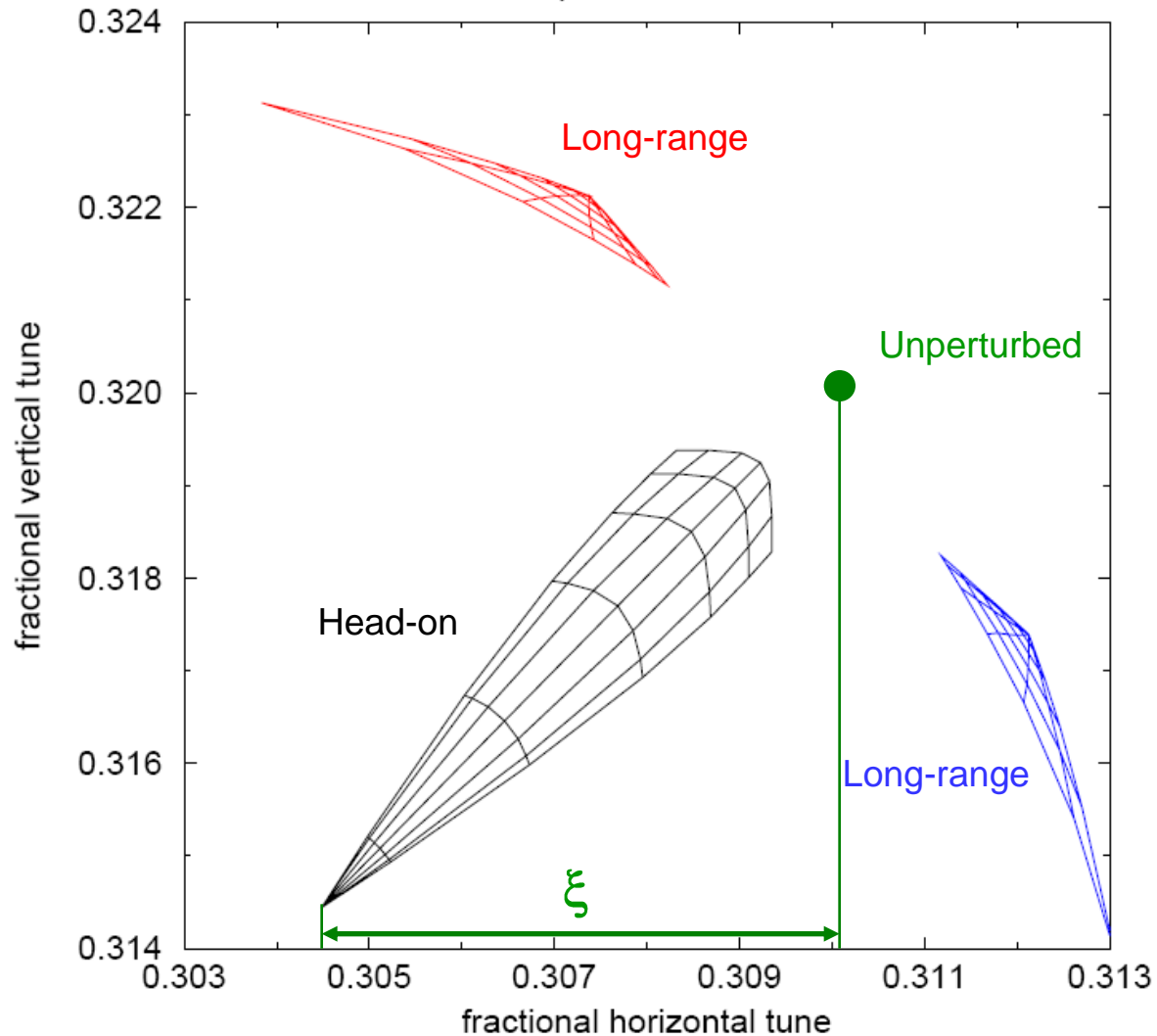
$$L = \frac{\xi_{total} N_b n_b f_{rev} \gamma}{k r_p \beta^*}$$



Beam-beam tune footprint

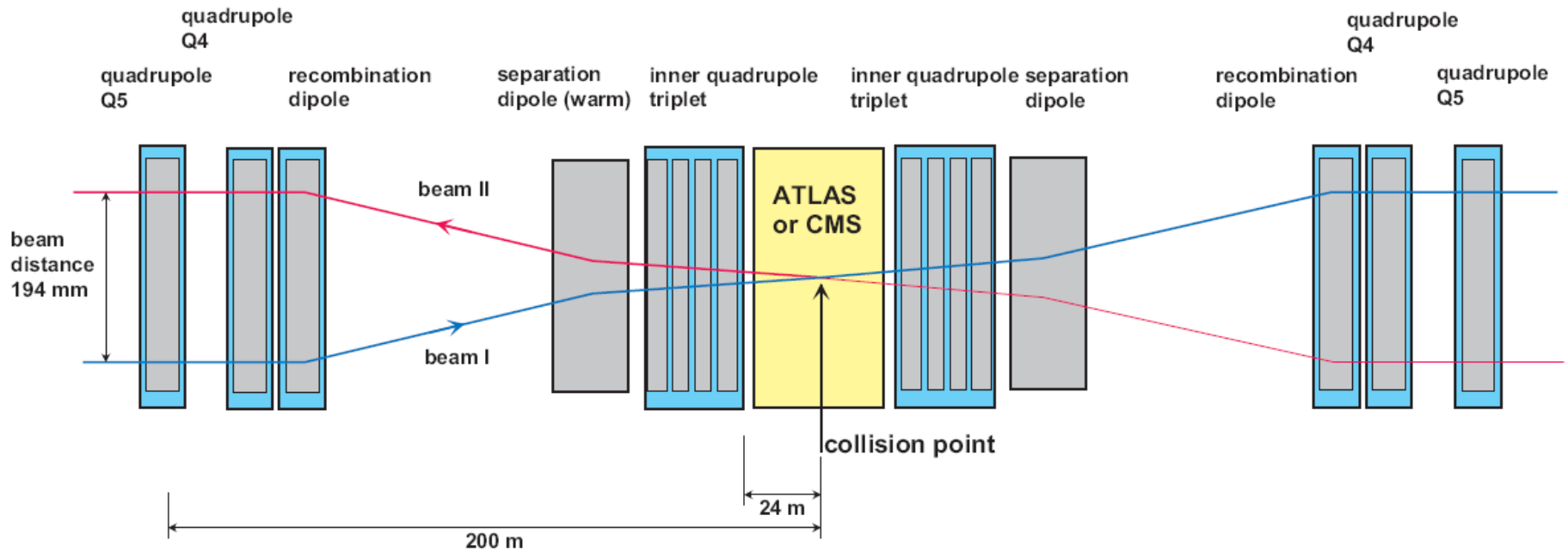
LHC collision, IP1 and IP5 only

head-on and parasitic at ± 150 μ rad



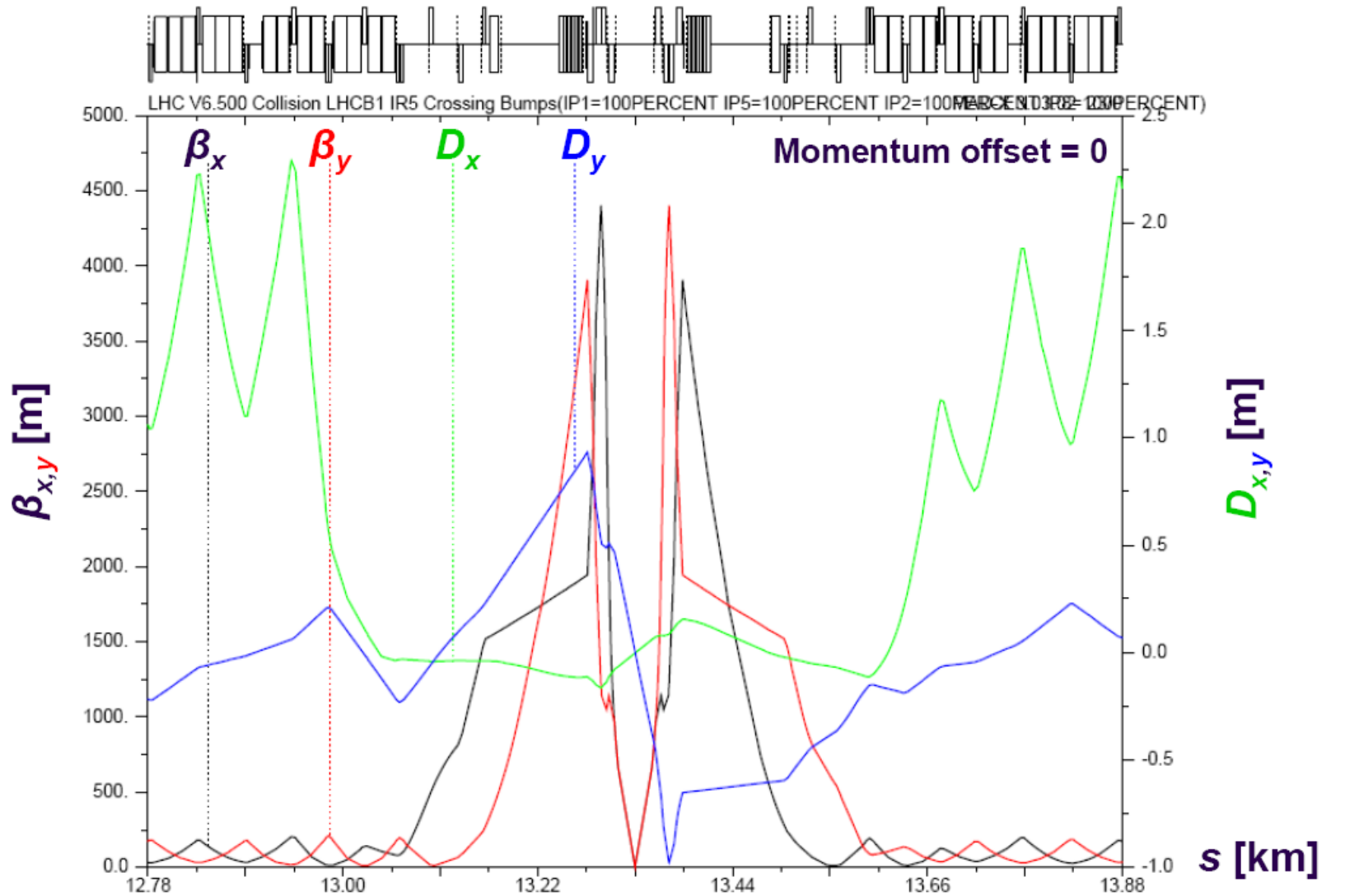


Layout of high-luminosity collision region





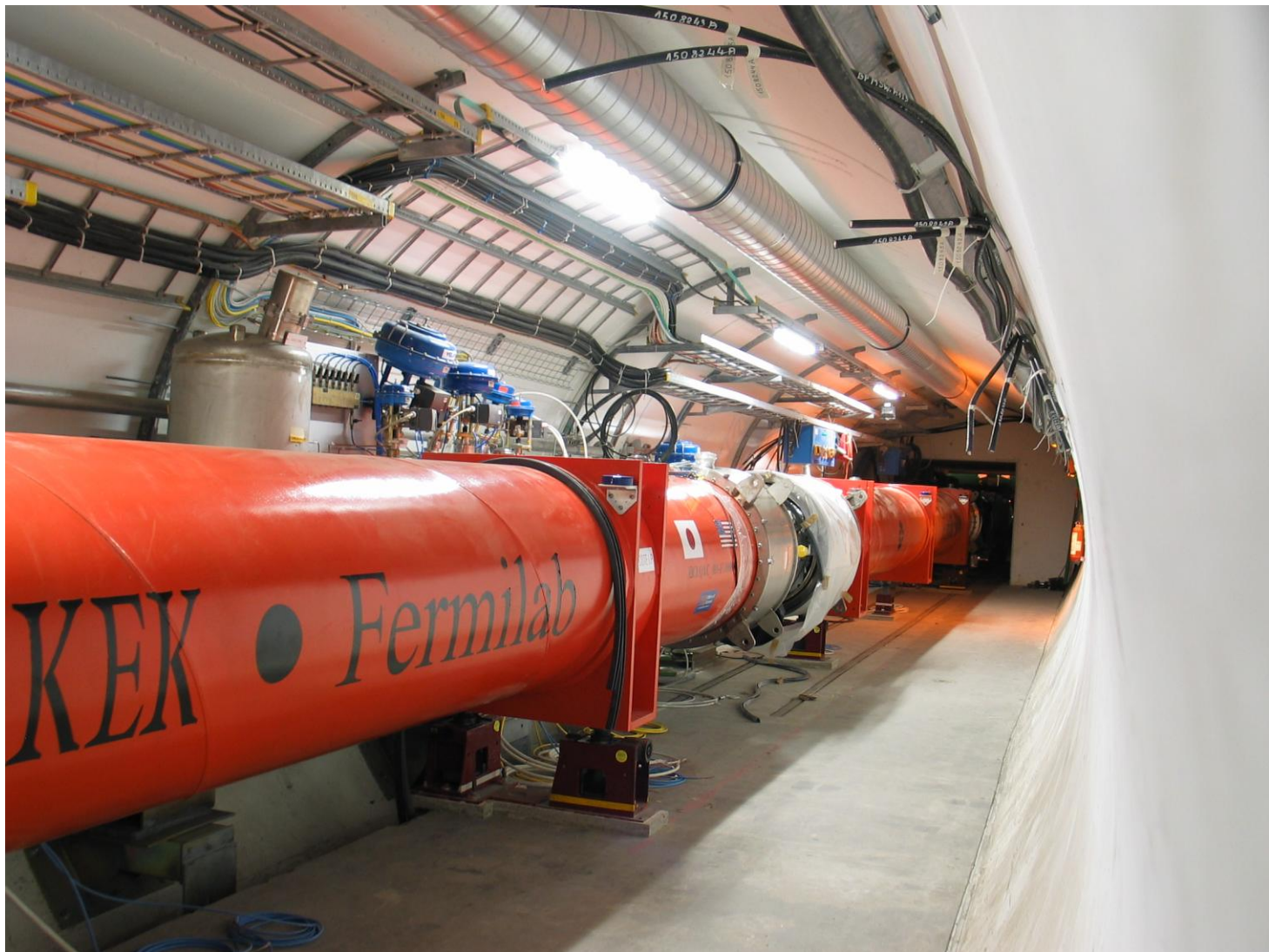
High-luminosity insertion optics





High-luminosity insertion

Inner triplet installed at LHC point 5





Luminosity lifetime

- Luminosity will decay with time due to degradation of beam intensity and emittance, by several processes
 - intra-beam scattering, i.e. multiple Coulomb scattering between particles in the same bunch
 - nuclear scattering of particles by residual gas molecules
 - the collisions themselves

~ 45 hours initially, 29 h as N_{total} and L decay $\longrightarrow \tau_{nuclear} = \frac{N_{total}}{k L \sigma_{total}}$

- Overall

$$\frac{1}{\tau_L} = \frac{1}{\tau_{IBS}} + \frac{2}{\tau_{gas}} + \frac{1}{\tau_{nuclear}}$$

~ 15 h, at least one fill per day $\longrightarrow \tau_L$

~ 80 h $\longrightarrow \tau_{IBS}$

~ 100 h, must be large w.r. to other processes $\longrightarrow \tau_{gas}$

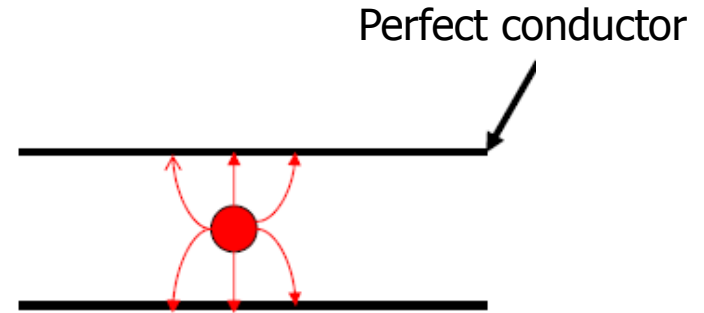
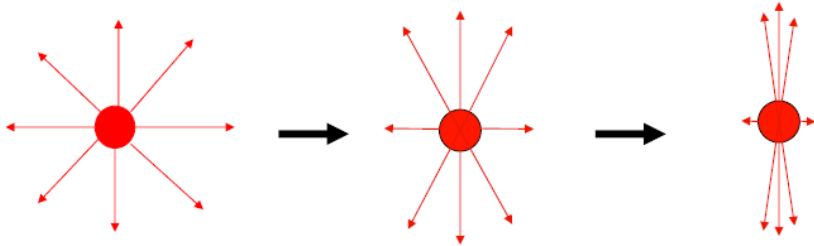
~ 29 h $\longrightarrow \tau_{nuclear}$



Contents

- The LHC in a nutshell
- **Performance**
 - Energy
 - Luminosity
 - **Collective effects**
 - Dynamic aperture
- Technology
 - Superconducting magnets
 - Powering and protection
 - Cryogenics
 - Vacuum

Beam impedance



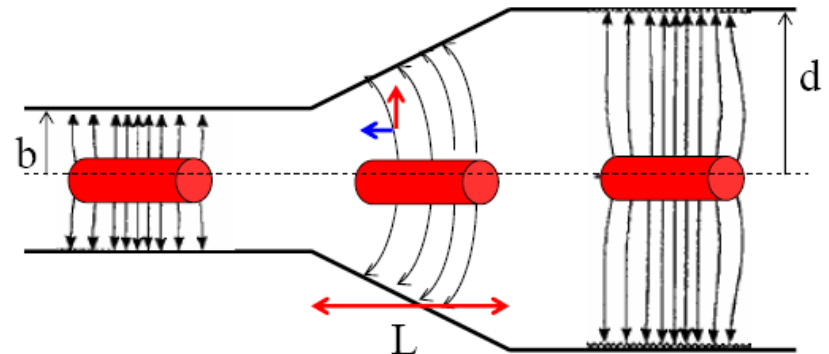
In case of resistive wall or change of cross-section, there is an interaction between the (charged) beam and the wall

⇒ energy dissipation (heating)

⇒ beam instabilities

This interaction can be described by an impedance $Z(\omega)$

Resistive wall or change of cross-section





Low transverse impedance for beam stability

- Transverse impedance

$$Z_{\perp}(\omega) \sim \rho R / \omega b^3$$

ρ wall electrical resistivity

R average machine radius

b half-aperture of beam pipe

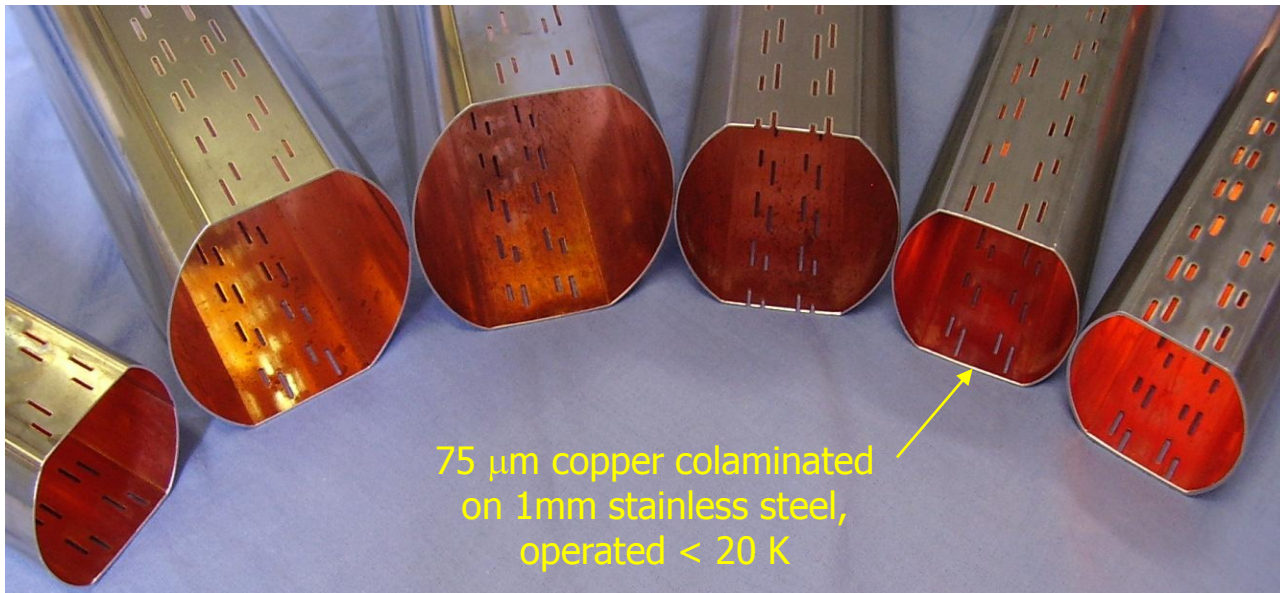
- Transverse resistive-wall instability

- dominant in large machines with small aperture

- compensated by beam feedback, provided growth is slow enough (~ 100 turns)

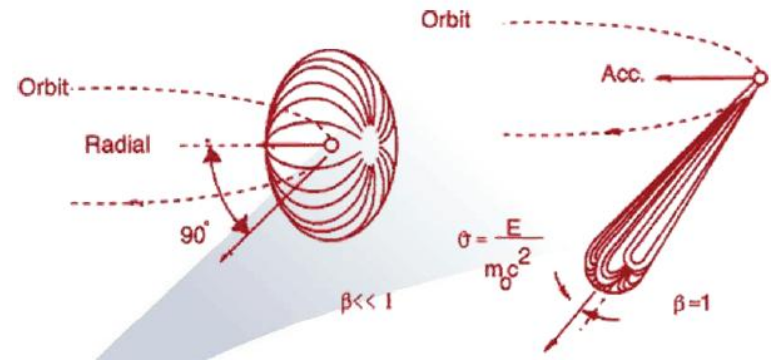
- maximize growth time $\tau \sim 1/Z_{\perp}(\omega)$ i.e. reduce $Z_{\perp}(\omega)$

\Rightarrow *low ρ , i.e. low-temperature wall coated with >0.05 mm copper*



Synchrotron radiation

- Charged particle beams bent in a magnetic field undergo centripetal acceleration and emit e-m radiation
- When beams are relativistic, radiation is emitted in a narrow cone



- Radiated power

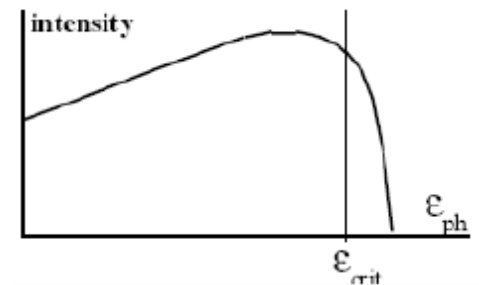
Free space impedance

$$P_{syn} = \frac{Z_0 e^2 c \gamma^4}{3 R} N_b n_b f_{rev} \sim \text{beam current}$$

Bending radius

- Critical photon energy

$$u_c = \frac{3}{2} \hbar c \frac{\gamma^3}{R}$$

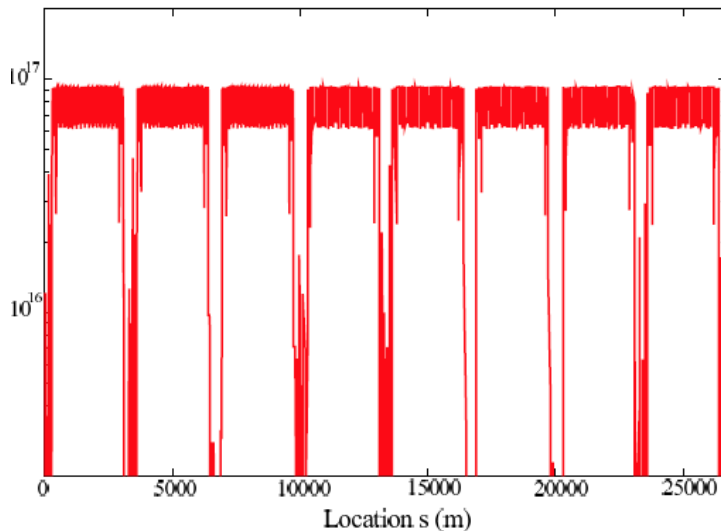




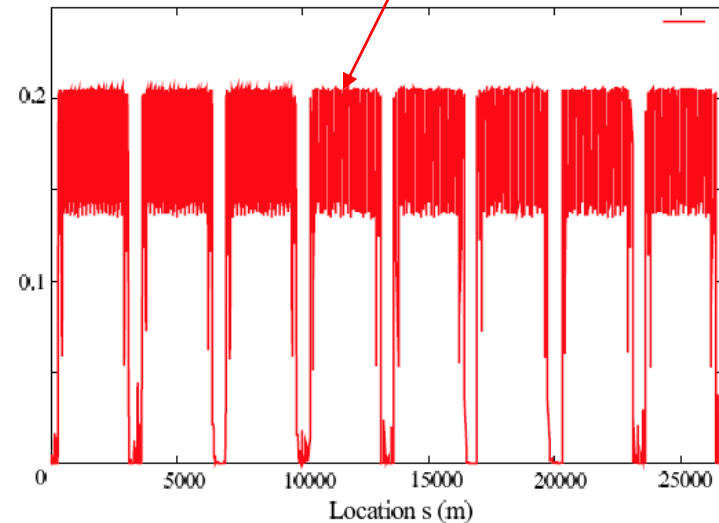
Synchrotron radiation

parameter	450 GeV	7 TeV	
total power / beam	0.066 W	3886 W	large at low T
energy loss per turn	0.11 eV	6.7 keV	
average photon flux per metre and second	0.4×10^{16}	6.8×10^{16}	
photon critical energy	0.01 eV	43.13 eV	UV, easy to screen
longit. emittance damping time	5.5 yr	12.9 h	
transv. emittance damping time	11 yr	26 h	

Photon Flux on Wall (s⁻¹ m⁻²)



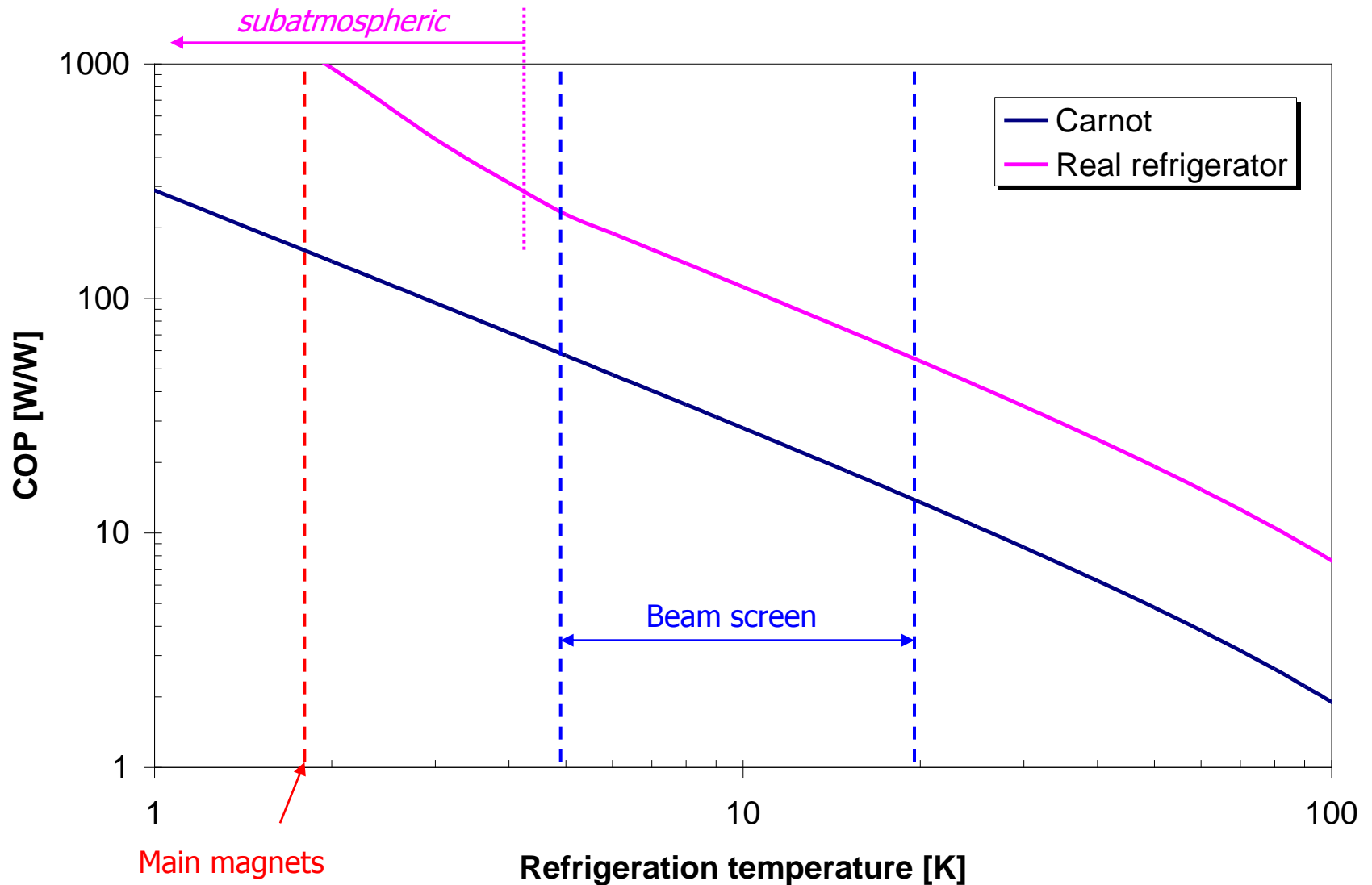
Heat Load (W/m)



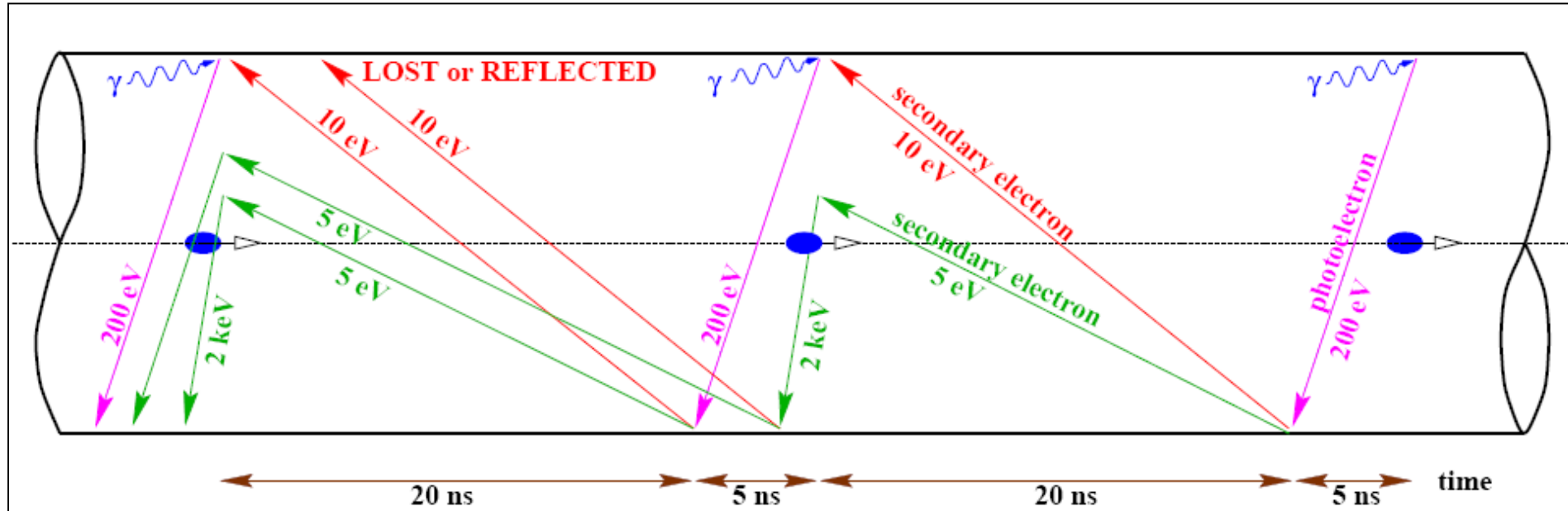


COP of cryogenic refrigeration & beam screen

Intercepting beam-induced heating at higher temperature



The electron cloud effect



Resonant acceleration of electrons extracted from the wall (photo-electrons and secondary electrons), by the electrical field of the successive bunches.

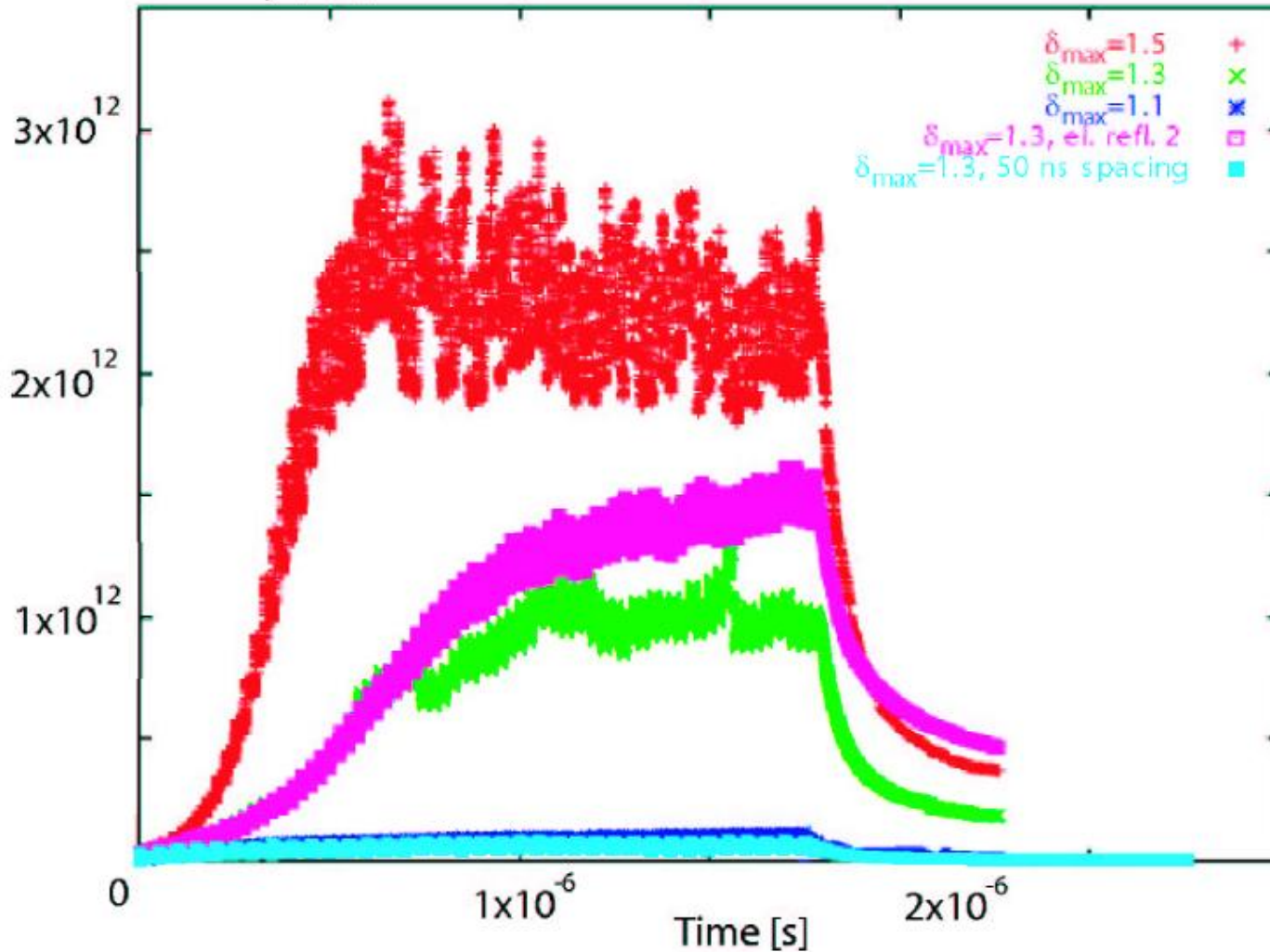
Governed by:

- photon irradiation of the wall \Rightarrow *low reflectivity surface*
- bunch repetition rate \Rightarrow *increase bunch spacing*
- secondary electron yield \Rightarrow *low-SEY surface and beam cleaning*



Simulated build-up of electron cloud, for different values of SEY

Volume Density [m^{-3}]

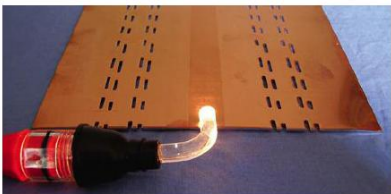
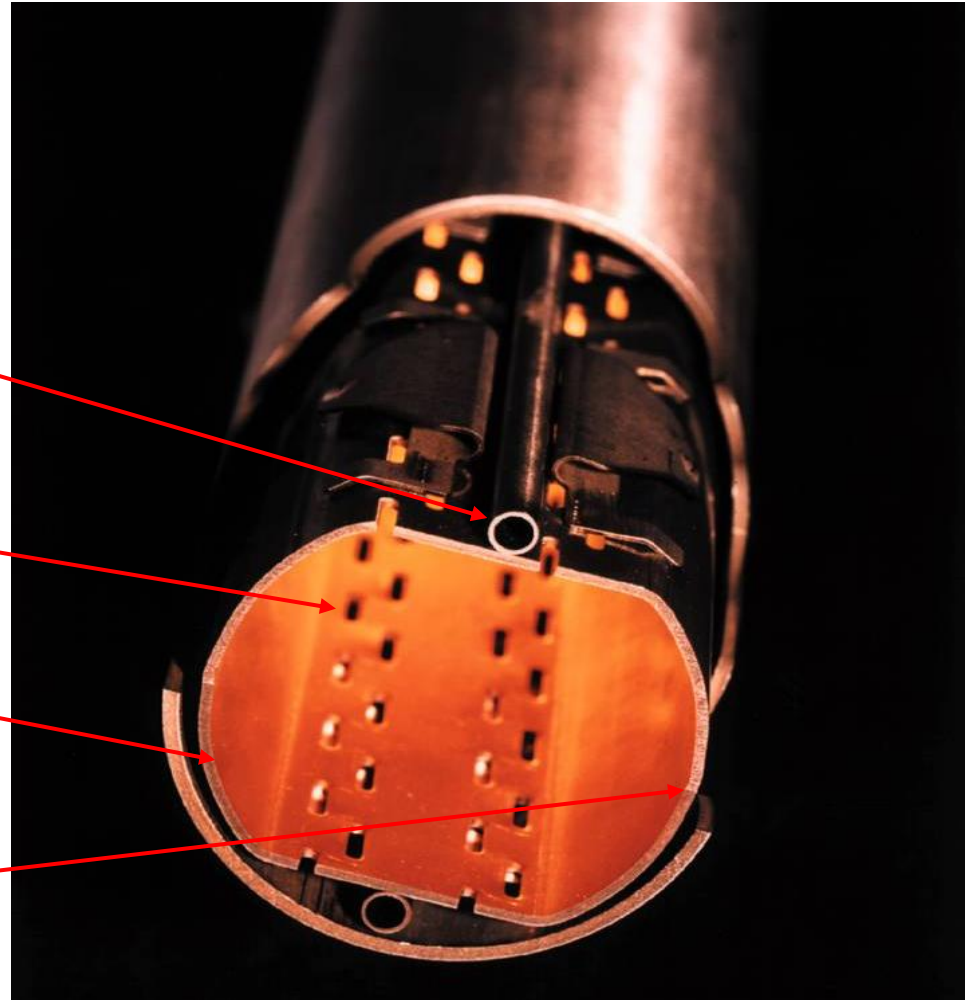




The beam screen

A multi-function component required by beam physics

- Interception of beam-induced heat loads at 5-20 K (supercritical helium)
- Shielding of the 1.9 K cryopumping surface from synchrotron radiation (pumping holes)
- High-conductivity copper lining for low beam impedance
- Low-reflectivity sawtooth surface at equator to reduce photoemission and electron cloud



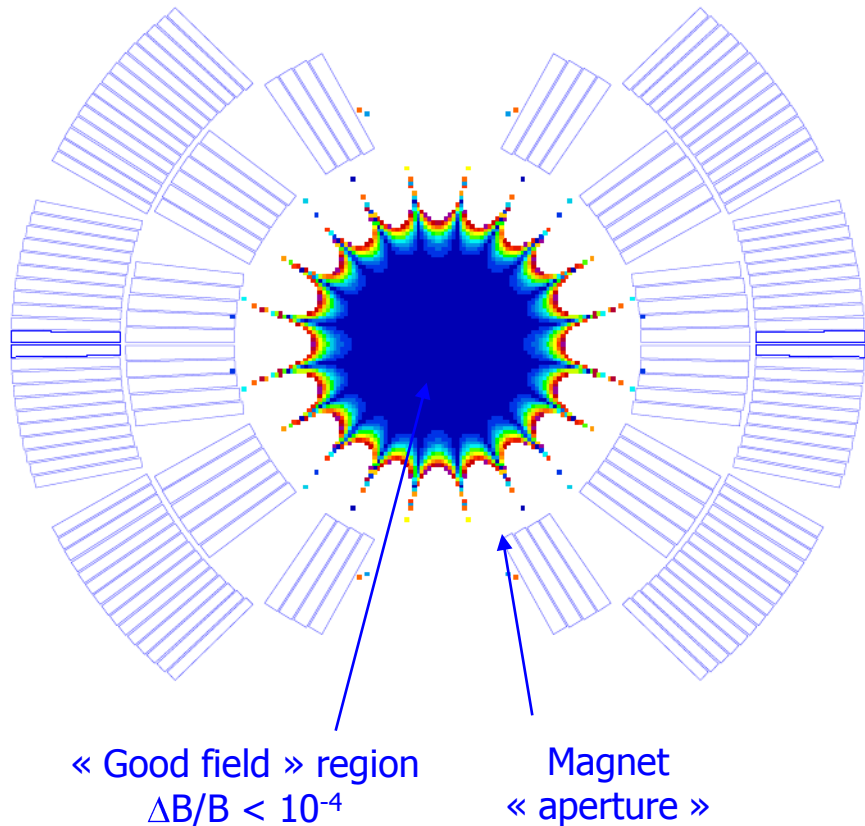


Contents

- The LHC in a nutshell
- **Performance**
 - Energy
 - Luminosity
 - Collective effects
 - **Dynamic aperture**
- Technology
 - Superconducting magnets
 - Powering and protection
 - Cryogenics
 - Vacuum



Field quality in superconducting magnets

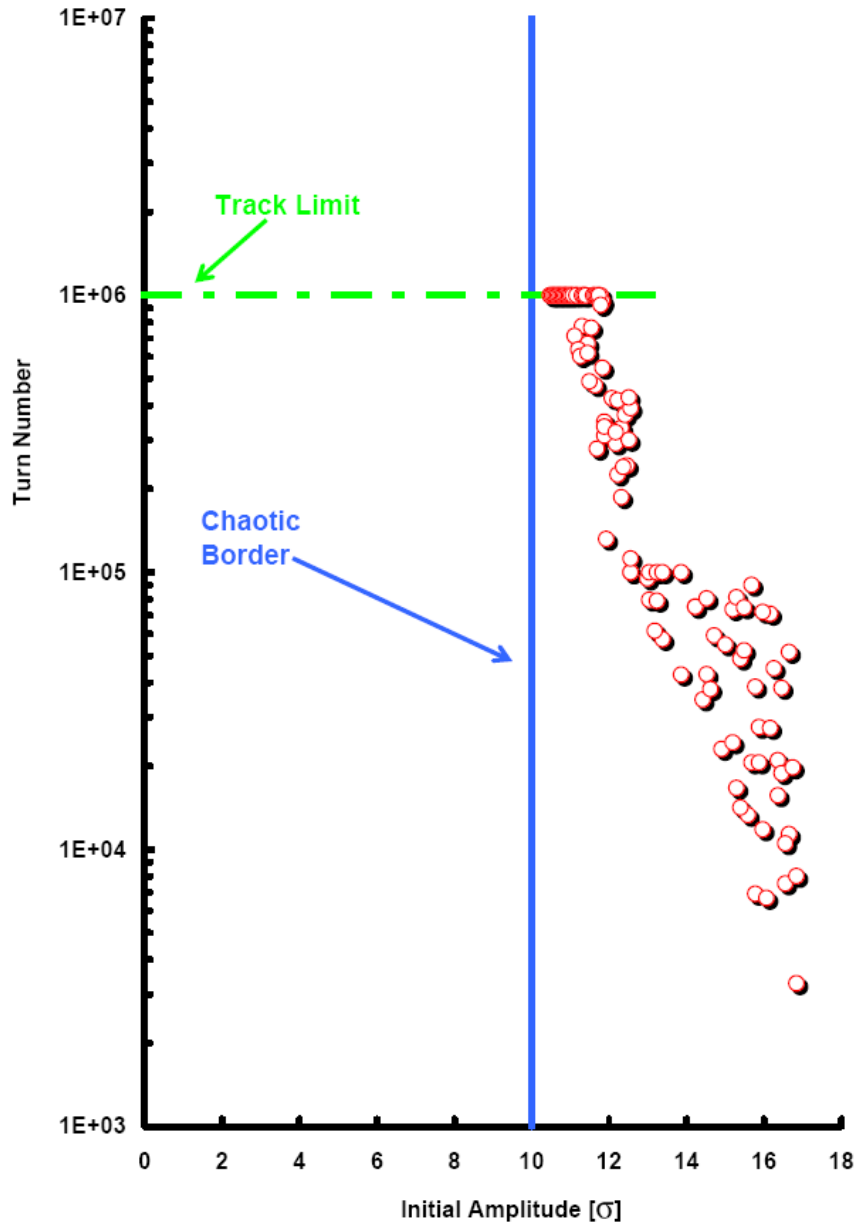


- In superconducting magnets, the field quality is determined by the positioning precision of a finite number of conductors and not by the geometry of the iron yoke, so it can never be as good as in conventional “iron-dominated” magnets
- As a consequence, the « good field » region is substantially smaller than the magnet aperture
- **Dynamic aperture** = aperture inside which particle orbits are stable
- Dynamic aperture estimated by computer « tracking » of particle orbits around virtual machines with distributed random and systematic imperfections
- Tracking results are used to define maximum systematic and random deviations of each field multipole

$$B_y + iB_x = B_1 \sum_{n=1}^{\infty} (b_n + ia_n) \left(\frac{x + iy}{r_{ref}} \right)^{n-1}$$



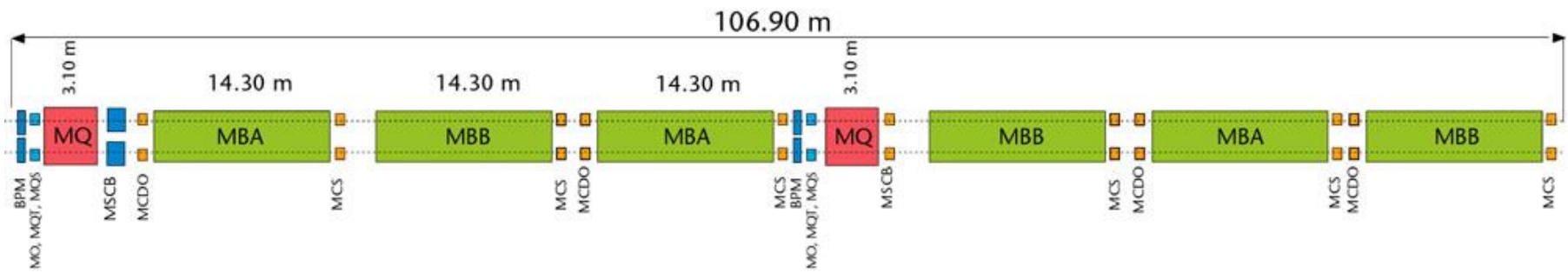
Dynamic aperture from tracking simulations



From tracking simulations to real d.a.

Source or Uncertainty	Impact	D.A. in σ
Target for tracking 10^5 turns		12
Finite mesh size	-5%	
Linear Imperfections ^a	-5%	
Amplitude ratio x_i/y_i plane	-5%	
Extrapolation to $4 \cdot 10^7$ turns	-7%	9.4
Time dependent multipoles	-10%	
Ripple	-10%	7.5
safety margin	-20%	6.0

Schematic layout of one LHC cell (23 periods per arc)



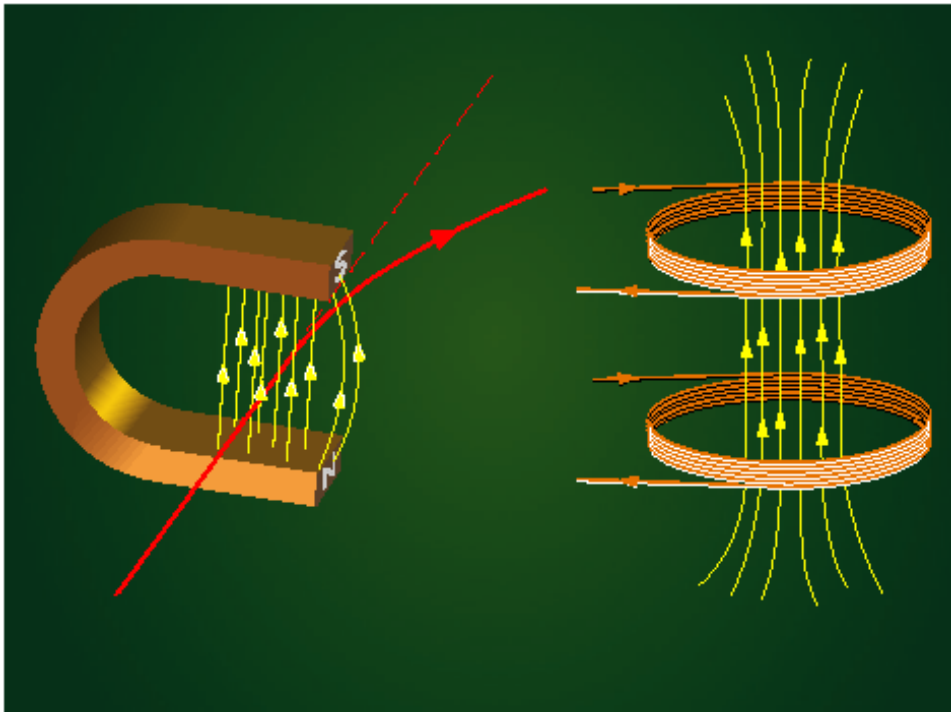
- MQ: Lattice Quadrupole
- MO: Landau Octupole
- MQT: Tuning Quadrupole
- MQS: Skew Quadrupole
- MSCB: Combined Lattice Sextupole (MS) or skew sextupole (MSS) and Orbit Corrector (MCB)
- BPM: Beam position monitor
- MBA: Dipole magnet Type A
- MBB: Dipole magnet Type B
- MCS: Local Sextupole corrector
- MCDO: Local combined decapole and octupole corrector



Contents

- › The LHC in a nutshell
- › Performance
 - Energy
 - Luminosity
 - Collective effects
 - Dynamic aperture
- **Technology**
 - **Superconducting magnets**
 - Powering and protection
 - Cryogenics
 - Vacuum

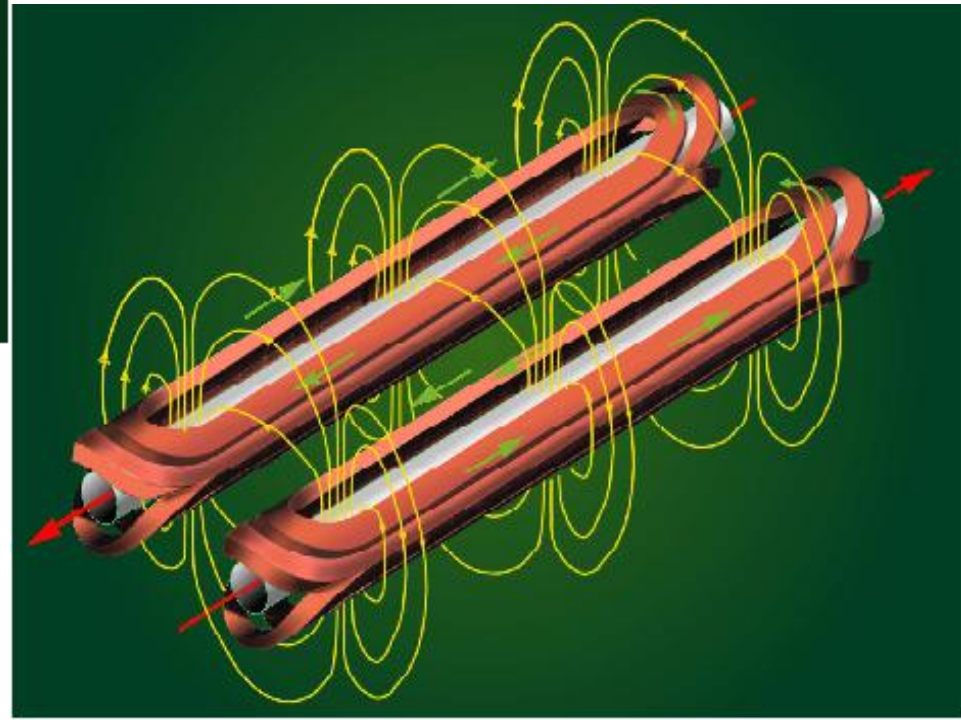
Superconducting accelerator magnets



In a superconducting magnet, the field level and geometry is basically given by the current distribution in the coils

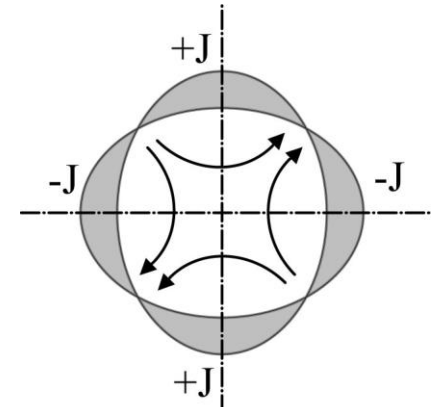
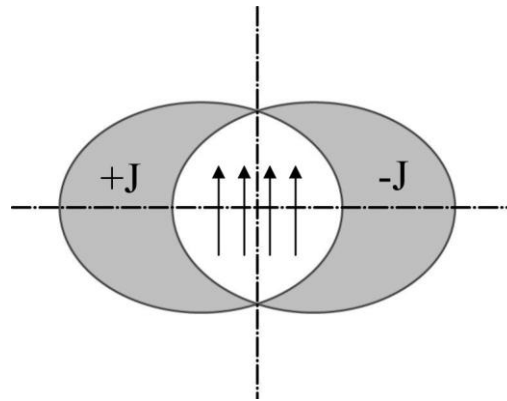
To match the geometry of the beam tubes, the coils are saddle-shaped & elongated

In the LHC, two sets of coils create opposite fields in the neighbouring apertures

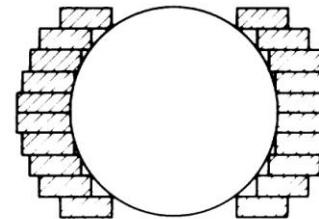
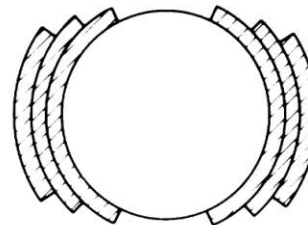
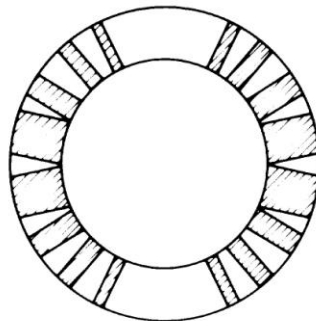
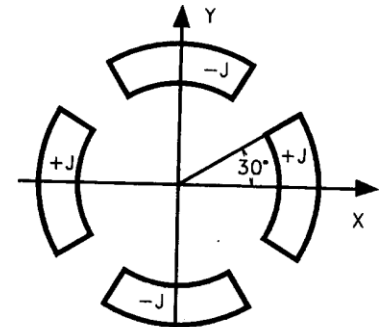
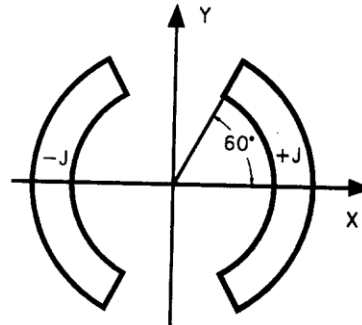


Current distributions

Two intersecting ellipses with uniform current density generate uniform dipole and quadrupole fields \Rightarrow "cos θ " geometry



In practice, this can be approximated by current sheets, leading to "block" or "layer" coil designs



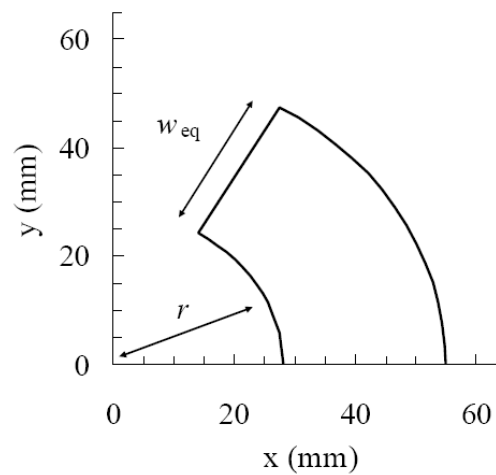
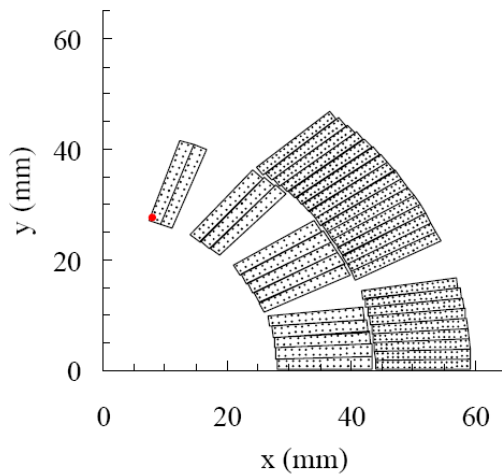


Field of single-layer dipole coil

$$B = \frac{\mu_0 \sqrt{3}}{\pi} \mathbf{j}_{tech} w$$

Average current density in coil

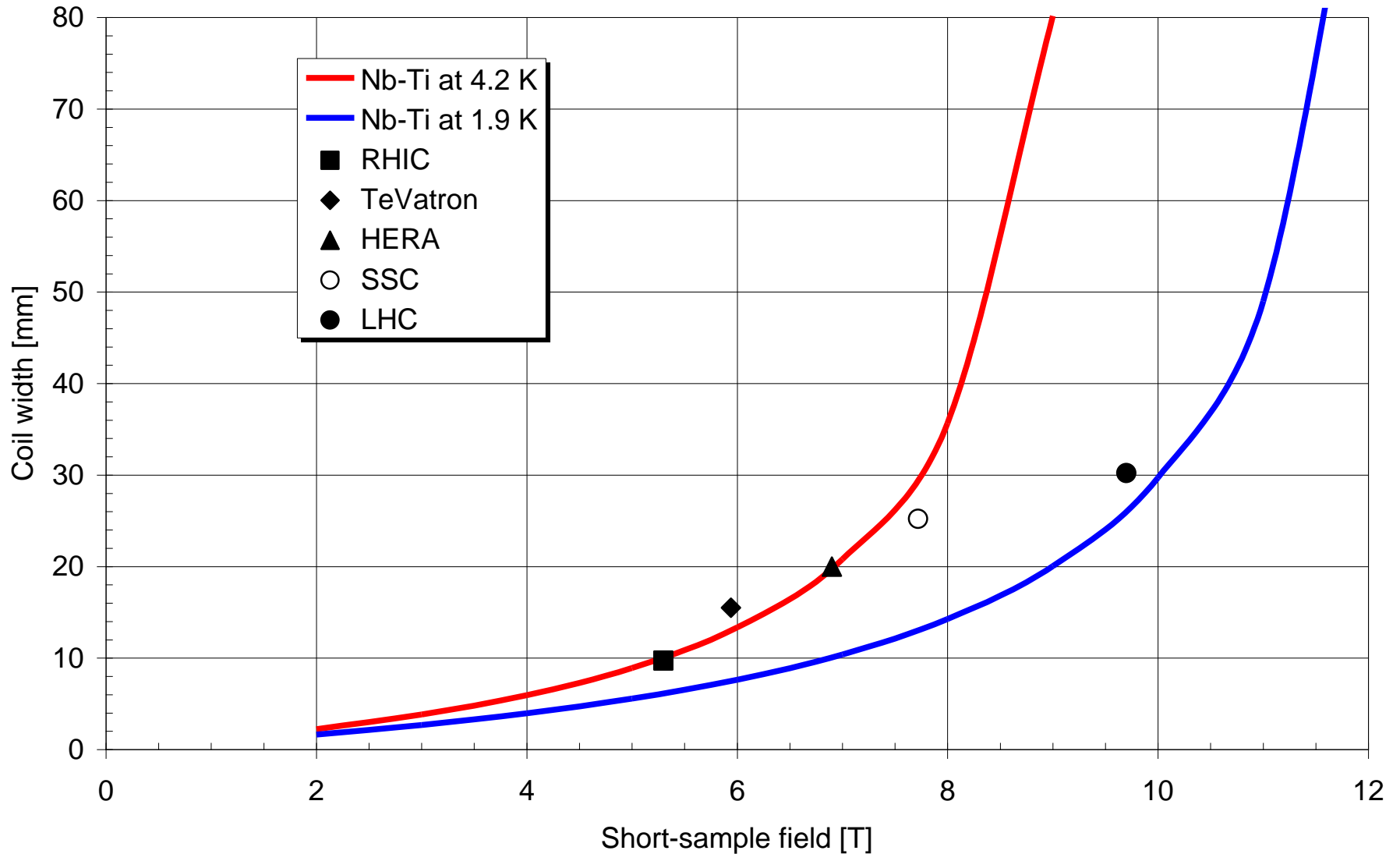
Coil width





Superconducting $\cos \theta$ dipoles in Nb-Ti

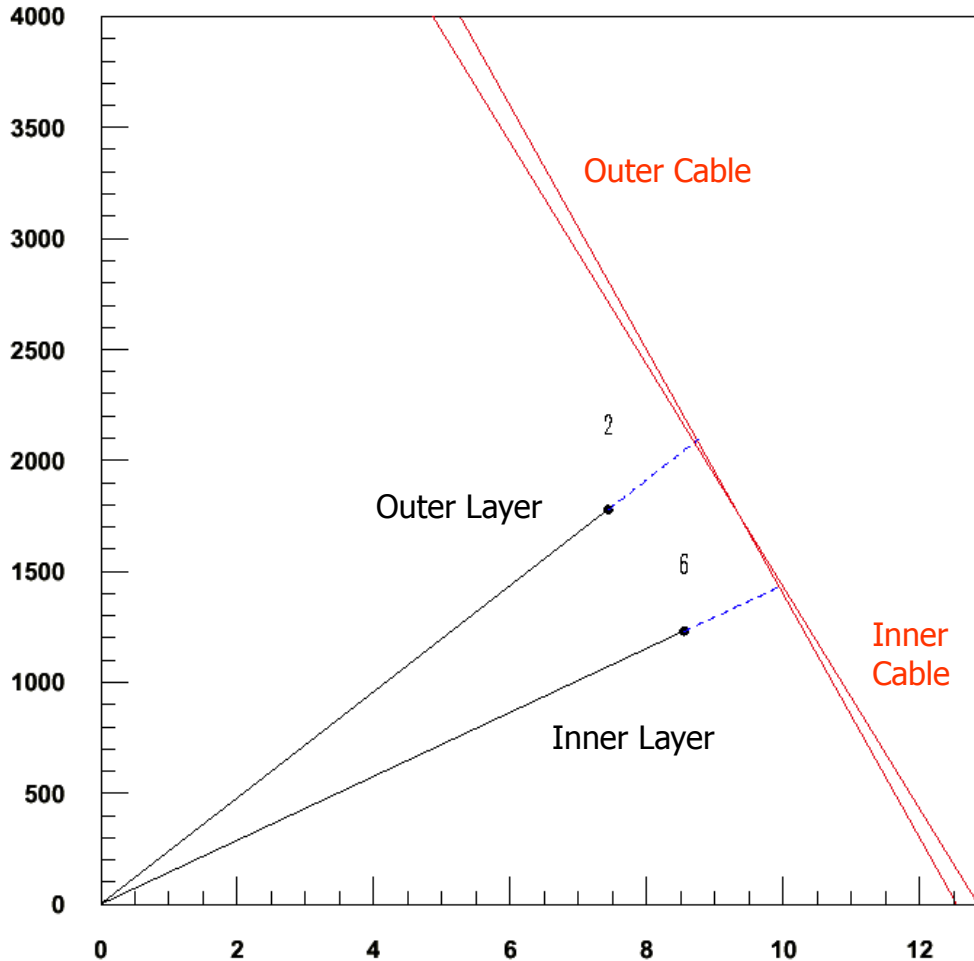
Coil width vs field



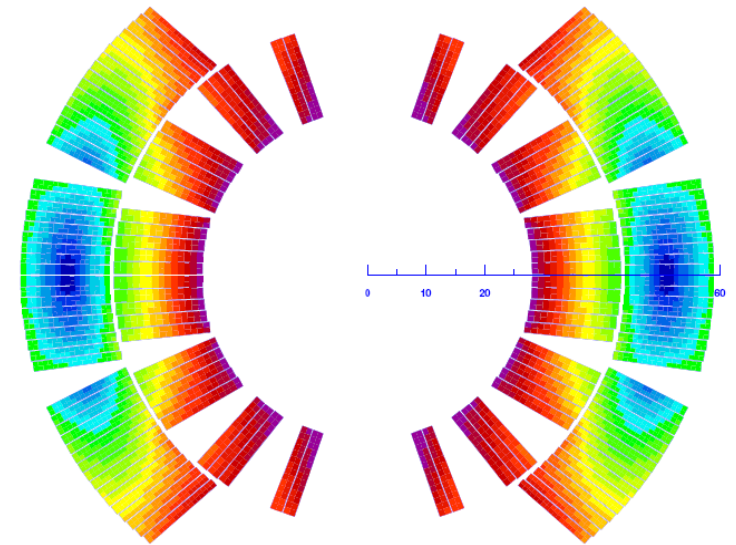


Load lines of LHC main dipole

J [A/mm²]



B_{peak} [T]



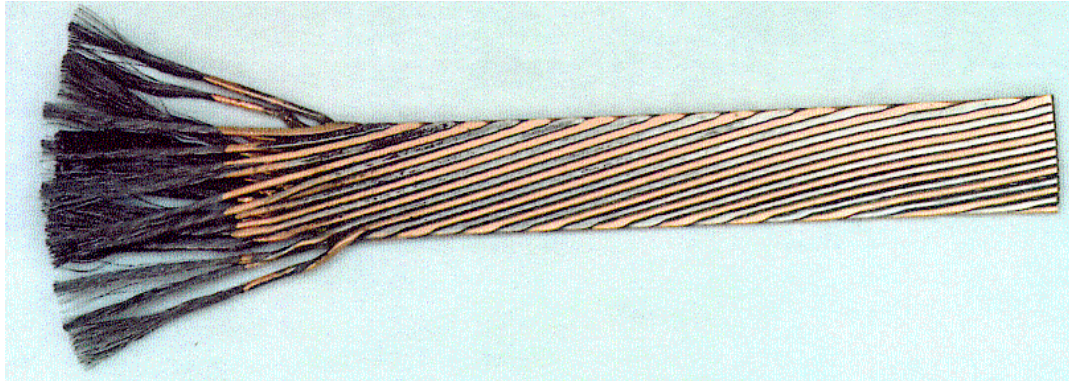
Current grading permits the outer cable, which sees a lower field, to operate at higher current density

Inter-layer splice in graded coil





7500 km of high-performance superconducting cable



Cable with etched strands showing Nb-Ti filaments

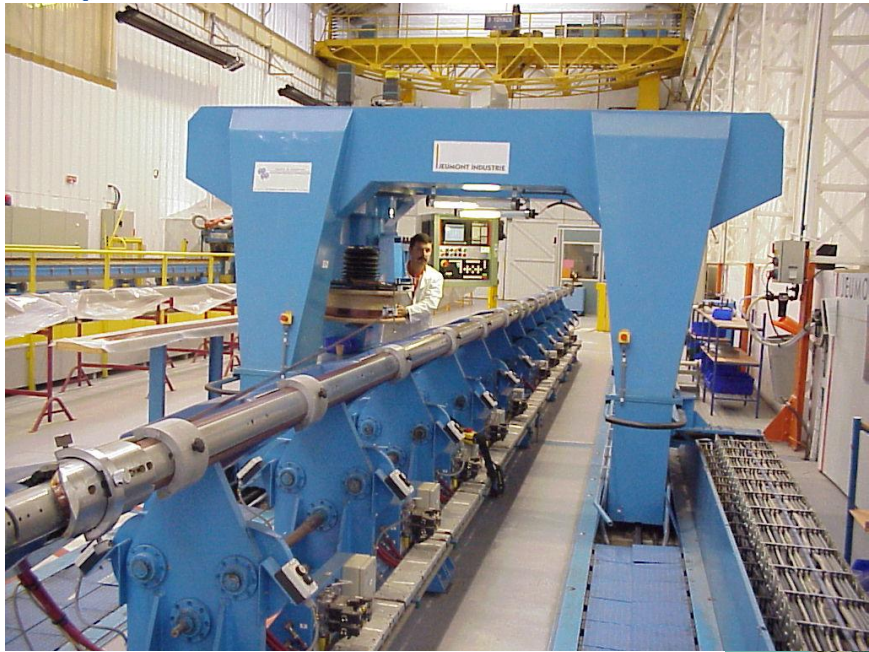
Cable insulation by double polyimide wrap

	Inner Cable	Outer Cable
Number of strands	28	36
Strand diameter	1.065 mm	0.825 mm
Filament diameter	7 μm	6 μm
Number of filaments	~ 8900	~ 6520
Cable width	15.1 mm	15.1 mm
Mid-thickness	1.900 mm	1.480 mm
Keystone angle	1.25	0.90
Transposition length	115 mm	100 mm
Ratio Cu/Sc	≥ 1.6	≥ 1.9

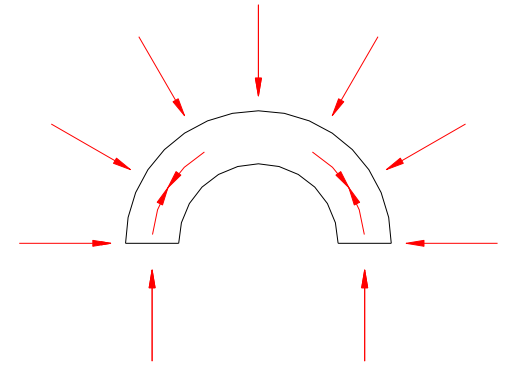
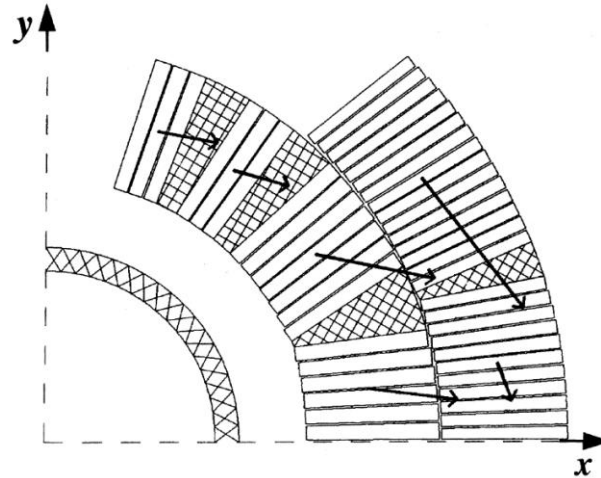
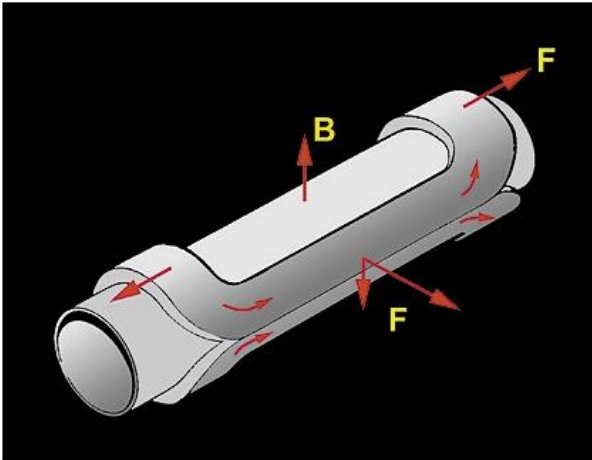




Manufacturing of superconducting coils



Electromagnetic forces



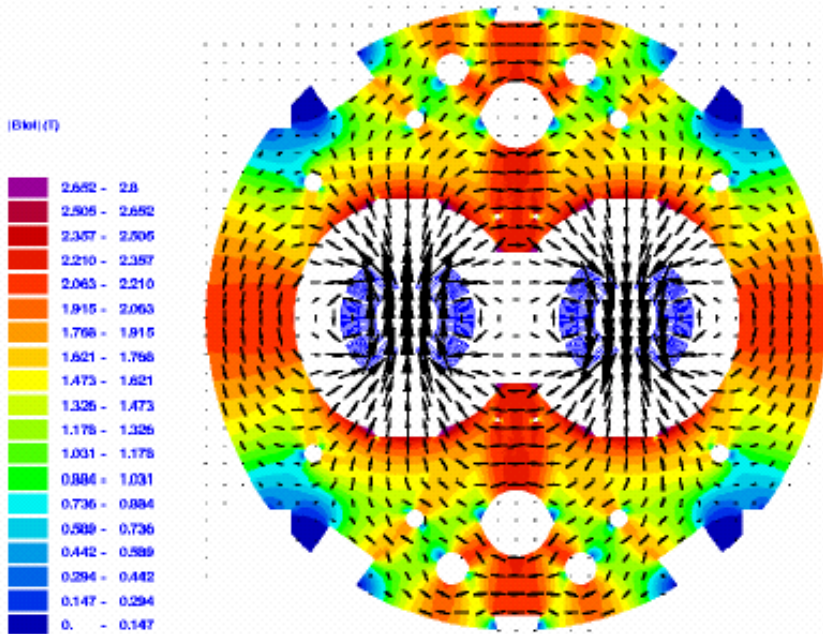
High magnetic field acting on high current generates large **electromagnetic forces** at right angle, which cannot be resisted by the mechanical strength of the conductor: saddle-shaped coils of accelerator magnets are not self-supporting

$$B = 10 \text{ T}, I = 10 \text{ kA} \Rightarrow 10^5 \text{ N/m per turn !}$$

⇒ **“roman arch”** coil geometry to contain the azimuthal component

⇒ external **support structure** against the radial component

Twin-aperture dipole magnet



Limited transverse space in tunnel \Rightarrow **compact** cross-section

Flux closure within twin magnet yoke \Rightarrow **magnetically efficient** design, limited stray field

Stainless steel collars resting on iron yoke inside preshrunk cylindrical shell \Rightarrow **rigid** structure



Assembly of dipole cold masses





Final assembly of cryomagnets at CERN



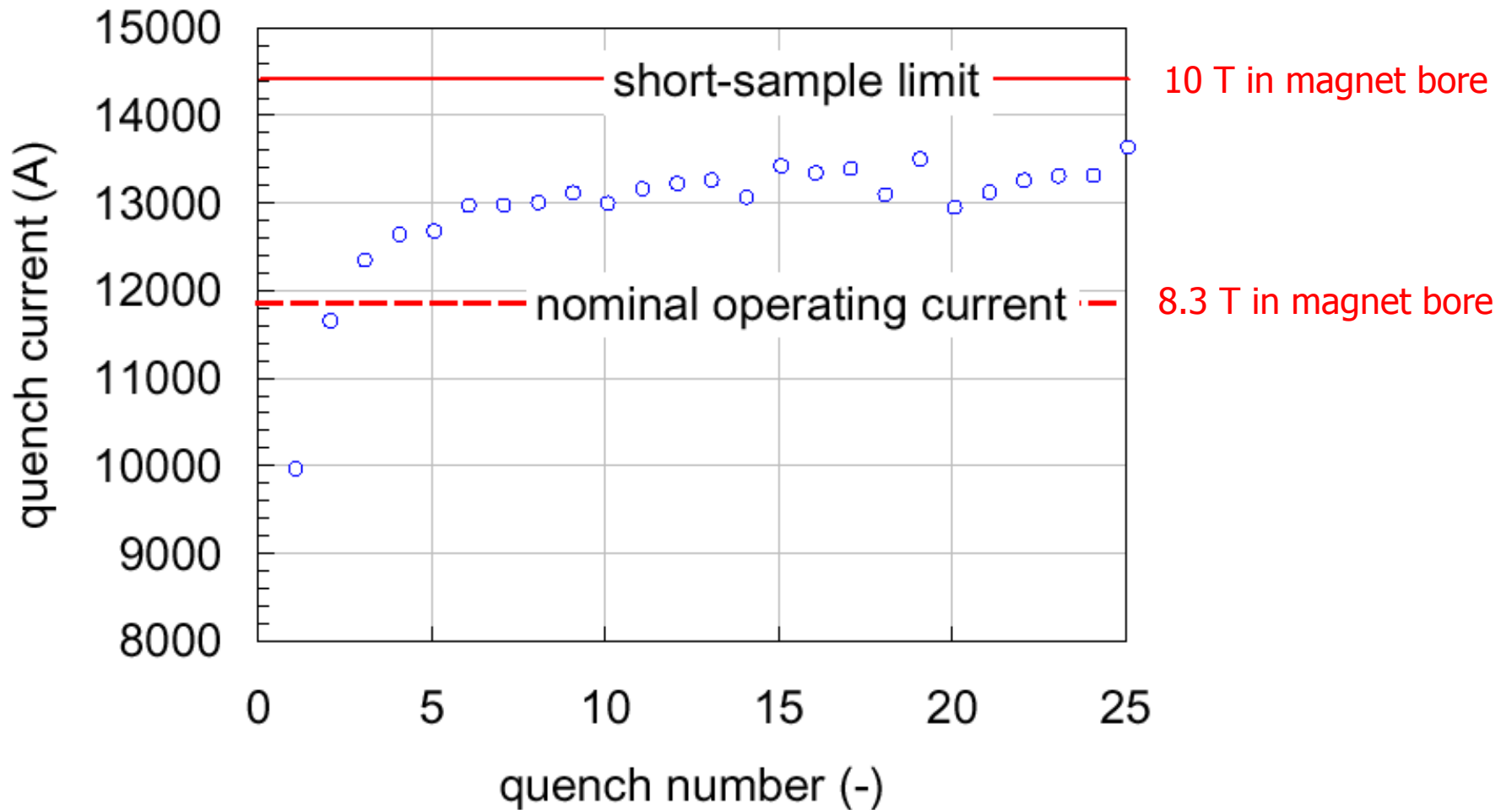


Cryogenic tests of magnets



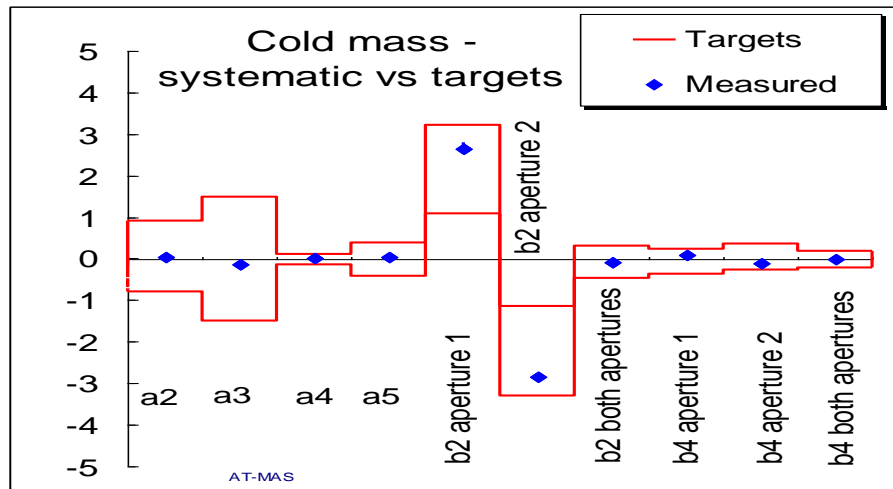
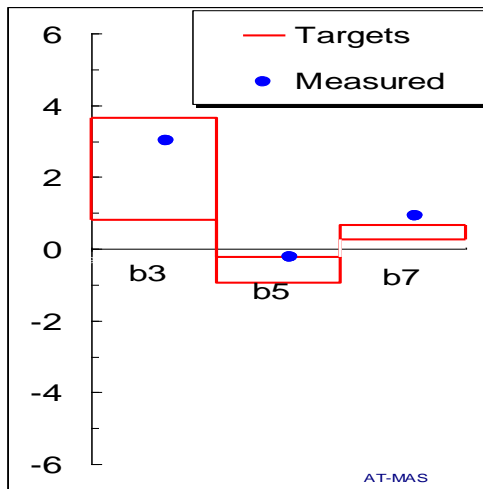
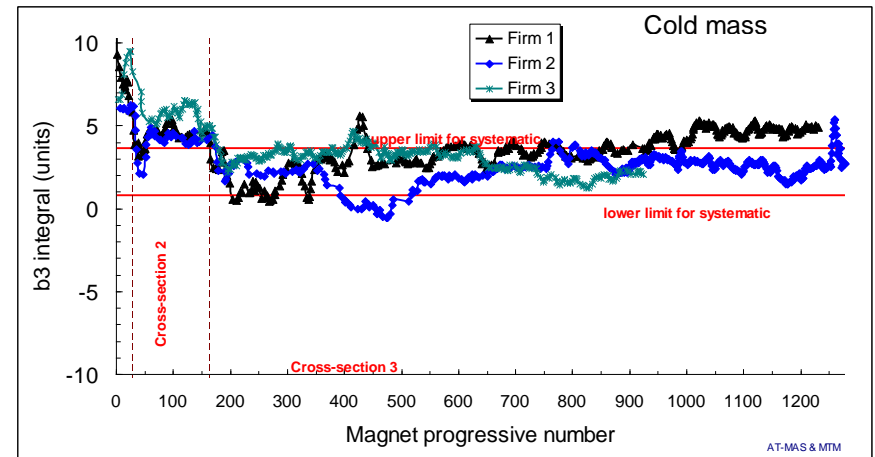
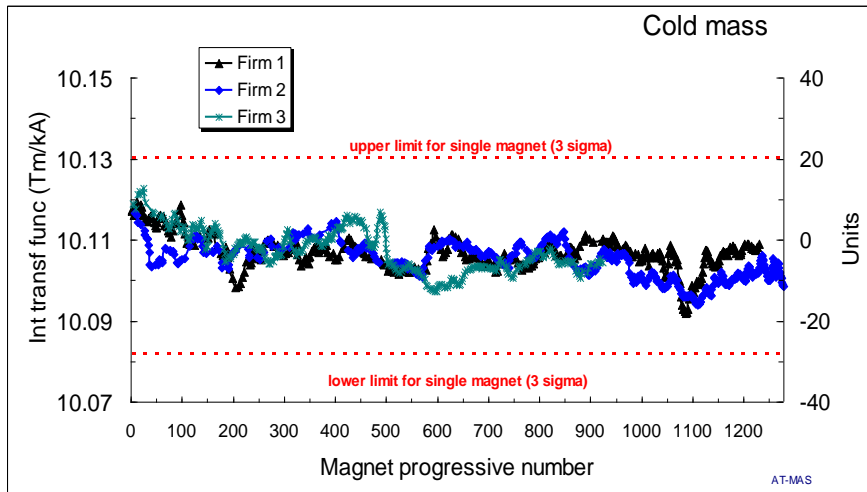


Training of superconducting magnets



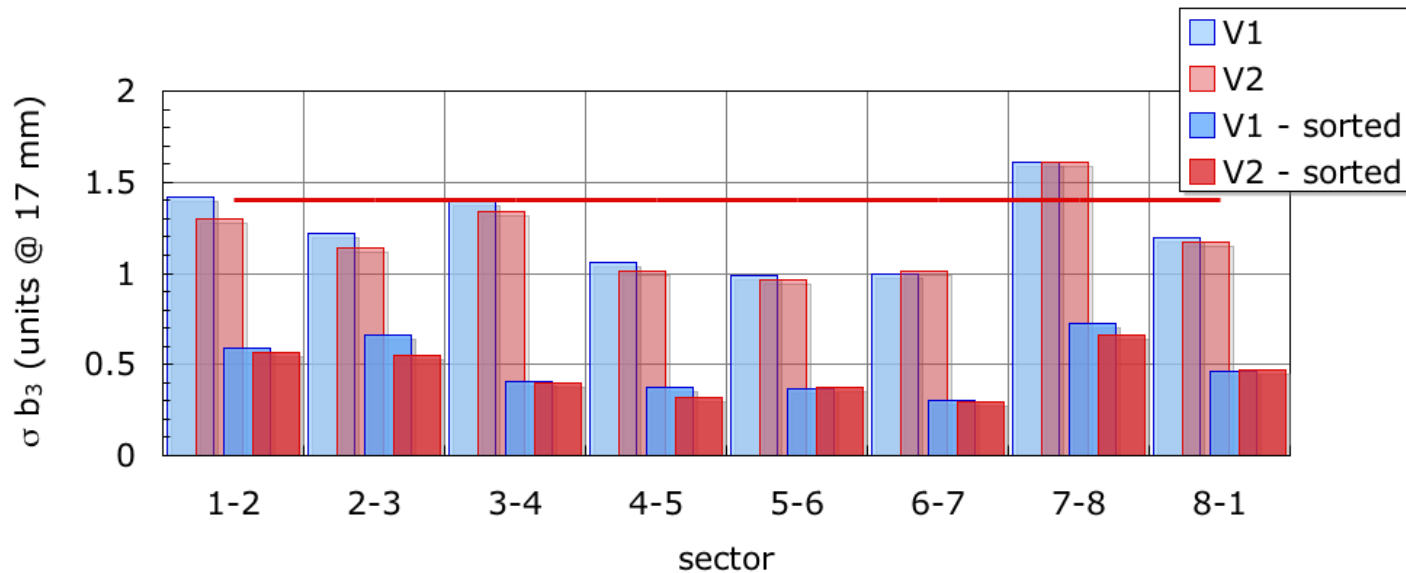
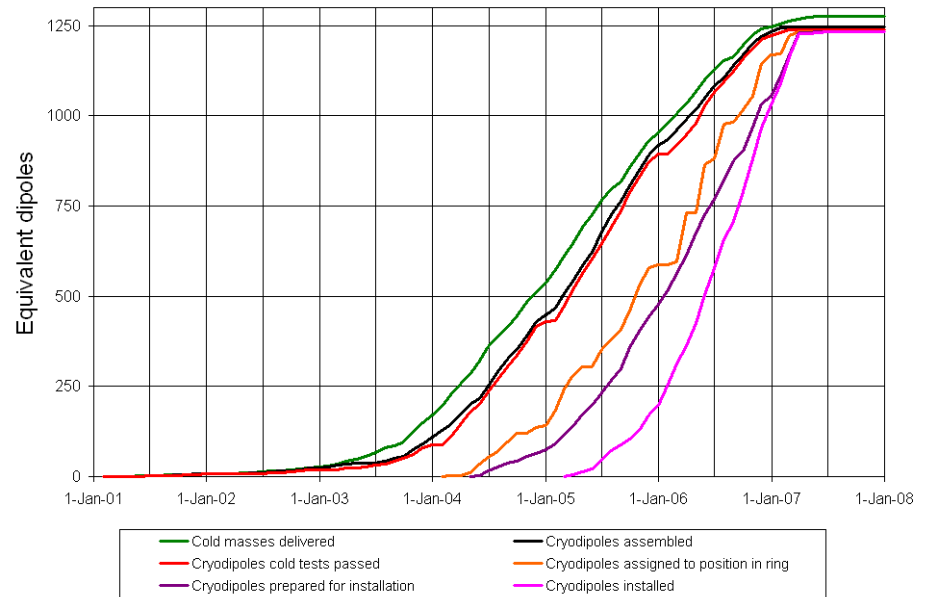


Dipole field quality in series production



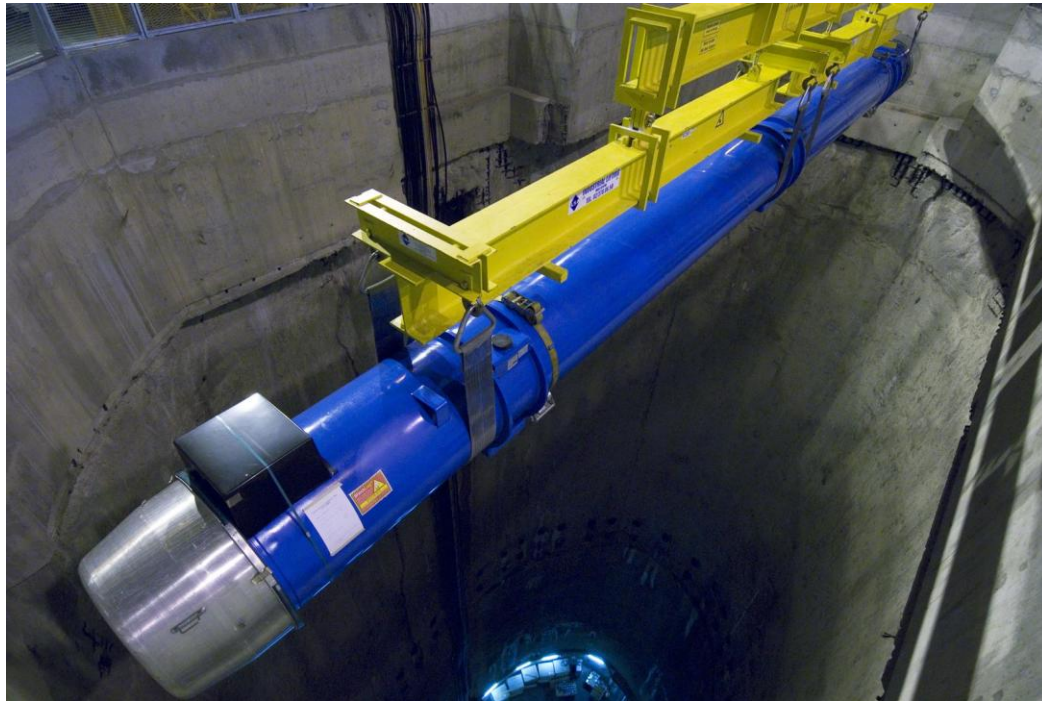


Buffer storage allows sorting, reduces dispersion

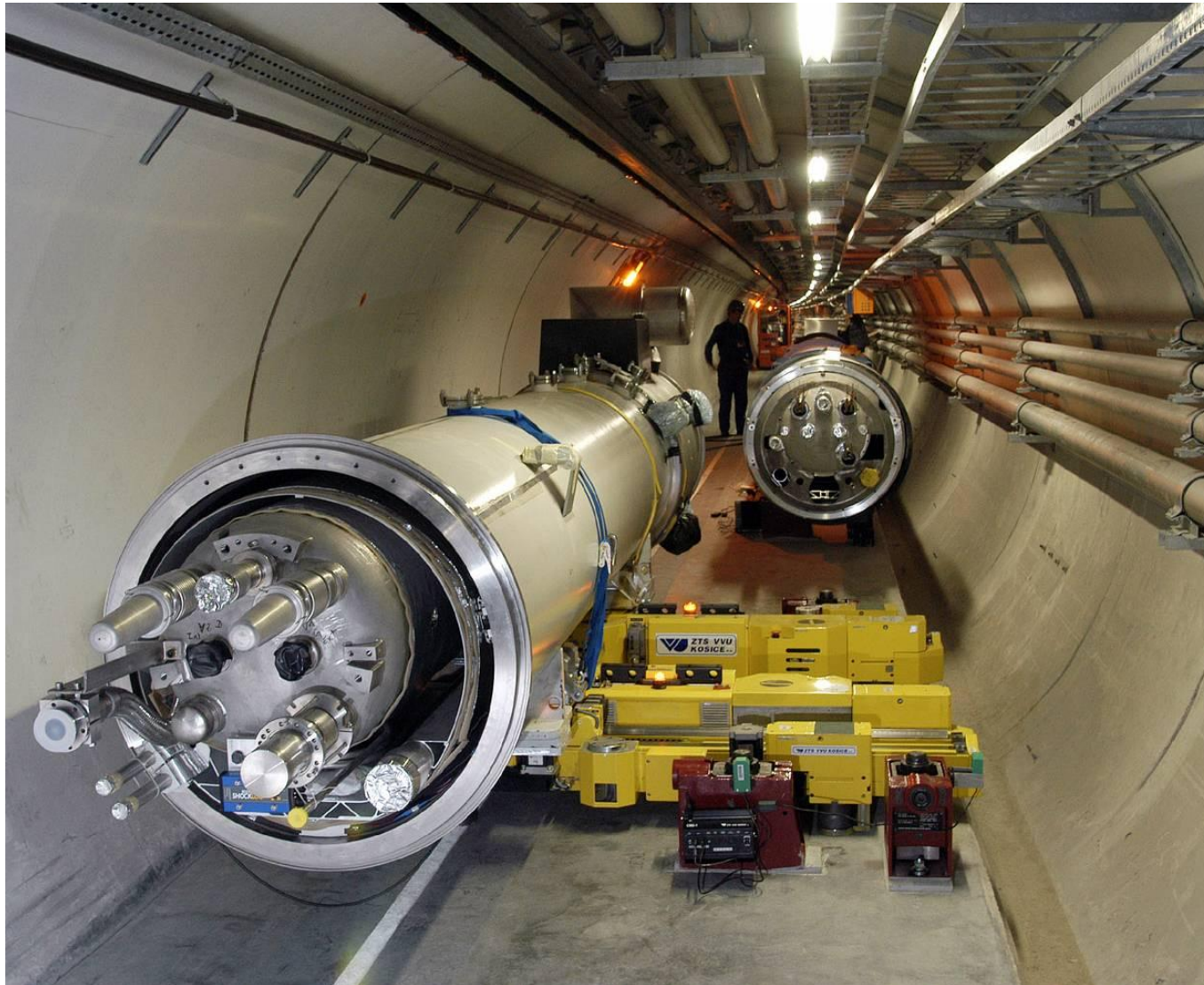




Lowering of magnets in tunnel



Cryomagnet installation in tunnel





Interconnections in tunnel

65'000 electrical joints

Induction-heated soldering

Ultrasonic welding

Very low residual resistance

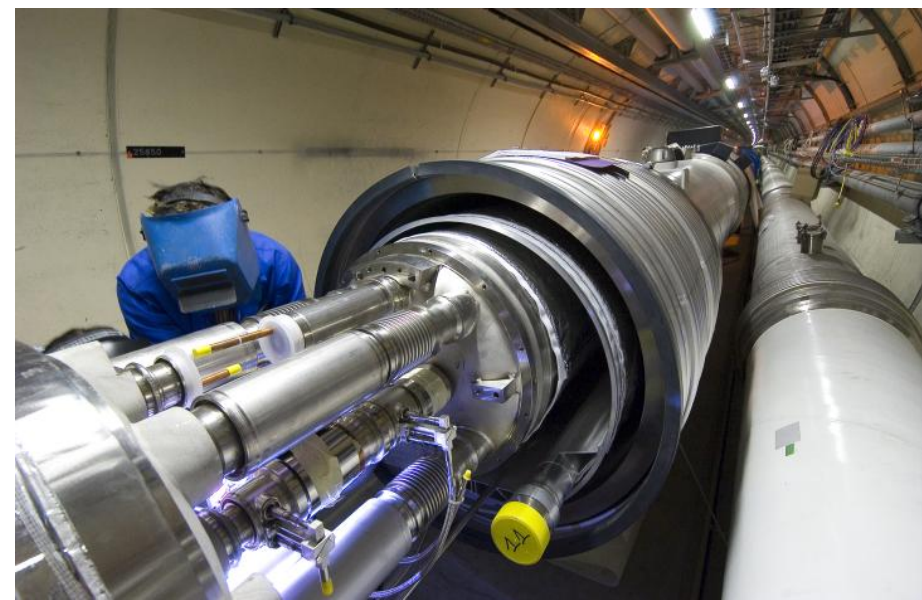
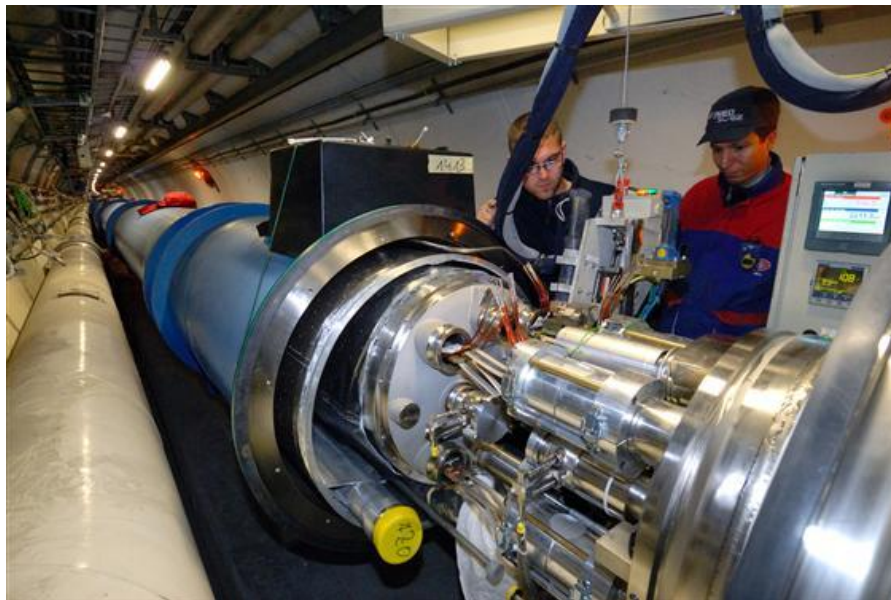
HV electrical insulation

40'000 cryogenic junctions

Orbital TIG welding

Weld quality

Helium leaktightness



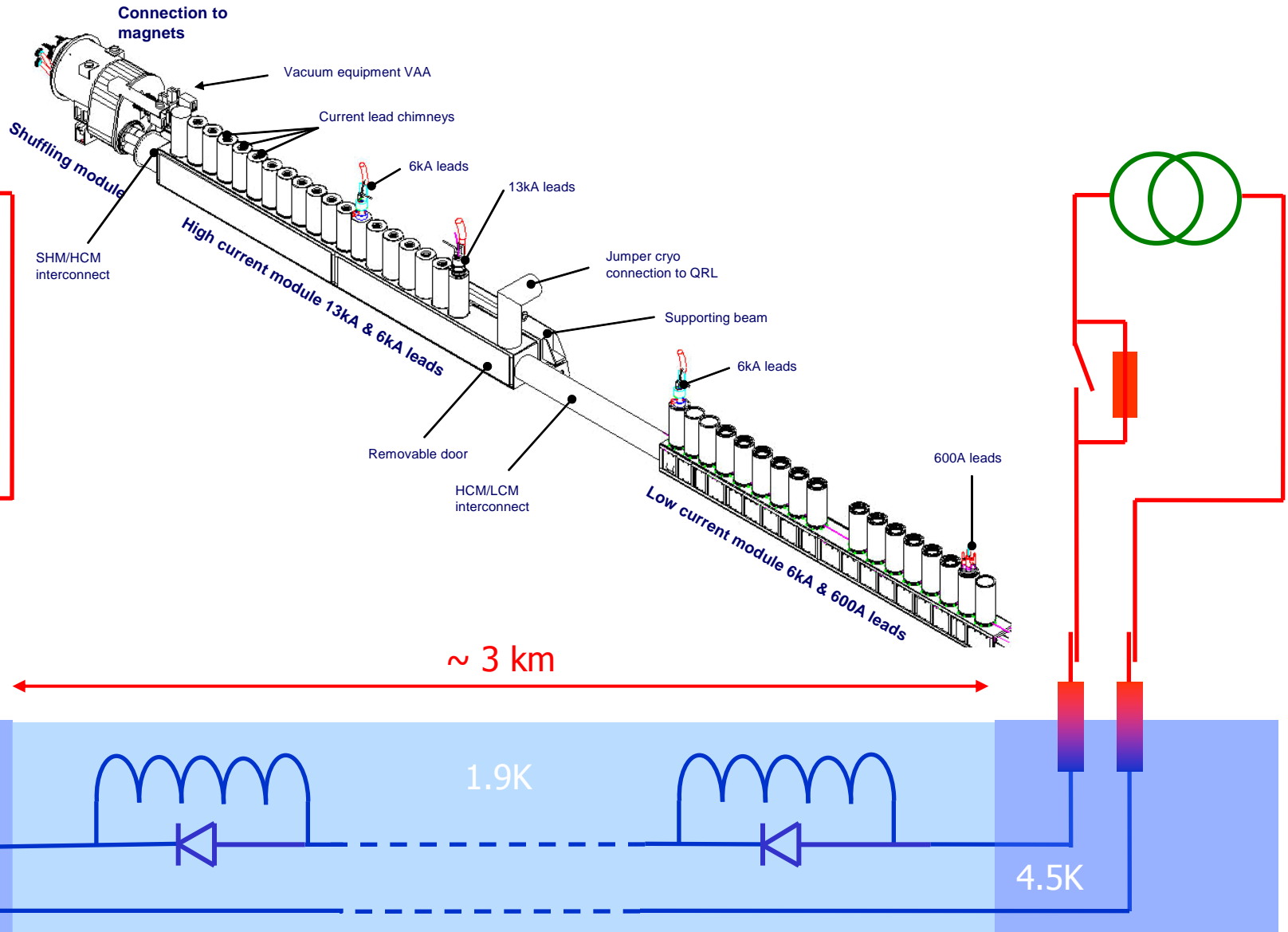


Contents

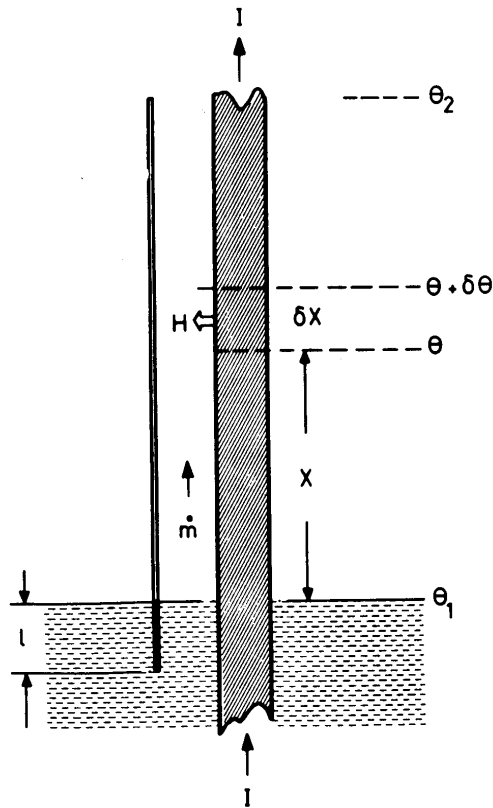
- The LHC in a nutshell
- Performance
 - Energy
 - Luminosity
 - Collective effects
 - Dynamic aperture
- **Technology**
 - Superconducting magnets
 - **Powering and protection**
 - Cryogenics
 - Vacuum



Arc electrical feedbox



Cryogenic current leads



Heat transfer processes at work

- Solid conduction
- Joule heating
- Convective cooling by He vapor

Metals are good electrical AND thermal conductors (Wiedemann-Franz-Lorentz law)

Optimal sizing of current lead results from compromise between heat conduction and Joule heating

Superconductors do not follow WFL law

They are perfect electrical conductors with low thermal conductivity

They can make excellent current leads... up to their transition temperature!

⇒ niche application for "high-temperature" superconductors



Current leads using HTS superconductor

	Resistive (WFL)	HTS (4 to 50 K) Resistive (> 50 K)
Heat inleak to liquid helium	1.1 W/kA	0.1 W/kA
Exergy loss	430 W/kA	150 W/kA
Electrical power of refrigerator	1430 W/kA	500 W/kA

Sum of currents into LHC ~ 1.7 MA,
i.e. need current leads for 3.4 MA
total rating (in and out)

Economy ~ 3400 W in liquid helium
 ~ 5000 l/h liquid helium

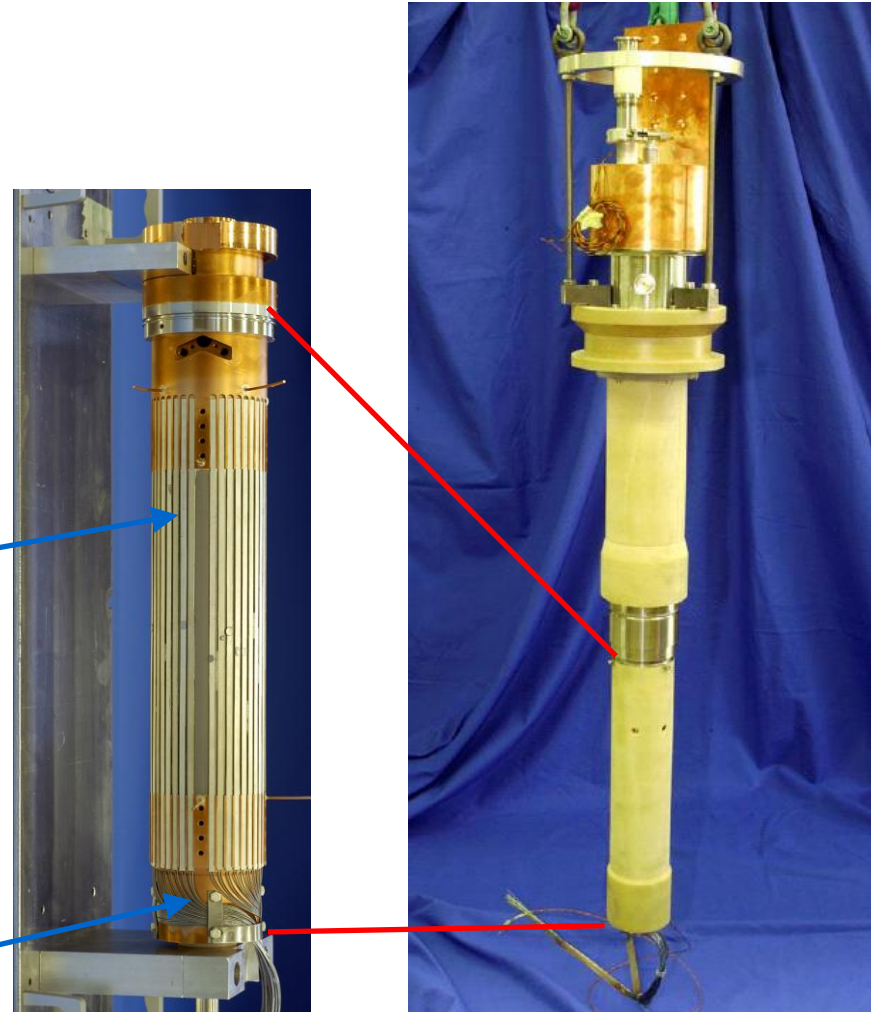
\Rightarrow capital: save extra cryoplant

\Rightarrow operation: save ~ 3.2 MW

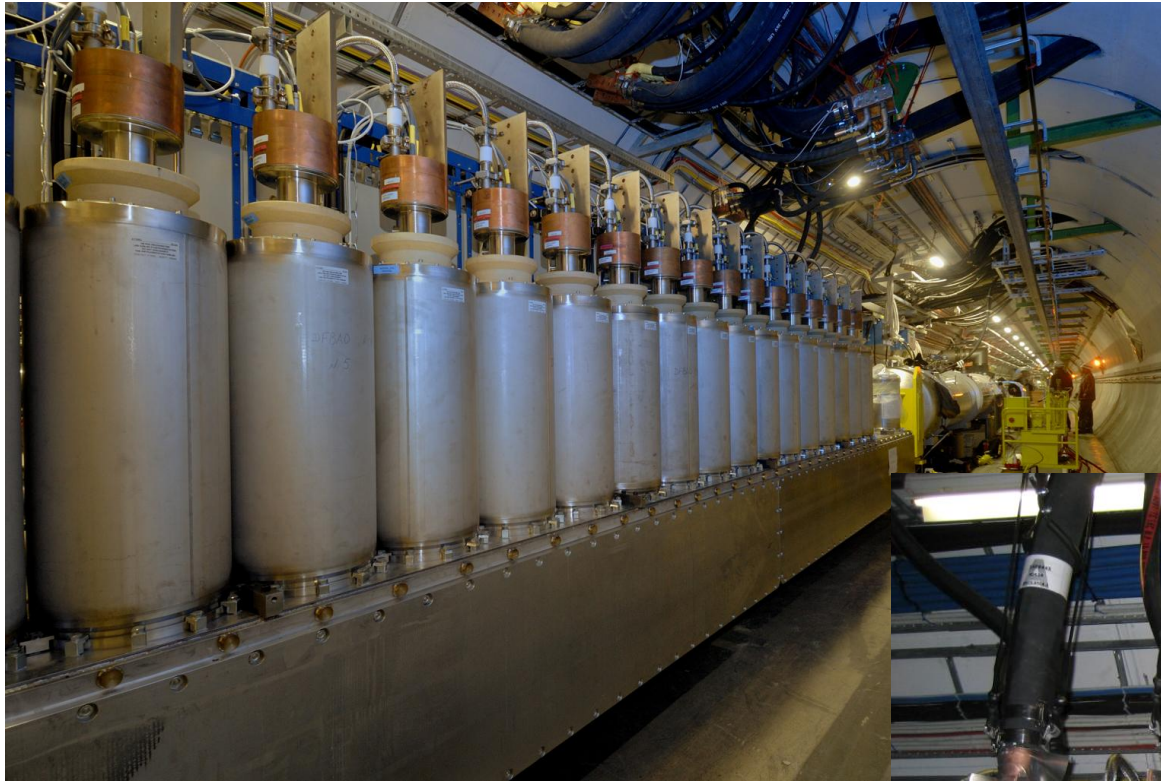
13 kA HTS current lead for LHC

BSCCO
2223 tapes

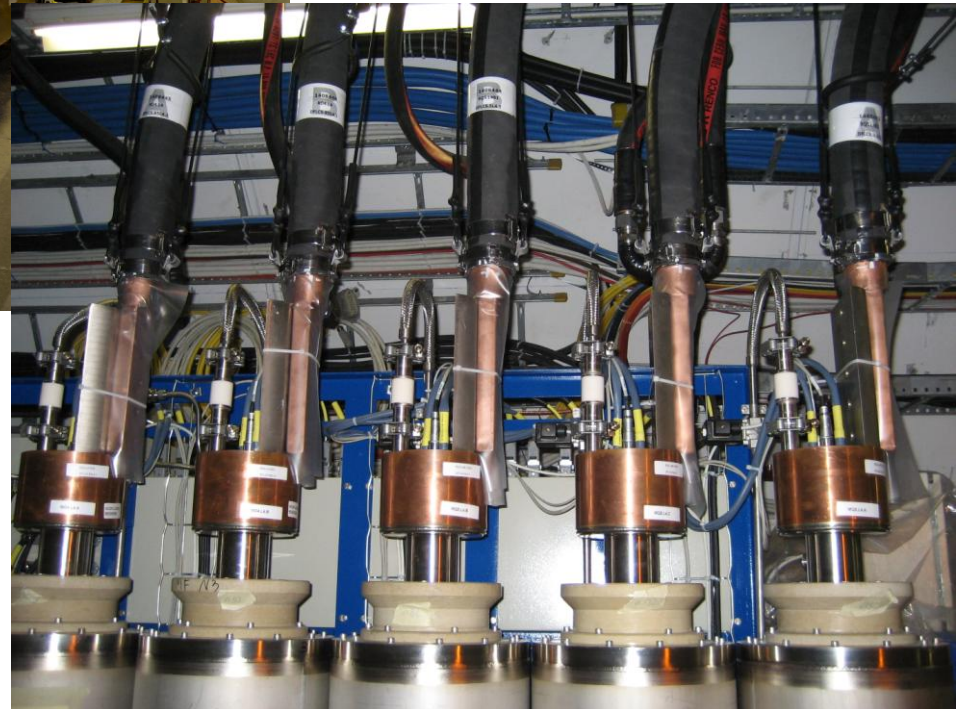
Nb-Ti
wires



HTS current leads in the LHC tunnel



6 & 13 kA leads on electrical feed-box



Water-cooled cables on current lead lugs



Superconductors are basically unstable!

Heat capacity of materials drops at low temperatures

$$\Delta T = \Delta E / \gamma C$$

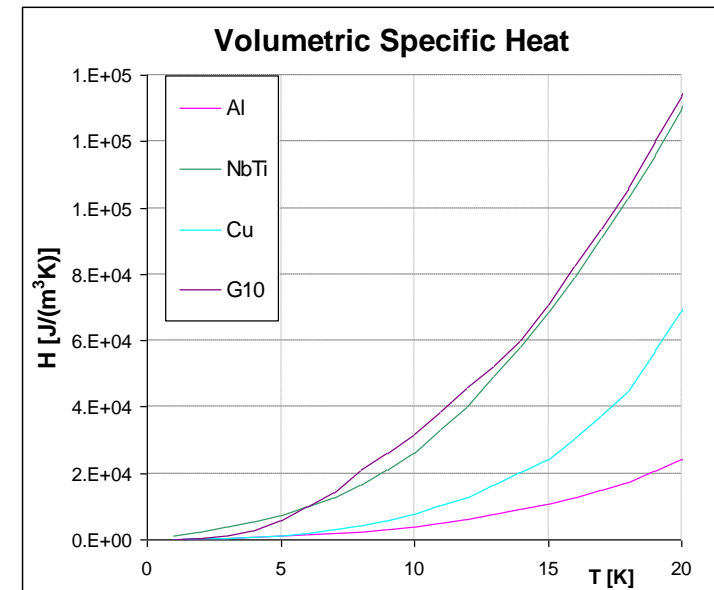
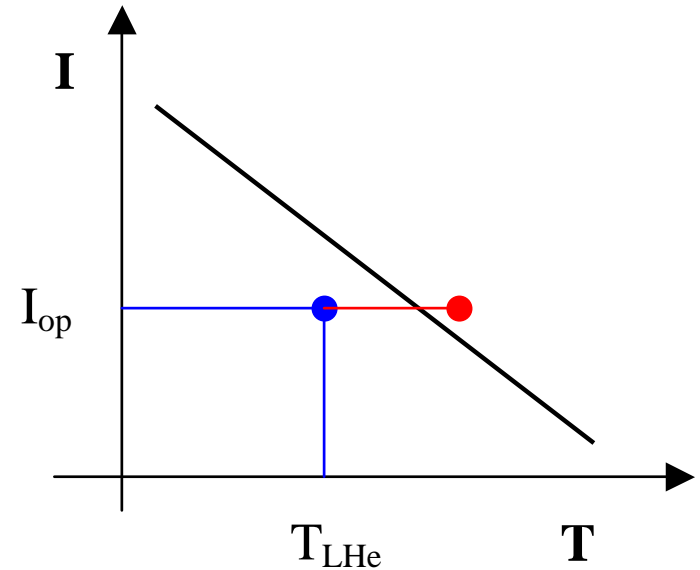
ΔE of few μJ on a superconducting strand in the cable generates ΔT pushing the operating point beyond the critical surface \Rightarrow *resistive transition* ("quench")

Temperature margin of superconductor $\sim 1.5 \text{ K}$

Specific quench energy $\sim 10 \text{ mJ/cm}^3$

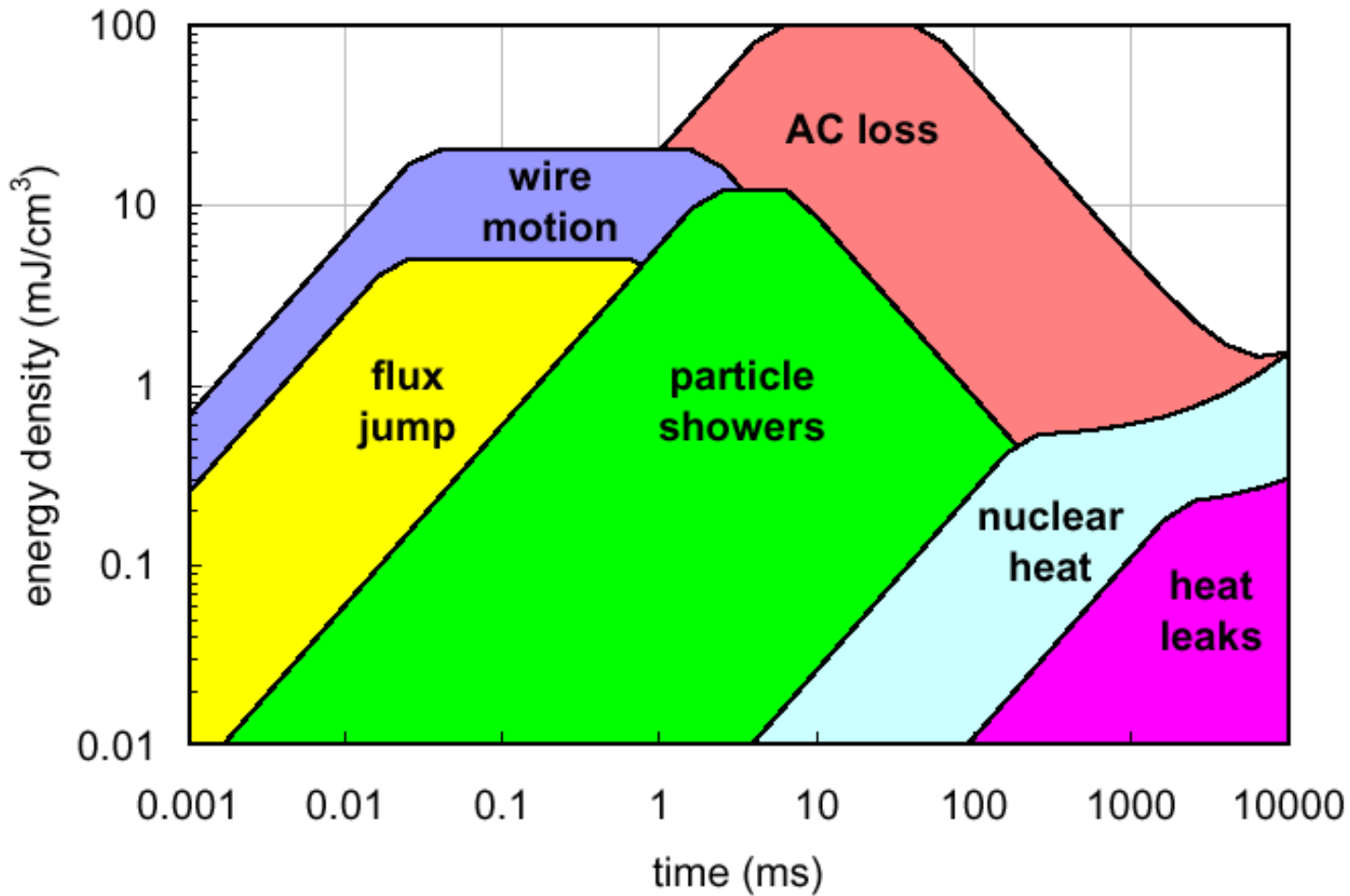
Energy stored inductively in magnet 6.9 MJ

Energy stored in beam 360 MJ

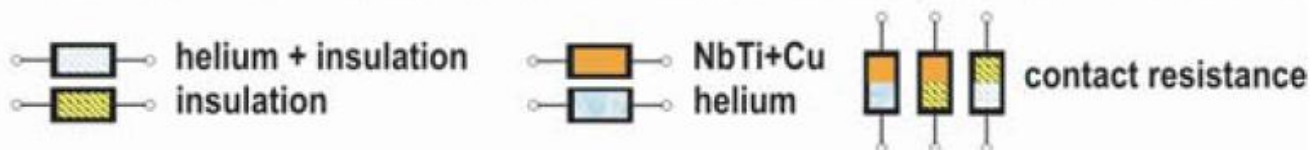
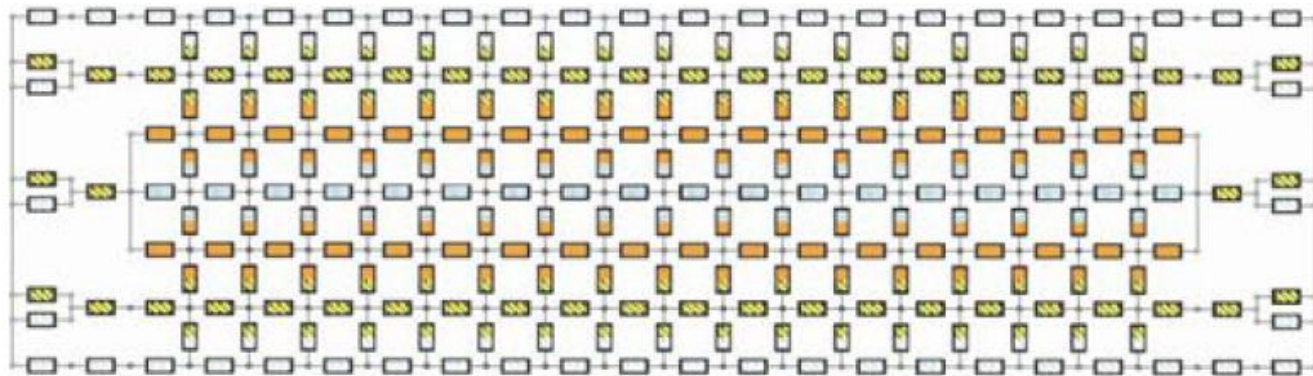
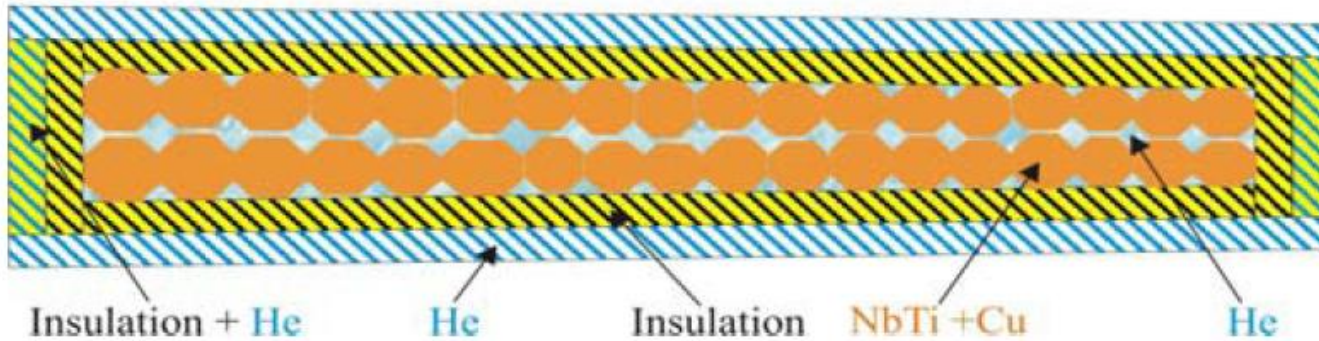
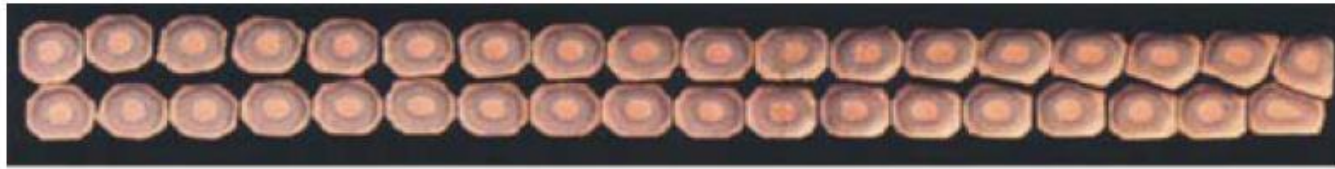




Perturbation spectrum of superconductor

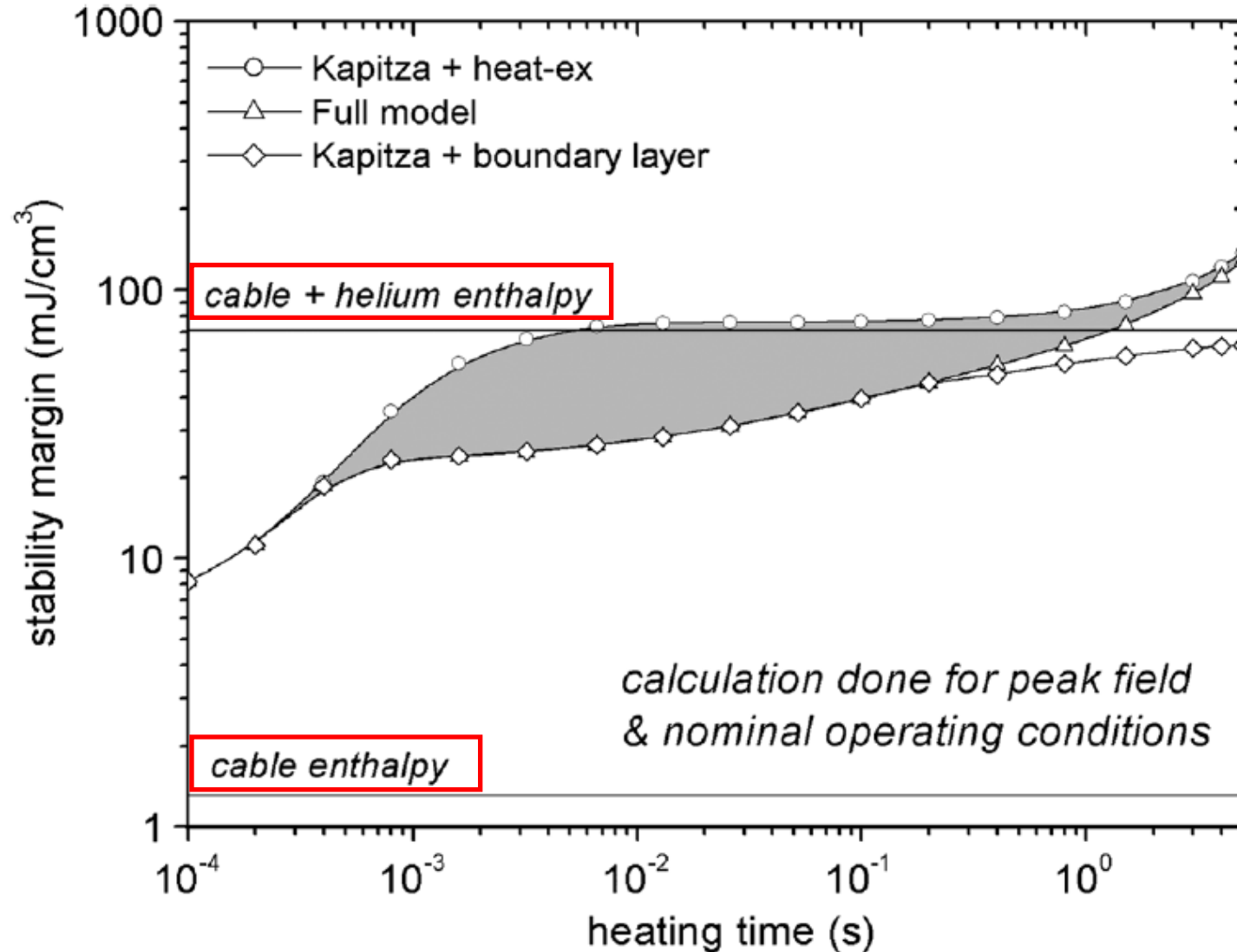


Network model of superconducting cable





Transient stability of superconducting cable





Hot spot temperature after a quench

Assume that quenched section is heated only by Joule effect and adiabatic (no conduction)

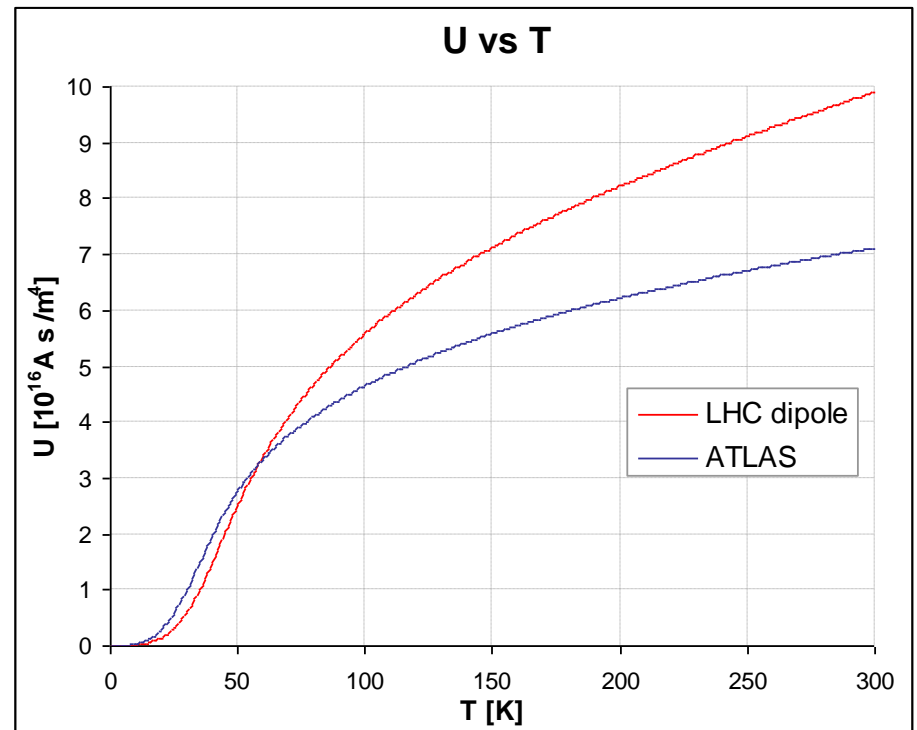
$$J^2(t) \rho(T) dt = \gamma C(T) dT \quad \int_0^\infty J^2(t) dt = \int_{T_{op}}^{T_m} \frac{\gamma C(T)}{\rho(T)} dT \quad J_0^2 T_d = U(T_m)$$

MIITs

To avoid too high hot spot temperature, speed up the quench propagation by any means

- 1) **Heater**: must be activated fast and reliably (20 ms)
- 2) “**Quench-back**” inductively propagated

This goes against having LHe in good contact with the conductor (i.e. against stability)!

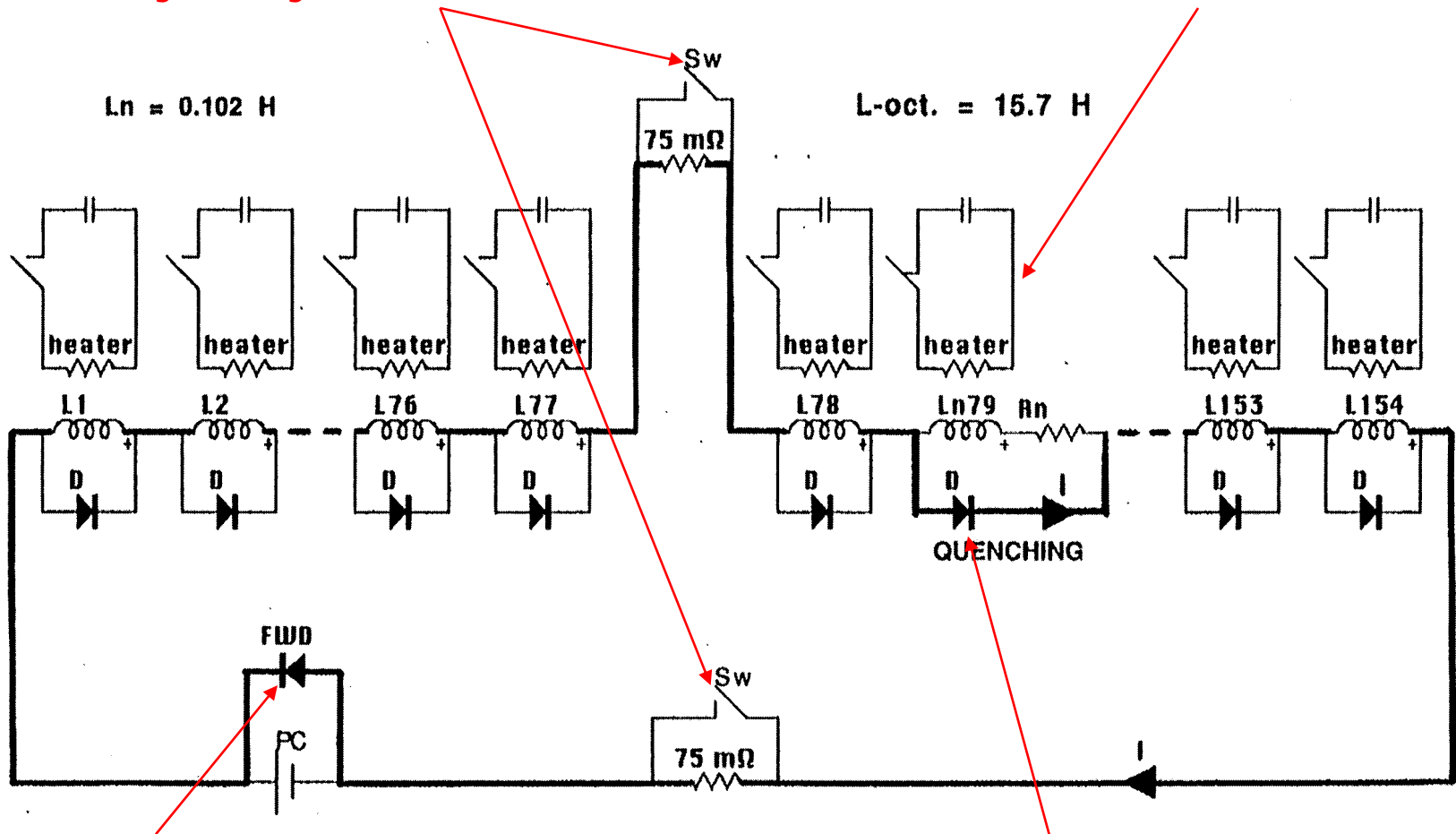




LHC magnet circuit protection scheme

Dissipate energy of magnet string by inserting discharge resistor in circuit

Fire heater to spread the quench over maximum coil volume and limit temperature



Free-wheeling diode across power converter

Diode bypasses quenched magnet during current discharge in string

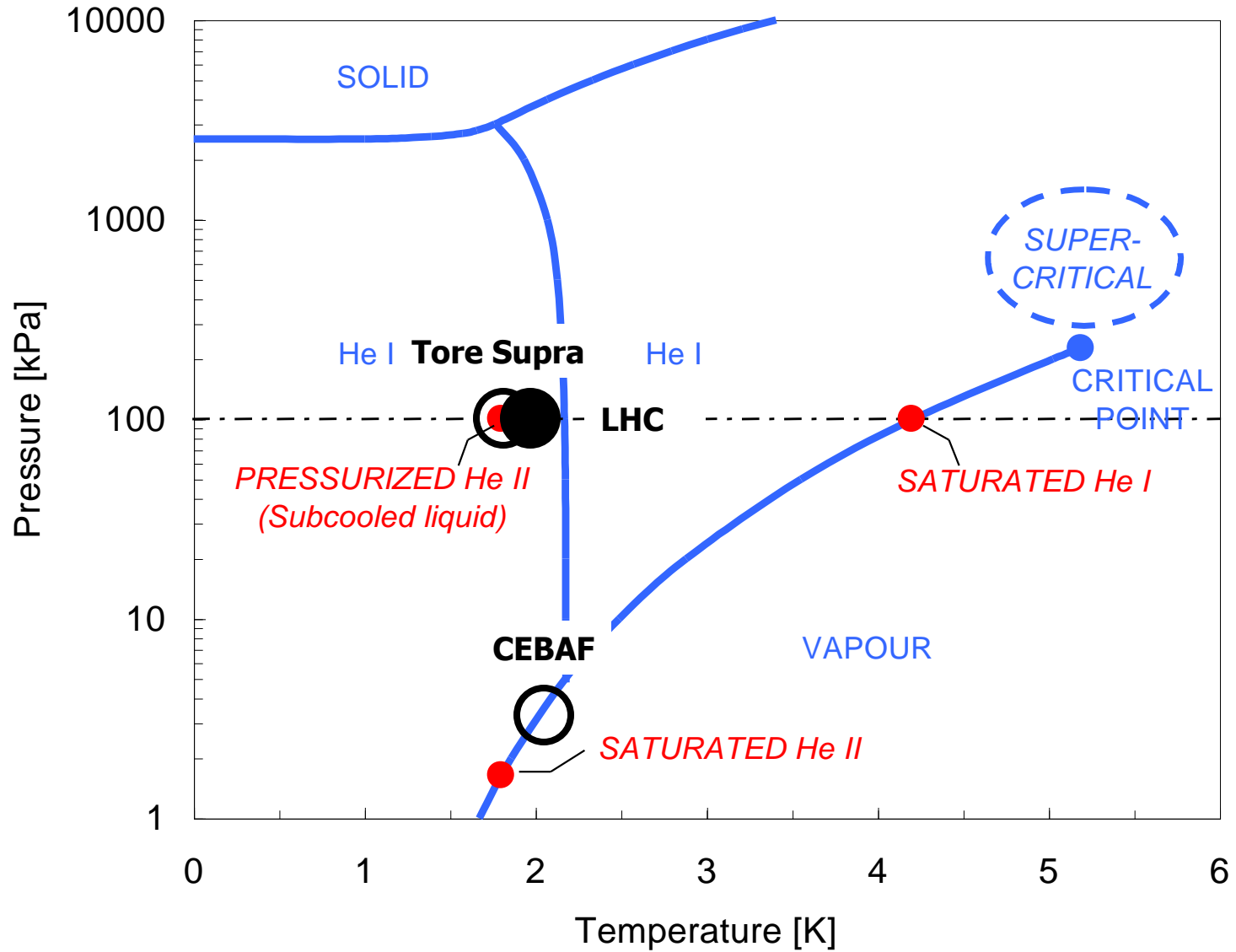


Contents

- The LHC in a nutshell
- Performance
 - Energy
 - Luminosity
 - Collective effects
 - Dynamic aperture
- **Technology**
 - Superconducting magnets
 - Powering and protection
 - **Cryogenics**
 - Vacuum

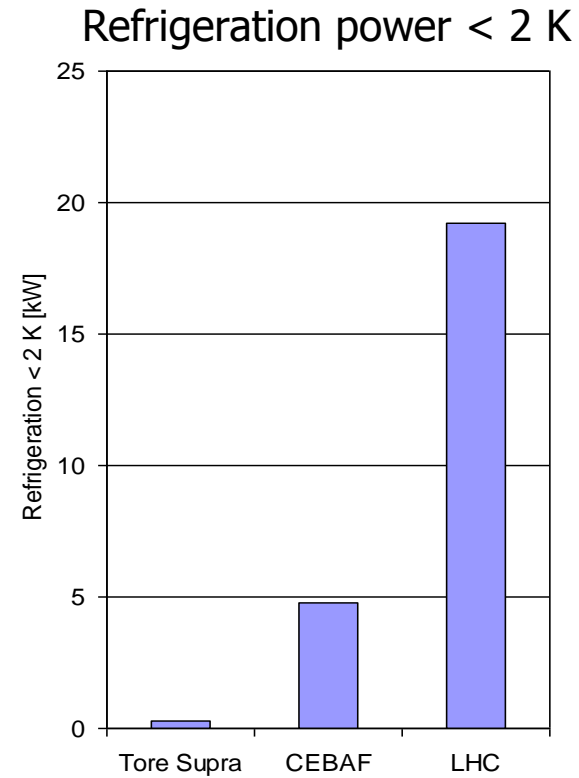
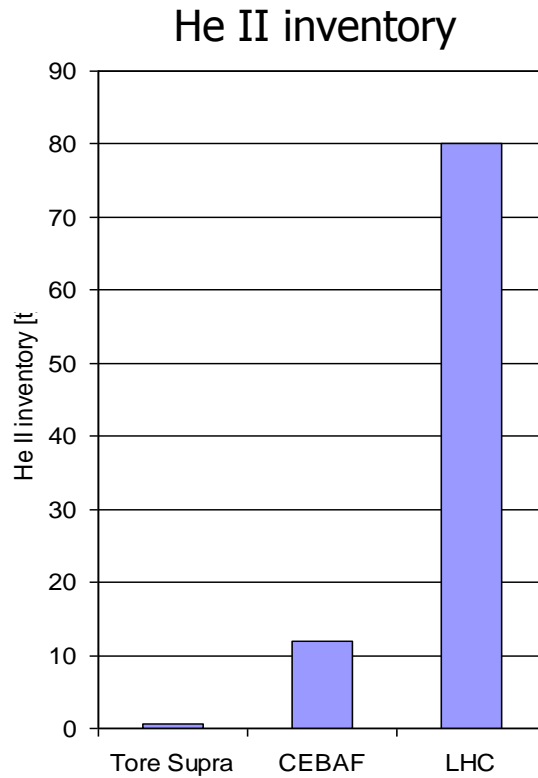


Cooling with superfluid helium

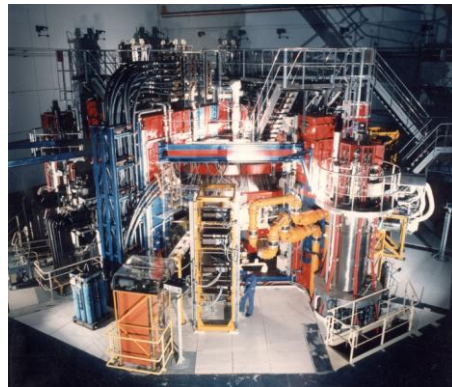




Large-scale superfluid helium systems



Tore Supra tokamak,
Cadarache (France)



CEBAF accelerator,
Newport News (USA)

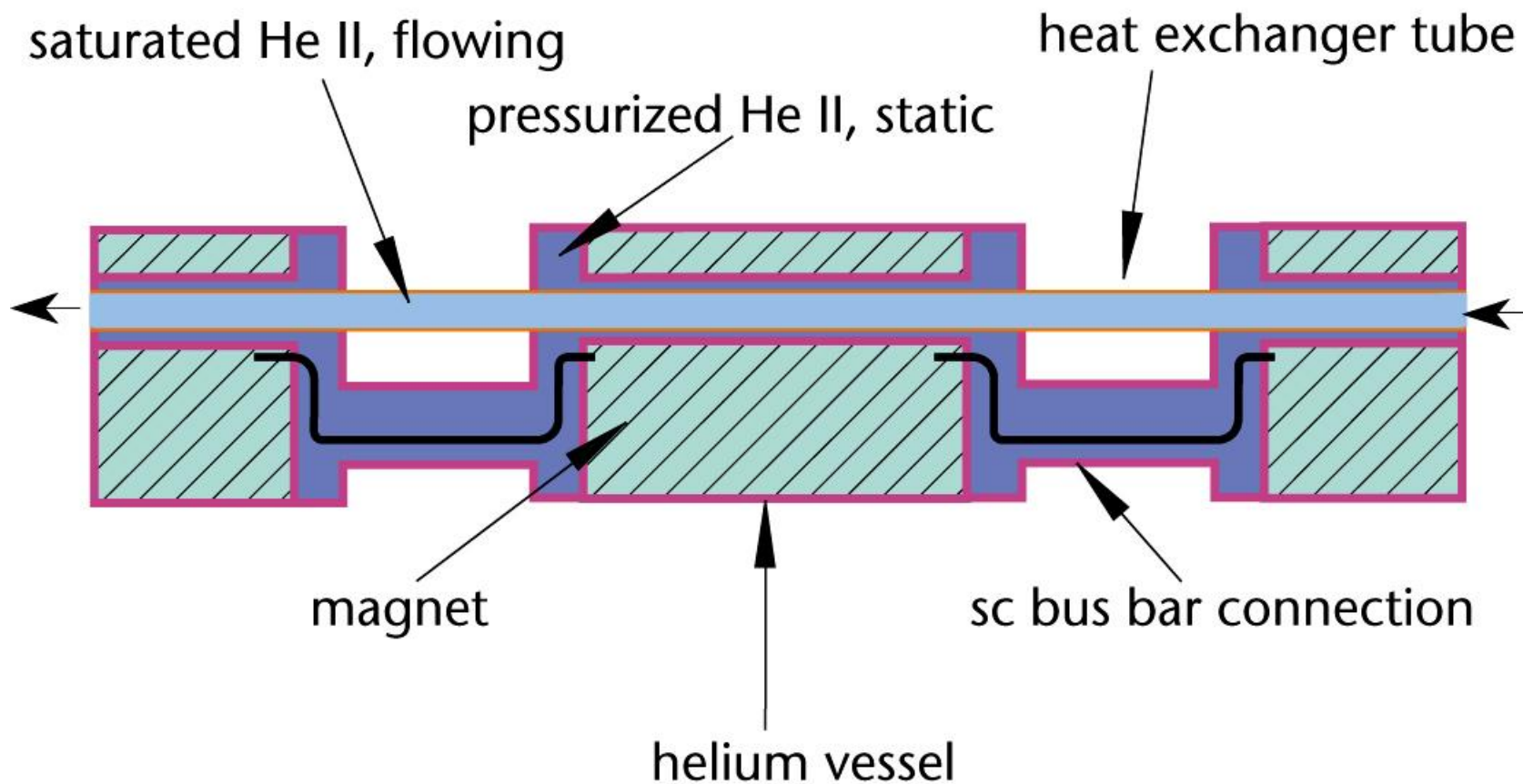


Thermophysical properties of He II

- Temperature < 2.17 K
- Low effective viscosity
 - 100 times lower than water at normal boiling point
- Very high specific heat
 - 10^5 times that of the conductor by unit mass
 - 2×10^3 times that of conductor by unit volume
- Very high thermal conductivity
 - 10^3 times that of OFHC copper, cryogenic grade
 - Peaking at 1.9 K
 - Still, insufficient for transporting heat over large distances across small temperature gradients

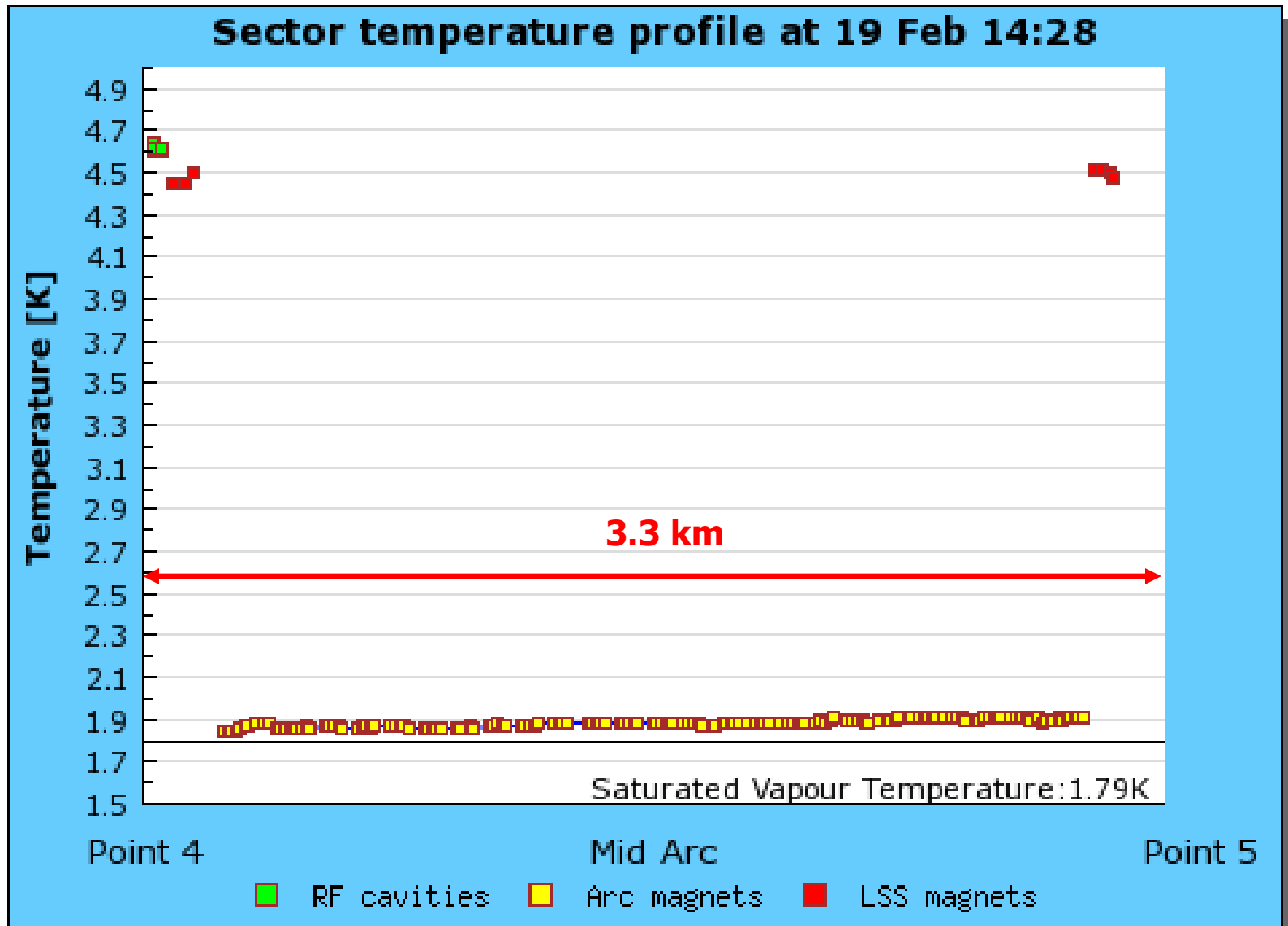


LHC magnet string cooling scheme



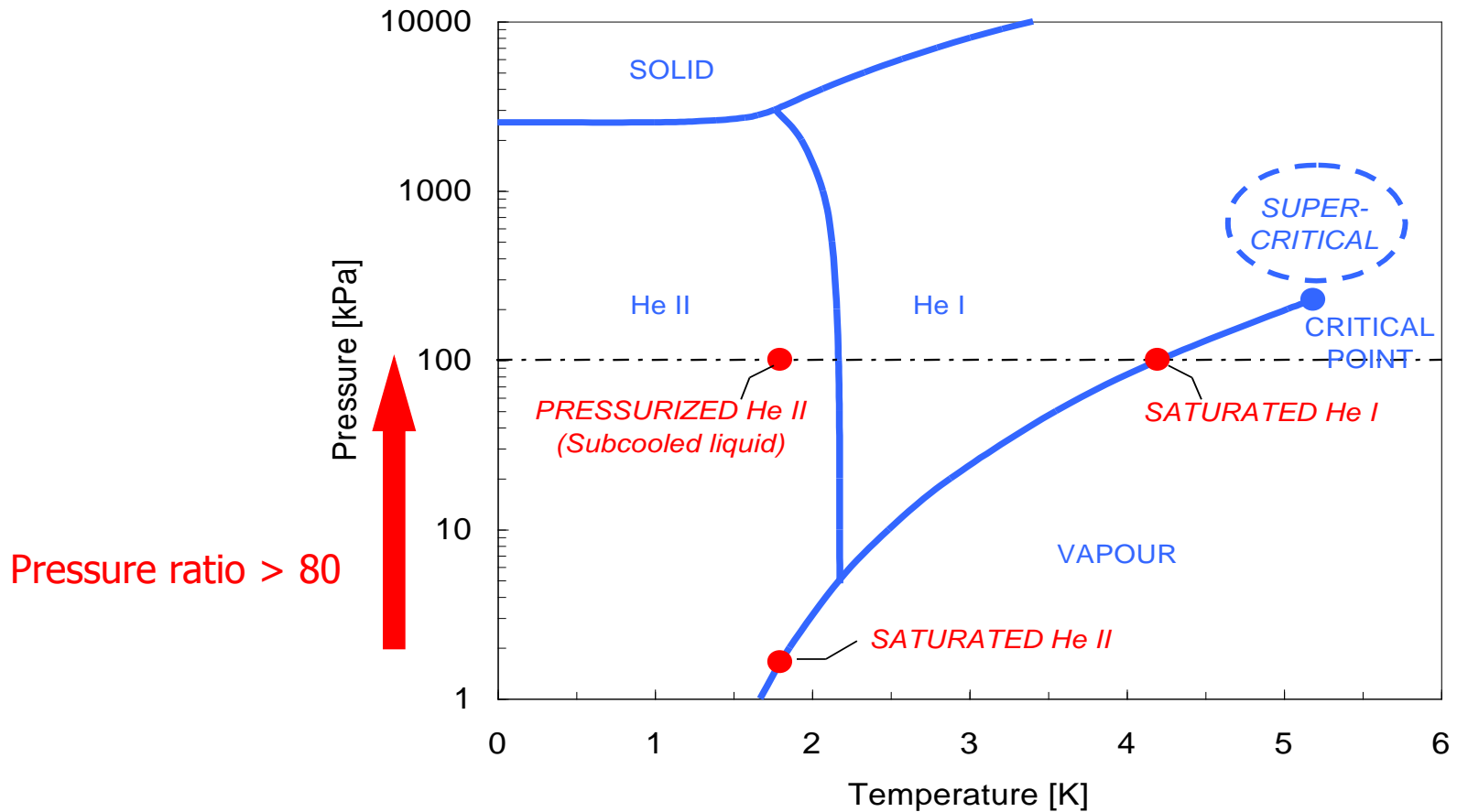


Cryogenic operation of LHC sector





Challenges of high-power 1.8 K refrigeration



- Compression of large mass flow-rate of He vapor across high pressure ratio \Rightarrow intake He at maximum density, i.e. cold
- Need contact-less, vane-less machine \Rightarrow hydrodynamic compressor
- Compression heat rejected at low temperature \Rightarrow thermodynamic efficiency



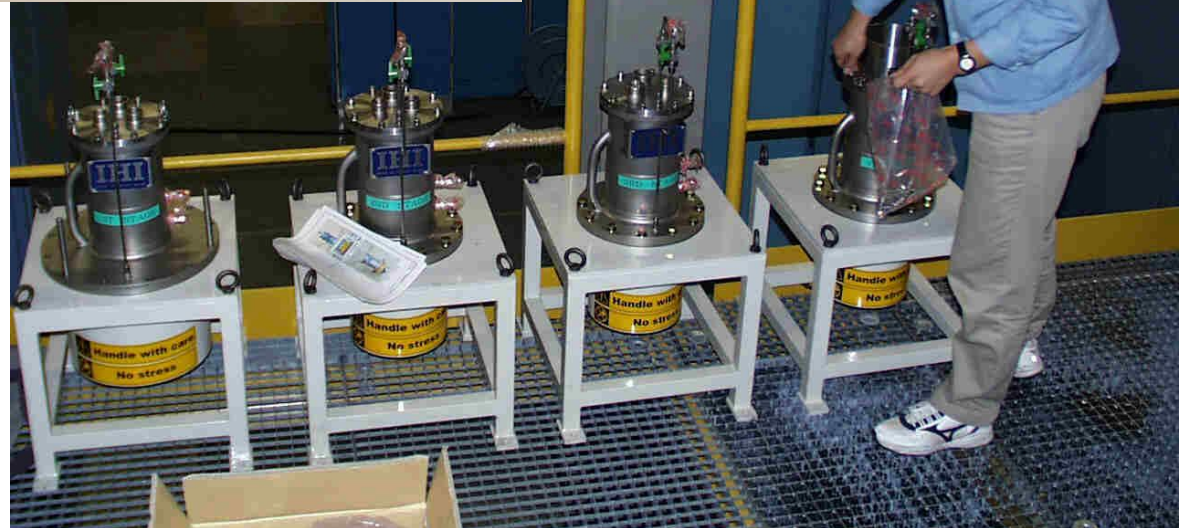
Cold compressors for 1.8 K refrigeration



Axial-centrifugal impeller



Cartridge 1st stage



4 cold compressor stages

Thermal insulation techniques

Multi-layer reflective insulation



10 layers around cold mass at 1.9 K

30 layers around thermal shield at 50-75 K

Cold surface area in LHC ~ 9 hectares!

Thermal radiation from 290 K (black-body)
 $\sim 400 \text{ W/m}^2 = 4 \text{ MW/ha}$

Heat flux from 290 K across 30 layers MLI
 $\sim 1 \text{ W/m}^2 = 10 \text{ kW/ha}$



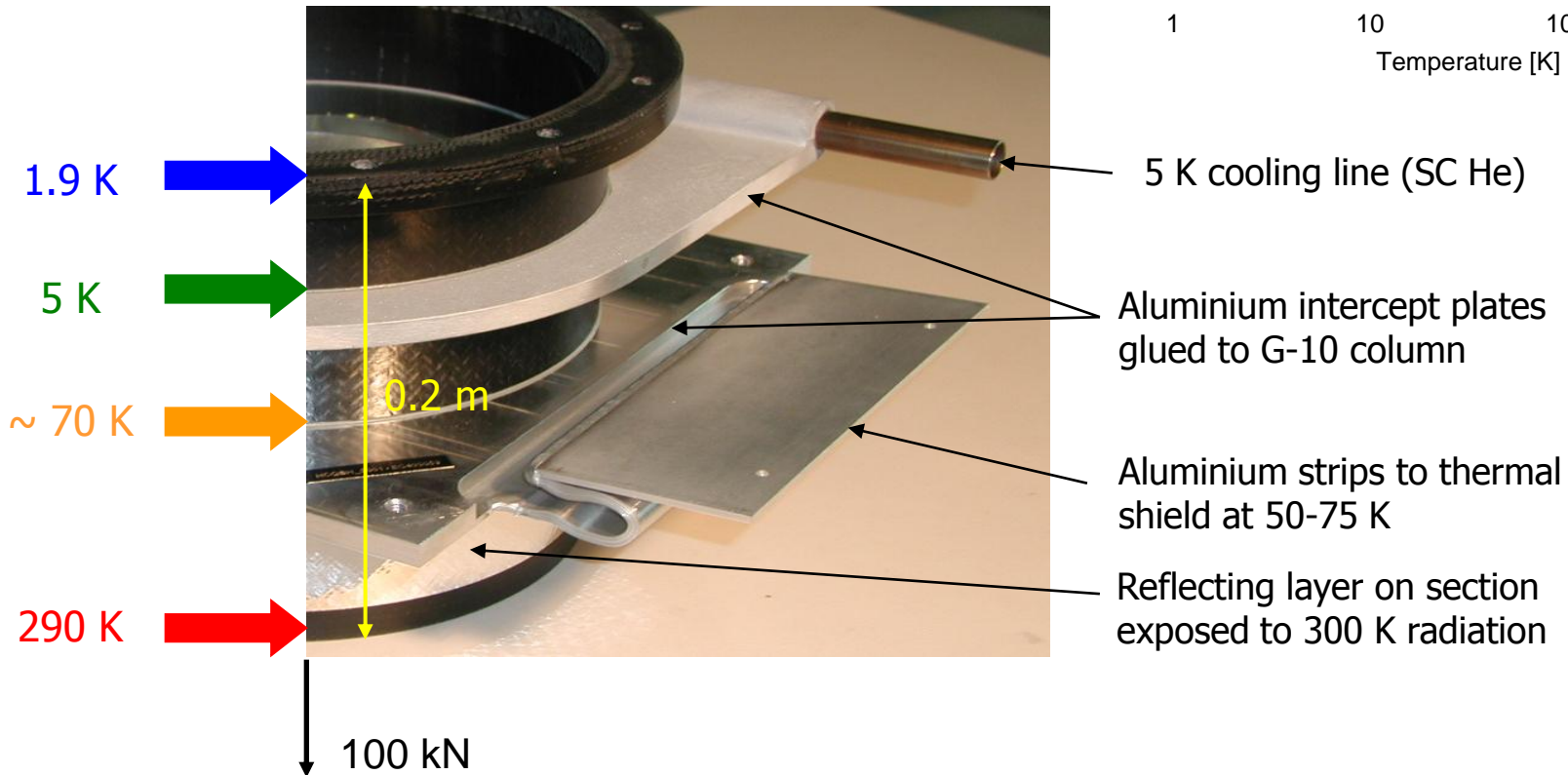
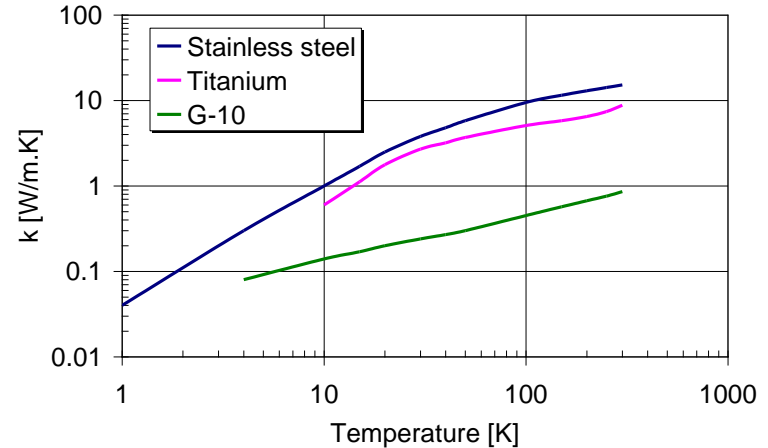
Thermal insulation techniques

Low-conduction non-metallic support posts

LHC cold mass to be supported = 37'500 tons

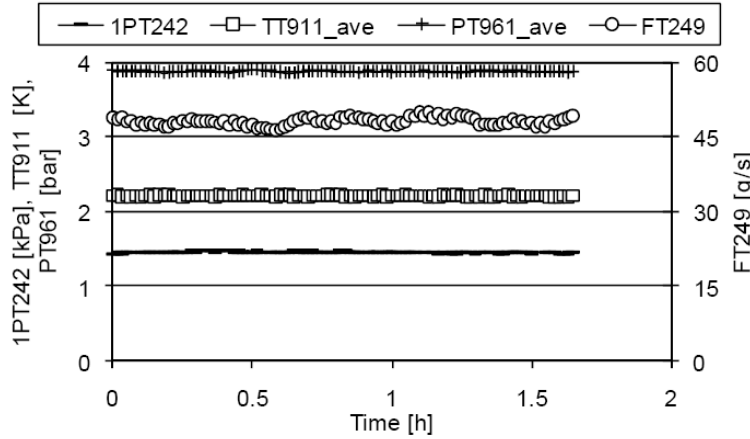
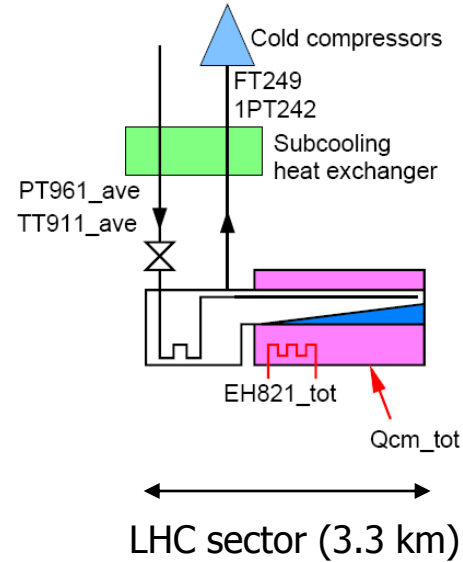
Conduction length = support height ~ 0.2 m

At a compressive stress of 50 N/mm², this requires a total support cross-section of 7.5 m², representing a large thermal conduction path



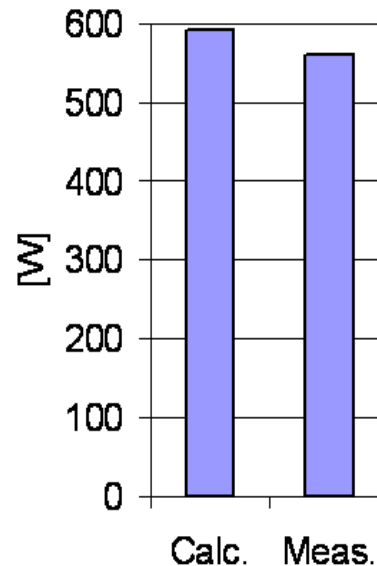


Heat inleak measurements on full sectors confirm thermal budget

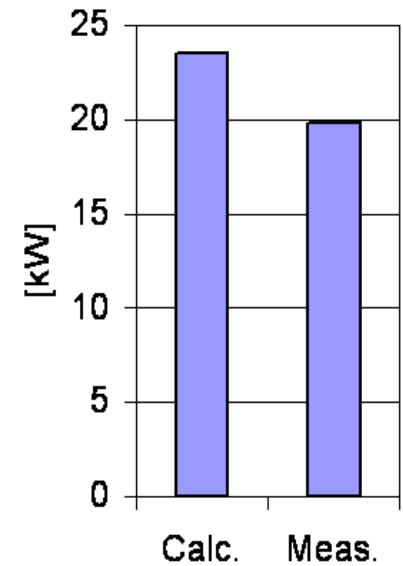


Temperatures and pressures stabilized, flow-rate integrated

Total S7-8 @ 1.9 K



Total @ 50-75 K



$$\dot{Q} = \dot{m} \Delta h \left(P, T \right)$$

Measured (pointing to \dot{Q} , \dot{m} , and Δh)
 He property tables (pointing to P, T)



Contents

- The LHC in a nutshell
- Performance
 - Energy
 - Luminosity
 - Collective effects
 - Dynamic aperture
- **Technology**
 - Superconducting magnets
 - Powering and protection
 - Cryogenics
 - **Vacuum**



Beam vacuum lifetime

- Dominated by nuclear scattering of protons on residual gas
- Lifetime of 100 h required to
 - Limit decay of beam intensity
 - Reduce energy deposited by scattered protons to ~ 30 mW/m

$$\frac{1}{\tau_{gas}} = -\frac{1}{N} \frac{dN}{dt} = v \sum_i \sigma_i n_i$$

Scattering cross-section

Gas density

Proton velocity

Sum over gas species

- Partial pressure

$$P_i = n_i k_B T$$

Proportional to temperature for given gas density



Beam vacuum lifetime

Gas species	Nuclear scattering cross-section [mbarn]	Gas density for 100 h lifetime [m^{-3}]	Pressure at 5 K for 100 h lifetime [Pa]
H ₂	95	9.8 E14	6.7 E-8
He	126	7.4 E14	5.1 E-8
CH ₄	566	1.6 E14	1.1 E-8
H ₂ O	565	1.6 E14	1.1 E-8
CO	854	1.1 E14	7.5 E-9
CO ₂	1320	0.7 E14	4.9 E-9



Vacuum in presence of beam

- Without beam

$$P = \frac{Q}{S}$$

Dynamic pressure

Outgassing rate

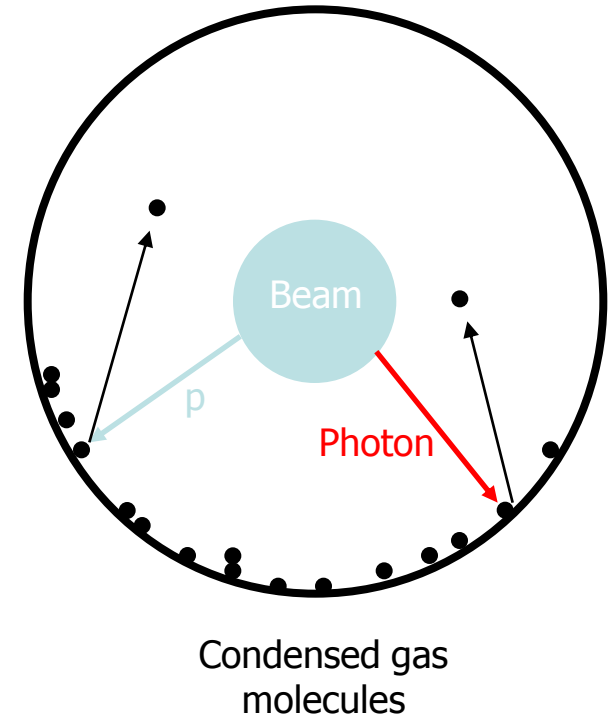
Pumping speed

- With beam

$$P = \frac{Q + \eta \dot{\Gamma}}{S}$$

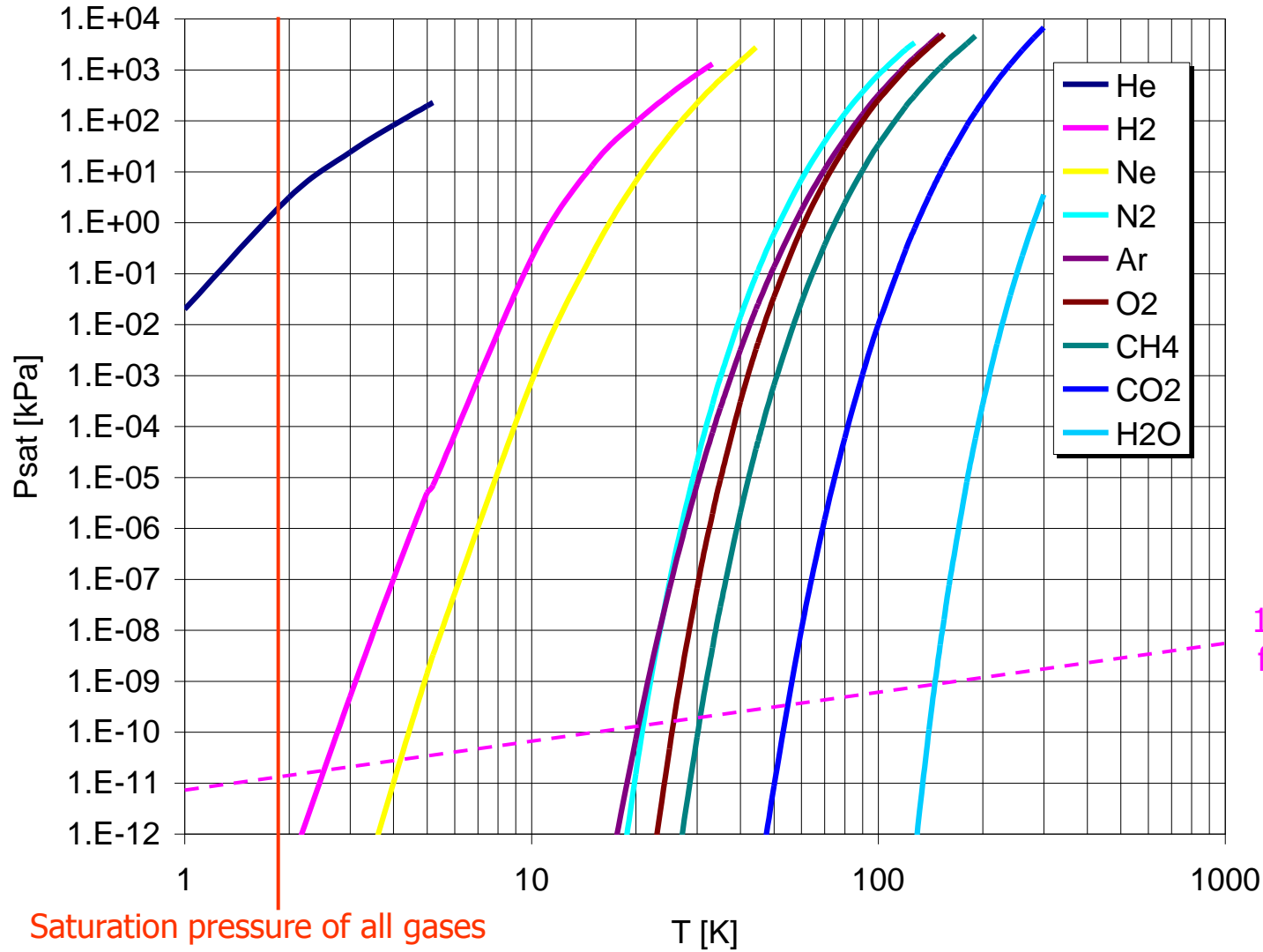
Photon/electron/ion desorption yield

Photon/electron/ion flux





Cryopumping of beam vacuum at 1.9 K

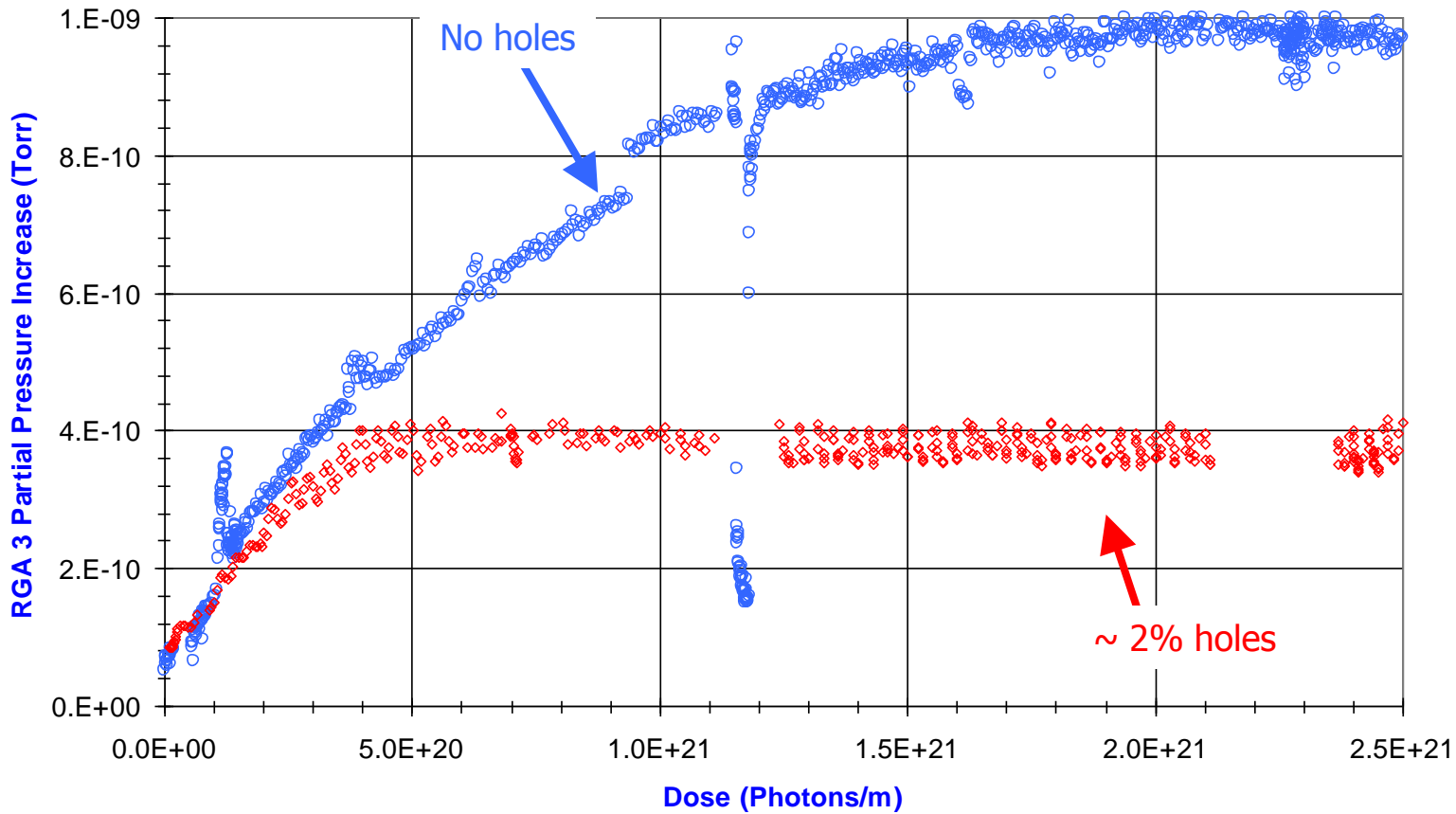


Saturation pressure of all gases except helium vanish at 1.9 K

100 h lifetime for hydrogen

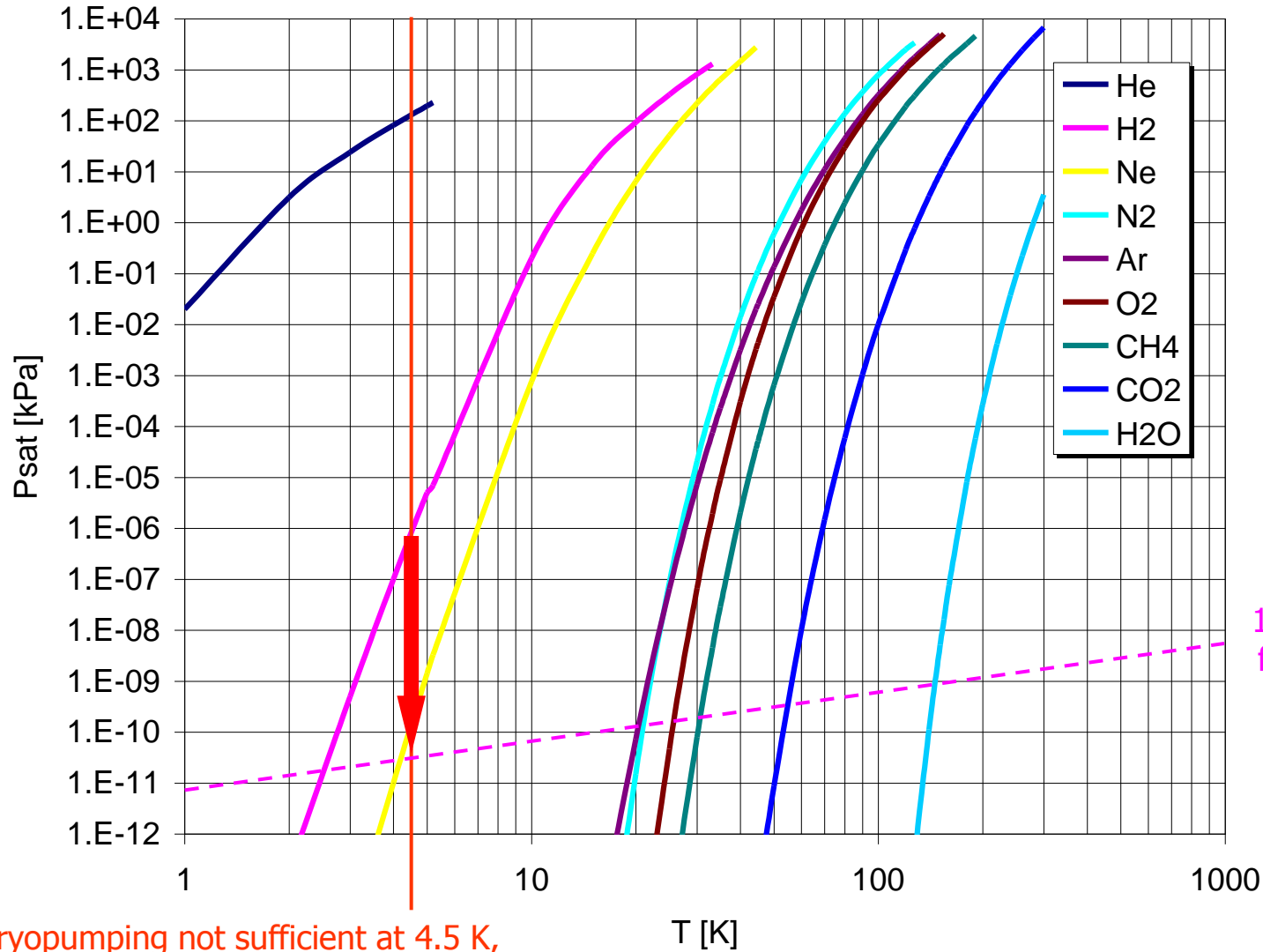


Pumping desorbed gas through the beam screen





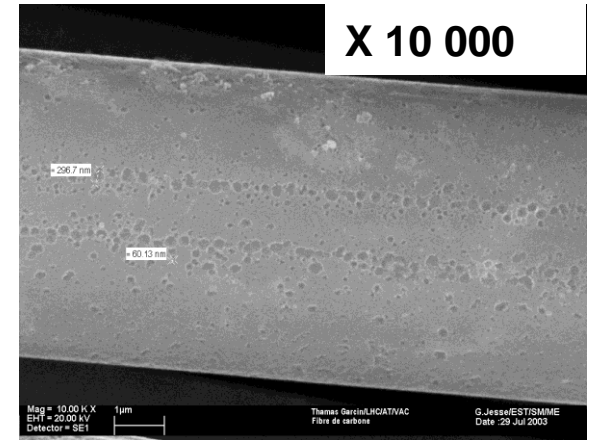
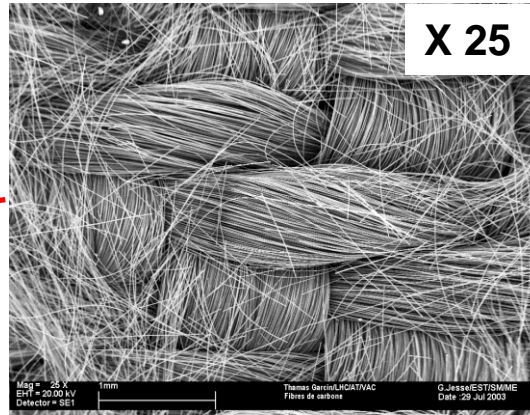
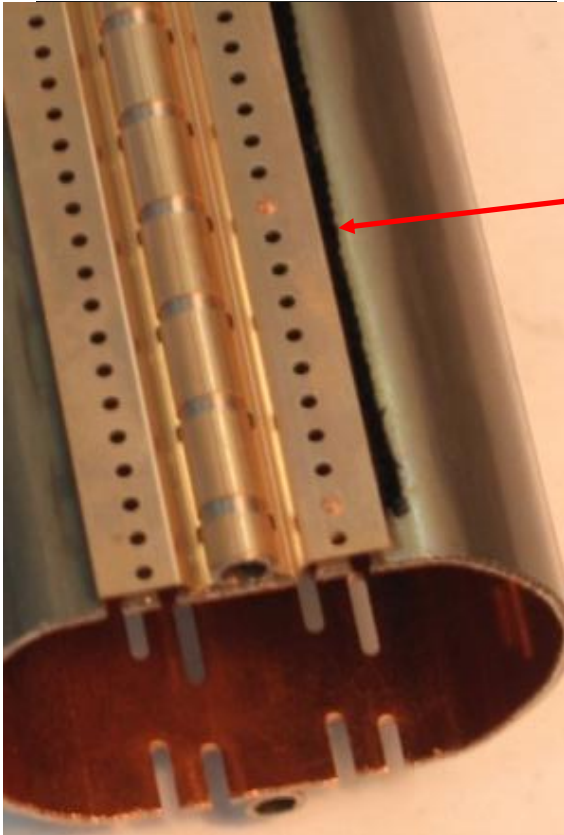
Cryosorption of beam vacuum at 4.5 K



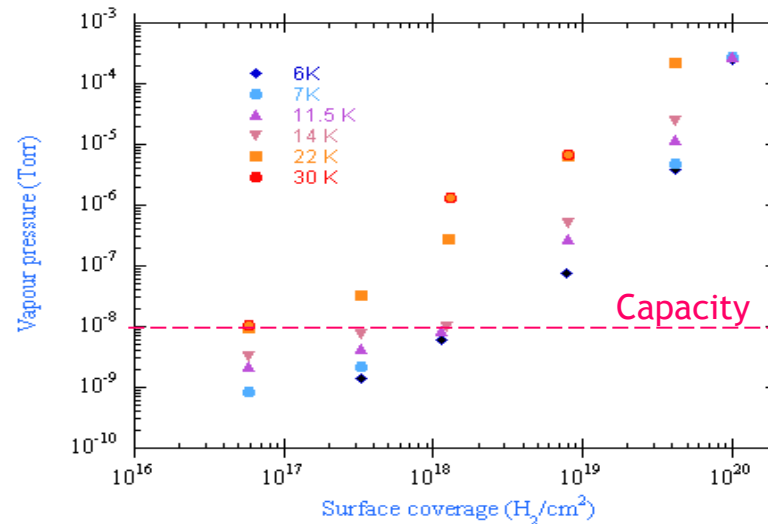
100 h lifetime
for hydrogen

Crypumping not sufficient at 4.5 K,
use cryosorption

Cryosorber



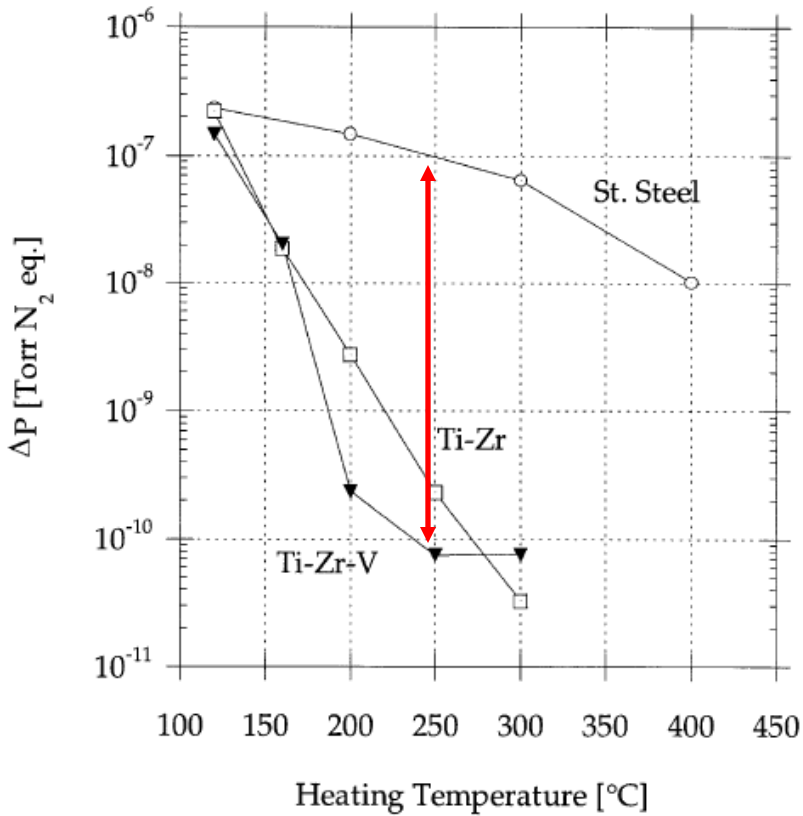
Carbon fiber mesh on the beam screen, to pump hydrogen
Capacity sufficient for regeneration only during annual shutdown



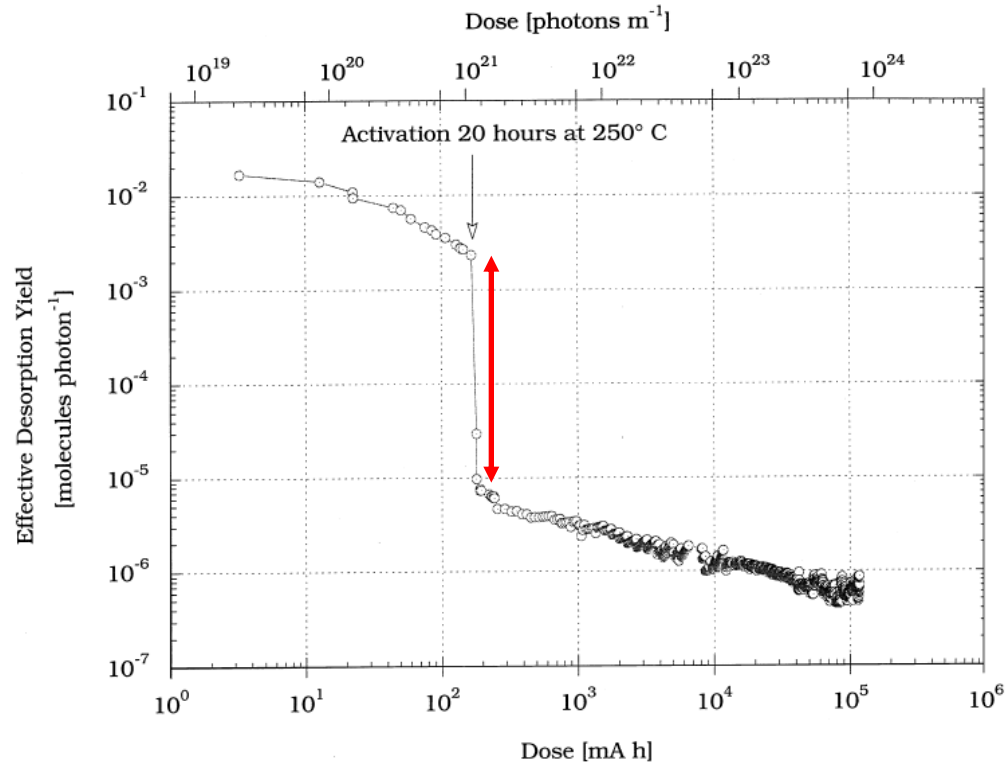


Non-evaporable getter coated vacuum chambers

Distributed pumping integrated into beam pipe



Pressure increase by 500 eV electron bombardment of surface at 20° C, after heating for 2 hours



Effective molecular desorption yield as a function of photon dose, on TiZrV NEG coating of stainless steel chamber



Beam vacuum in long straight sections



Cold-to-warm
transition

NEG-coated copper
vacuum chambers



Some references

- L. Evans (editor), *The Large Hadron Collider, a marvel of technology*, EPFL/CRC Press, Lausanne/Boca Raton (2009)
- LHC Design Report, Volume I, *The LHC Main Ring*, CERN-2004-003 (2004)
<http://cdsweb.cern.ch/record/782076?ln=en>
- L. Evans, *LHC accelerator physics and technology challenges*, Proc. PAC1999 New York, JACoW (1999) 21-25
<http://cdsweb.cern.ch/record/386693?ln=en>
- L. Rossi, *The Large Hadron Collider and the role of superconductivity in one of the largest scientific enterprises*, IEEE Trans. Applied Superconductivity **17** (2007) 1005-1014
<http://cdsweb.cern.ch/record/1048661?ln=en>
- Ph. Lebrun, *Cryogenics for the Large Hadron Collider*, IEEE Trans. Applied Superconductivity **10** (2000) 1500-1506
<http://cdsweb.cern.ch/record/438911?ln=en>
- J.M. Jiménez, *LHC : the world's largest vacuum systems being operated at CERN*, Vacuum **84** (2009) 2-7
<http://cdsweb.cern.ch/record/1281361?ln=en>